NUB-3244/Th-04
astro-ph/0402371

Astrophysical Origins of Ultrahigh Energy Cosmic Rays

Diego F. Torres[a] and Luis A. Anchordoqui[b]

[a] *Lawrence Livermore National Laboratory, 7000 East Ave., L-413, Livermore, CA 94550, USA*

[b] *Department of Physics, Northeastern University Boston, MA 02115, USA*

dtorres@igpp.ucllnl.org
l.anchordoqui@neu.edu

Abstract

In the first part of this review we discuss the basic observational features at the end of the cosmic ray energy spectrum. We also present there the main characteristics of each of the experiments involved in the detection of these particles. We then briefly discuss the status of the chemical composition and the distribution of arrival directions of cosmic rays. After that, we examine the energy losses during propagation, introducing the Greisen-Zaptsepin-Kuzmin (GZK) cutoff, and discuss the level of confidence with which each experiment have detected particles beyond the GZK energy limit. In the second part of the review, we discuss astrophysical environments able to accelerate particles up to such high energies, including active galactic nuclei, large scale galactic wind termination shocks, relativistic jets and hot-spots of Fanaroff-Riley radiogalaxies, pulsars, magnetars, quasar remnants, starbursts, colliding galaxies, and gamma ray burst fireballs. In the third part of the review we provide a brief summary of scenarios which try to explain the super-GZK events with the help of new physics beyond the standard model. In the last section, we give an overview on neutrino telescopes and existing limits on the energy spectrum and discuss some of the prospects for a new (multi-particle) astronomy. Finally, we outline how extraterrestrial neutrino fluxes can be used to probe new physics beyond the electroweak scale.

Solicited Review Article Prepared for Reports on Progress in Physics

PREFACE

Reviewing cosmic ray physics is a risky business. Theoretical models continue to appear at an amazing rate, both in the astrophysical and more exotic domains. We warn the reader: we do not (nor we could) intend to make an homogeneous coverage of all the ideas of our fellow colleagues. Reading differently focused reviews on the issue (quoted here along the way) is, in our view, the best approach to such a wide topic of research.

Contents

I. THERE'S SOMETHING ABOUT COSMIC RAY OBSERVATIONS

A. Experiments and future projects

The cosmic ray (CR) spectrum spans over roughly 11 decades of energy. Continuously running monitoring using sophisticated equipment on high altitude balloons and ingenious installations on the Earth's surface encompass a plummeting flux that goes down from 10^4 m^{-2} s^{-1} at $\sim 10^9$ eV to 10^{-2} km^{-2} yr^{-1} at $\sim 10^{20}$ eV. Its shape is remarkably featureless, with little deviation from a constant power law across this large energy range. The small change in slope, from $\propto E^{-2.7}$ to $\propto E^{-3.0}$, near $10^{15.5}$ eV is known as the "knee". The spectrum steepens further to $E^{-3.3}$ above the "dip" ($\approx 10^{17.7}$ eV), and then flattens to $E^{-2.7}$ at the "ankle" ($\approx 10^{19}$ eV). Within statistical uncertainty of current observations, which is large above 10^{20} eV, the upper end of the spectrum is consistent with a simple extrapolation at that slope to the highest energies, possibly with a slight accumulation around $10^{19.5}$ eV (For recent surveys of experimental data the reader is referred to [1, 2, 3, 4, 5, 6]).

It is a lucky coincidence that at the energy ($\sim 10^{14}$ eV) where direct measurement of CRs becomes limited by detector area and exposure time, the resulting air showers that such particles produce when they strike the upper atmosphere become big enough to be detectable at ground level. There are several techniques that can be employed in the process of detection:

(i) Direct detection of shower particles is the most commonly used method, and involves constructing an array of sensors spread over a large area to sample particle densities as the shower arrives at the Earth's surface. The pioneering development of the air shower techniques (and the first use of plastic scintillation detectors for the dual use of measuring arrival directions and particle densities) was started at the Agassiz Station of the Harvard College Observatory, a work carried out between 1954 and 1957 [7, 8, 9]. The existence of primary particles with energies greater than 10^{18} eV was established by the observation of one shower with more than 10^9 particles. Soon afterwards, this technique flourished with measurements of ultra high energy cosmic rays (UHECRs) with the Volcano Ranch experiment in the 60 s [10, 11, 12], as well as with several other arrays, such as Haverah Park in England [13], Yakutsk in Russia [14, 15], the Sydney University Giant Airshower Recorder in Australia (SUGAR) [16], and the Akeno Giant Air Shower Array (AGASA) in Japan [17, 18].

(ii) Another well-established method of detection involves measurement of the longitudinal development (number of particles versus atmospheric depth) of the extensive air shower (EAS) by sensing the fluorescence light produced via interactions of the charged particles in the atmosphere. The emitted light is typically in the 300 - 400 nm ultraviolet range to which the atmosphere is quite transparent. Under favorable at-

mospheric conditions, EASs can be detected at distances as large as 20 km, about 2 attenuation lengths in a standard desert atmosphere at ground level. However, observations can only be done on clear Moon*less* nights, resulting in an average 10% duty cycle. The fluorescence technique has so far been implemented only in the Dugway desert (Utah). Following a successful trial at Volcano Ranch [19] the group from the University of Utah built a device containing two separated Fly's Eyes [20, 21]. The two-eye configuration monitored the sky from 1986 until 1993. As an up-scaled version of Fly's Eye, the High Resolution (HiRes) Fly's Eye detector begun operations in May 1997 [22, 23]. In monocular mode, the effective acceptance of this instrument is $\sim 350(1000)$ km^2 sr at $10^{19}\,(10^{20})$ eV, on average about 6 times the Fly's Eye acceptance, and the threshold energy is 10^{17} eV. This takes into account a 10% duty cycle.

(iii) A more recently proposed technique uses radar echos from the column of ionized air produced by the shower. This idea suggested already in 1940 [24], has been recently re-explored [25, 26] as either an independent method to study air showers, or as a complement to existing fluorescence and surface detectors. A proposal has recently been put forth to evaluate the method using the Jicamarca radar system near Lima, Peru [27].

In order to increase the statistics at the high end of the spectrum significantly, two projects are now under preparation:

(i) The Pierre Auger Observatory (PAO), currently under construction in Argentina, is the first experiment designed to work in a hybrid mode incorporating both a ground-based array of 1600 particle detectors spread over 3000 km^2 with fluorescence telescopes placed on the boundaries of the surface array [28]. A second array will be set up in the Northern hemisphere to cover the whole sky. Such a full-sky coverage is very important to allow sensitive anisotropy analysis. The overall aperture (2 sites) for CRs with primary zenith angle $< 60^\circ$ and primary energy $> 10^{19}$ eV is $\approx 1.4 \times 10^4$ km^2 sr.

(ii) The mission "Extreme Universe Space Observatory" (EUSO) will observe the fluorescence signal of CRs, with energy $> 4 \times 10^{19}$ eV, looking downward from the International Space Station to the dark side of the Earth atmosphere [29, 30]. The characteristic wide angle optics of the instrument (with opening field of view $\pm 30^\circ$ at an average orbit altitude of ≈ 400 km) yields a geometric aperture of $\approx 5 \times 10^5$ km^2 sr, taking into account a 10% duty cycle. The monocular stand-alone configuration of the telescope will serve as a pathfinder mission to develop the required technology to observe the fluorescent trails of EASs from space.

The experimental input for γ-ray physics will be further enriched by dedicated Čerenkov detectors like HESS [31], MAGIC [32], CANGAROO [33], and VERITAS [34], as well as satellites like GLAST [35, 36] and AGILE [37].

B. Primary species

When a CR enters the Earth atmosphere it collides with a nucleus of an air atom, producing a roughly conical cascade of billions of elementary particles which reaches the ground in the form of a giant "saucer" traveling at nearly the speed of light.

Unfortunately, because of the highly indirect method of measurement, extracting precise information from EASs has proved to be exceedingly difficult. The most fundamental problem is that the first generations of particles in the cascade are subject to large inherent fluctuations and consequently this limits the event-by-event energy resolution of the experiments. In addition, the center-of-mass energy of the first few cascade steps is well beyond any reached in collider experiments. Therefore, one needs to rely on hadronic interaction models that attempt to extrapolate, using different mixtures of theory and phenomenology, our understanding of particle physics. At present, the different approaches used to model the underlying physics of $p\bar{p}$ collisions show clear differences in multiplicity predictions which increase with rising energy [38, 39, 40]. Therefore, distinguishing between a proton and a nucleus shower is extremely difficult at the highest energies [41, 42].

Fortunately, photon and hadron primaries can be distinguished by comparing the rate of vertical to inclined showers, a technique which exploits the attenuation of the electromagnetic shower component for large slant depths. Comparing the predicted rate to the rate observed by Haverah Park for showers in the range $60^\circ < \theta < 80^\circ$, Ave et al. [43] conclude that above 10^{19} eV, less than 48% of the primary CRs can be photons and above 4×10^{19} eV less than 50% can be photons. Both of these statements are made at the 95% CL.

The longitudinal development has a well defined maximum, usually referred to as $X_{\max}$, which increases with primary energy as more cascade generations are required to degrade the secondary particle energies. Evaluating $X_{\max}$ is a fundamental part of many of the composition studies done by detecting air showers. For showers of a given total energy, heavier nuclei have smaller $X_{\max}$ because the shower is already subdivided into A nucleons when it enters the atmosphere. Specifically, the way the average depth of maximum $\langle X_{\max} \rangle$ changes with energy depends on the primary composition and particle interactions according to

$$\langle X_{\max} \rangle = D_e \ln \left(\frac{E}{E_0} \right), \tag{1}$$

where D_e is the so-called "elongation rate" and E_0 is a characteristic energy that depends on the primary composition [44]. Therefore, since $\langle X_{\max} \rangle$ and D_e can be determined directly from the longitudinal shower profiles measured with a fluorescence detector, E_0 and thus the composition, can be extracted after estimating E from the

total fluorescence yield. Indeed, the parameter often measured is D_{10}, the rate of change of $\langle X_{\rm max}\rangle$ per *decade* of energy.

Another important observable which can be related to primary energy and chemical composition is the total number of muons N_μ reaching ground level. For vertical proton showers, numerical simulations [45] indicate that the muon production is related to the energy of the primary via [16]

$$E = 1.64 \times 10^{18} \left(\frac{N_\mu^p}{10^7}\right)^{1.073} \text{ eV}. \tag{2}$$

Thus, modeling a shower produced by a nucleus with energy E_A as the collection of A proton showers, each with energy A^{-1} of the nucleus energy, leads – using Eq. (2) – to $N_\mu^A \propto A(E_A/A)^{0.93}$ [46]. Consequently, one expects a CR nucleus to produce about $A^{0.07}$ more muons than a proton. This implies that an iron nucleus produces a shower with around 30% more muons than a proton shower of the same energy.

The analysis of the elongation rate and the spread in $X_{\rm max}$ at a given energy reported by the Fly's Eye Collaboration suggests a change from an iron dominated composition at $10^{17.5}$ eV to a proton dominated composition near 10^{19} eV [47, 48]. Such behavior of D_e is in agreement with an earlier analysis from Haverah Park [49]. However, the variation of the density of muons with energy reported by the Akeno Collaboration favours a composition that remains mixed over the $10^{18} - 10^{19}$ eV decade [50]. More recently, Wibig and Wolfendale [51] reanalyzed the Fly's Eye data considering not only proton and iron components (as in [47]) but a larger number of atomic mass hypotheses. Additionally, they adopted a different hadronic model that shifts the prediction of $X_{\rm max}$ for primary protons of 10^{18} eV from 730 g cm^{-2} [47] to 751 g cm^{-2}. The difference, although apparently small, has a significant effect on the mass composition inferred from the data. The study indicates that at the highest energies ($10^{18.5} - 10^{19}$ eV and somewhat above) there is a significant fraction of primaries with charge greater than unity. This result is more in accord with the conclusions of the Akeno group than those of the Fly's Eye group. Very recently, the Volcano Ranch data was re-analyzed taking into account a bi-modal proton-iron model [52]. The best fit gives a mixture with $75 \pm 5\%$ of iron, with corresponding percentage of protons. A summary of the diferent bi-modal analyses is shown in Fig. 1. Within statistical errors and systematic uncertainties introduced by hadronic interaction models, the data seem to indicate that iron is the dominant component of CRs between $\sim 10^{17}$ eV and $\sim 10^{19}$ eV. Nonetheless, in view of the low statistics at the end of the spectrum and the wide variety of uncertainties in these experiments, one may conservatively say that this is not a closed issue.

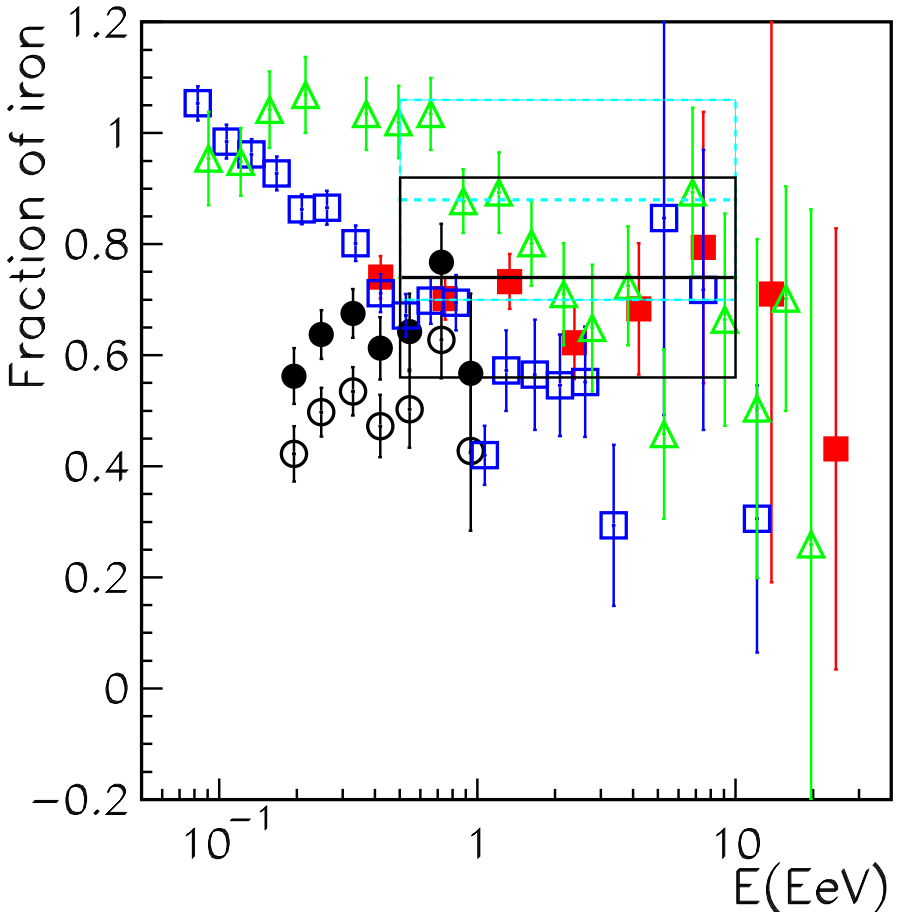

FIG. 1: Predicted fraction of iron nuclei in the CR beam at the top of the atmosphere from various experiments: Fly's Eye (△), AGASA A100 (■), AGASA A1 (□) using SIBYLL 1.5 as the hadronic interaction event generator [53] and Haverah Park [54], using QGSJET98 (●) and QGSJET01 (○) to process the hadronic collisions. The solid (dashed) line rectangle indicates the mean composition with the corresponding error estimated using the Volcano Ranch data and QGSJET98 (QGSJET01); the systematic shift in the fraction of iron induced by the hadronic event generator is 14% [55].

C. Distribution of arrival directions

The distribution of arrival directions is perhaps the most helpful observable in yielding clues about the CR origin. On the one hand, if cosmic rays cluster within a small angular region (see e.g. [56]) or show directional alignment with powerful compact objects (see e.g. [57]), one might be able to associate them with isolated sources in the sky. On the other hand, if the distribution of arrival directions exhibits a large-scale anisotropy, this could indicate whether or not certain classes of sources are associated

with large-scale structures (such as the Galactic plane or the Galactic halo).

Cosmic ray air shower detectors which experience stable operation over a period of a year or more can have a uniform exposure in right ascension, α. A traditional technique to search for large-scale anisotropies is then to fit the right ascension distribution of events to a sine wave with period $2\pi/m$ ($m^{\rm th}$ harmonic) to determine the components (x, y) of the Rayleigh vector [58]

$$x = \frac{2}{N}\sum_{i=1}^{N}\cos(m\,\alpha_i)\,, \quad y = \frac{2}{N}\sum_{i=1}^{N}\sin(m\,\alpha_i)\,. \tag{3}$$

The $m^{\rm th}$ harmonic amplitude of N measurements of α_i is given by the Rayleigh vector length $\mathcal{R} = (x^2 + y^2)^{1/2}$. The expected length of such a vector for values randomly sampled from a uniform phase distribution is $\mathcal{R}_0 = 2/\sqrt{N}$. The chance probability of obtaining an amplitude with length larger than that measured is $p(\geq \mathcal{R}) = e^{-k_0}$, where $k_0 = \mathcal{R}^2/\mathcal{R}_0^2$. To give a specific example, a vector of length $k_0 \geq 6.6$ would be required to claim an observation whose probability of arising from random fluctuation was 0.0013 (a "3σ" result) [6].

AGASA has revealed a correlation of the arrival direction of the cosmic rays to the Galactic Plane (GP) at the 4σ level [59]. The energy bin width which gives the maximum k_0-value corresponds to the region $10^{17.9}$ eV – $10^{18.3}$ eV where $k_0 = 11.1$, yielding a chance probability of $p(\geq \mathcal{R}^{\rm AGASA}_{E\sim{\rm EeV}}) \approx 1.5\times10^{-5}$. The GP excess, which is roughly 4% of the diffuse flux, is mostly concentrated in the direction of the Cygnus region, with a second spot towards the Galactic Center (GC) [60]. Evidence at the 3.2σ level for GP enhancement in a similar energy range has also been reported by the HiRes Collaboration [61]. The existence of a point-like excess in the direction of the GC has been confirmed via independent analysis [62] of data collected with SUGAR.[1] This is a remarkable level of agreement among experiments using a variety of techniques.

At lower energies ($\sim$ PeV), the Rayleigh analysis shows no evidence of anisotropy [64]. Hence, the excess from the GP is very suggestive of neutrons as candidate primaries, because the directional signal requires relatively-stable neutral primaries, and time-dilated neutrons can reach the Earth from typical Galactic distances when the neutron energy exceeds 10^{18} eV. Arguably, if the Galactic messengers are neutrons, then those with energies below 10^{18} eV will decay in flight, providing a flux of cosmic antineutrinos above 1 TeV that should be observable at kilometer-scale neutrino telescopes [65]. A measurement of the $\bar{\nu}$-flux will supply a strong confirmation of the GP neutron hypothesis.

[1] Interestingly, sub-TeV γ-ray emission from the direction of the GC has been observed using the CANGAROO-II Imaging Atmospheric Čerenkov Telescope [63].

For the ultra high energy ($\gtrsim 10^{19.6}$ eV) regime, all experiments to date have reported $k_0 \ll 6.6$, $\forall m < 5$ [66, 67, 68, 69].[2] This does not imply an isotropic distribution, but it merely means that available data are too sparse to claim a statistically significant measurement of anisotropy. In other words, there may exist anisotropies at a level too low to discern given existing statistics [70].

The right harmonic analyses are completely blind to intensity variations which depend only on declination, δ. Combining anisotropy searches in α over a range of declinations could dilute the results, since significant but out of phase Rayleigh vectors from different declination bands can cancel each other out. Moreover, the analysis methods that consider distributions in one celestial coordinate, while integrating away the second, have proved to be potentially misleading [71]. An unambiguous interpretation of anisotropy data requires two ingredients: *exposure to the full celestial sphere and analysis in terms of both celestial coordinates.* In this direction, a recent study [72] of the angular power spectrum of the distribution of arrival directions of CRs with energy $> 10^{19.6}$ eV, as seen by the AGASA and SUGAR experiments, shows no departures from either homogeneity or isotropy on an angular scale greater than 10°. Finally, the recently analyzed HiRes data is also statistically consistent with an isotropic distribution [73].

All in all, the simplest interpretation of the existing data is that, beyond the ankle, a new population of extragalactic CRs emerges to dominate the more steeply falling Galactic population. Moreover, there are two extreme explanations for the near observed isotropy beyond $10^{19.6}$ eV: one is to argue a cosmological origin for these events, and the other is that we have nearby sources (say, within the Local Supercluster) with a tangled magnetic field in the Galaxy, and beyond, which bends the particle orbits, camouflaging the exact location of the sources.

Although there seems to be a remarkable agreement among experiment on predictions about isotropy on large scale structure, this is certainly not the case when considering the two-point correlation function on a small angular scale. The analyses carried out by AGASA Collaboration seem to indicate that the pairing of events on the celestial sky could be occurring at higher than chance coincidence [56, 74]. Specifically, when showers with separation angle less than the angular resolution $\theta_{\rm min} = 2.5^\circ$ are paired up, AGASA finds five doublets and one triplet among the 58 events reported with mean energy above $10^{19.6}$ eV. The probability of observing these clusters by chance coincidence under an isotropic distribution was quoted as smaller than 1%. A third

[2] For the Fly's Eye data-sample the Rayleigh vector was computed using weighted showers, because it has had a nonuniform exposure in sideral time. A shower's weight depends on the hour of its sideral arrival time, and the 24 different weights are such that every time bin has the same weighted number of showers.

independent analysis [75], using the Goldberg–Weiler formalism [76], confirmed the result reported by AGASA Collaboration and further showed that the chance probability is extremely sensitive to the angular binning. The "world" data set has also been studied [77]. Six doublets and two triplets out of 92 events with energies $> 10^{19.6}$ eV were found, with the chance probability being less than 1% in the restricted region within $\pm 10^{\circ}$ of the super-Galactic plane. The angular two-point correlation function of a combined data sample of AGASA ($E > 4.8 \times 10^{19}$ eV) and Yakutsk ($E > 2.4 \times 10^{19}$ eV) was analyzed [78]. For a uniform distribution of sources, the probability of chance clustering is reported to be as small as 4×10^{-6}. Far from confirming what seemed a fascinating discovery, the recent analysis reported by the HiRes Collaboration showed that the data is consistent with no small-scale anisotropy among the highest energy events [79, 80].

The discovery of such clusters would be a tremendous breakthrough for the field, but the case for them is not yet proven. To calculate a meaningful statistical significance in such an analysis, it is important to define the search procedure *a priori* in order to ensure it is not inadvertently devised especially to suit the particular data set after having studied it. In the analyses carried out by AGASA Collaboration [56, 74], for instance, the angular bin size was not defined ahead of time. Very recently, with the aim to avoid accidental bias on the number of trials performed in selecting the angular bin, the original claim of AGASA Collaboration [56] was re-examined considering only the events observed after the claim [81]. This study showed that the evidence for clustering in the AGASA data set is weaker than was previously claimed, and consistent with the null hypothesis of isotropically distributed arrival directions.

Summing up, the clustering on small angular scale at the upper end of the spectrum remains an open question, and the increase in statistics and improved resolution attainable with PAO is awaited to solve the issue.

D. Propagation of UHECRs

In this section we briefly summarize the relevant interactions that CRs suffer on their trip to Earth. For a more detailed discussion the reader is refer to [1, 82, 83, 84, 85].

1. The GZK-cutoff

Ever since the discovery of the cosmic microwave background (CMB) standard physics implies there would be a cuttoff in the observed CR-spectrum. In the mid-60's Greisen, Zatsepin, and Kuzmin (GZK) [86, 87] pointed out that this photonic molasses makes the universe opaque to protons of sufficiently high energy, i.e., protons

with energies beyond the photopion production threshold,

$$E^{\rm th}_{p\gamma_{\rm CMB}} = \frac{m_\pi\,(m_p + m_\pi/2)}{\mathcal{E}_{\rm CMB}} \approx 6.8\times 10^{19}\,\left(\frac{\mathcal{E}_{\rm CMB}}{10^{-3}\ {\rm eV}}\right)^{-1}\ {\rm eV}\,, \tag{4}$$

where m_p (m_π) denotes the proton (pion) mass and $\mathcal{E}_{\rm CMB} \sim 10^{-3}$ eV is a typical CMB photon energy. After pion production, the proton (or perhaps, instead, a neutron) emerges with at least 50% of the incoming energy. This implies that the nucleon energy changes by an e-folding after a propagation distance $\lesssim (\sigma_{p\gamma}\, n_\gamma\, y)^{-1} \sim 15$ Mpc. Here, $n_\gamma \approx 410$ cm^{-3} is the number density of the CMB photons, $\sigma_{p\gamma} > 0.1$ mb is the photopion production cross section, and y is the average energy fraction (in the laboratory system) lost by a nucleon per interaction. Energy losses due to pair production become relevant below $\sim 10^{19}$ eV. For heavy nuclei, the giant dipole resonance can be excited at similar total energies and hence, for example, iron nuclei do not survive fragmentation over comparable distances. Additionally, the survival probability for extremely high energy ($\approx 10^{20}$ eV) γ-rays (propagating on magnetic fields $\gg 10^{-11}$ G) to a distance d, $p(>d) \approx \exp[-d/6.6\ {\rm Mpc}]$, becomes less than 10^{-4} after traversing a distance of 50 Mpc.[3]

In recent years, several studies on the propagation of CRs (including both analytical analyses and numerical simulations) have been carried out [89, 90, 91, 92, 93, 94, 95, 96, 97, 98, 99, 100, 101, 102, 103, 104, 105, 106, 107, 108, 109, 110]. A summary of the UHECR attenuation lengths for the above mentioned processes (as derived in these analyses) is given in Fig. 2. It is easily seen that our horizon shrinks dramatically for energies $\gtrsim 10^{20}$ eV. Therefore, if UHECRs originate at cosmological distances, the net effect of their interactions would yield a pile-up of particles around $4-5\times 10^{19}$ eV with the spectrum droping sharply thereafter. As one can infer from Fig. 2, the subtleties of the spectral shape depend on the nature of the primary species, yielding some ambiguity in the precise definition of the "GZK cutoff". In what follows we consider an event to supersed the cutoff if the lower energy limit at the 95% CL exceeds 7×10^{19} eV. This conforms closely to the strong criteria outlined in Ref. [111].

2. Propagation of CRs in a magnetized neighborhood of the Galaxy

In addition to the interactions with the radiation fields permeating the universe, CRs suffer deflections on extragalactic and Galactic magnetic fields.

Over the last few years, it has become evident that the observed near-isotropy of arrival directions can be easily explained if our Local Supercluster contains a large

[3] It should be stressed that if the extragalactic magnetic field is $< 10^{-12}$ G, photons with energy $\gg 10^{21}$ eV can reach us without significant energy loss from distant (redshift $z \gtrsim 0.03$) sources [88].

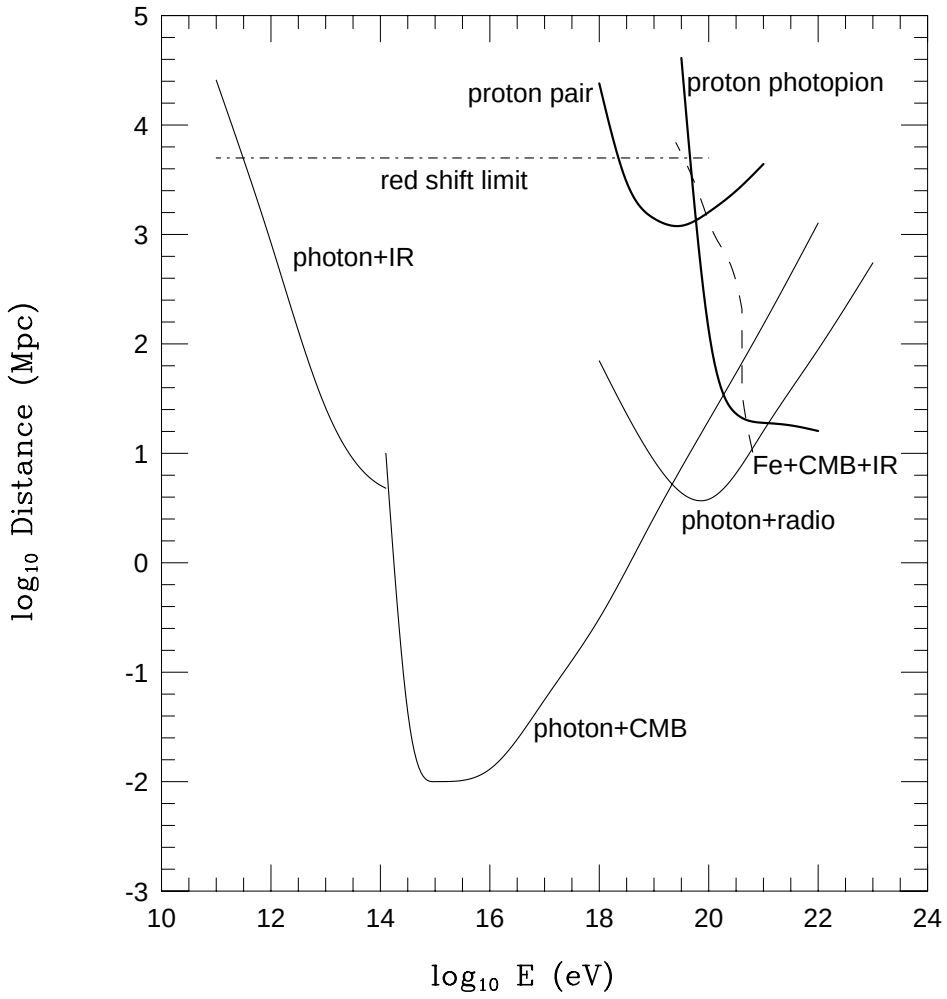

FIG. 2: Attenuation length of γ's, p's, and ^{56}Fe's in various background radiations as a function of energy. The 3 lowest and left-most thin solid curves refer to γ-rays, showing the attenuation by infra-red, microwave, and radio backgrounds. The upper, right-most thick solid curves refer to propagation of protons in the CMB, showing separately the effect of pair production and photopion production. The dashed-dotted line indicates the adiabatic fractional energy loss at the present cosmological epoch (see e.g. Appendix B of Ref. [1]). The dashed curve illustrates the attenuation of iron nuclei.

scale magnetic field which provides sufficient bending to the CR trajectories [112, 113]. Intergalactic field strengths and coherence lengths are not well established, but it is plausible to assume that fields have coherent directions on scales $\ell \approx 0.5 - 1$ Mpc. The Larmor radius of a CR of charge Ze propagating in a magnetic field $B_{\rm nG} \equiv B/10^{-9}$ G is given by

$$r_{\rm L} \approx \frac{100\ E_{20}}{Z\ B_{\rm nG}}\ {\rm Mpc}\ , \tag{5}$$

where E_{20} is the particle's energy in units of 10^{20} eV. For $r_{\rm L} \gg \ell$ the motion is not very different from a quasilinear trajectory, with small deflections away from the straight line path given by

$$\theta(E) \approx 0.3^\circ \, \frac{L_{\rm Mpc}\, Z\, B_{\rm nG}}{E_{20}}\,, \tag{6}$$

where $L_{\rm Mpc}$ is the propagation distance in units of Mpc. As the Larmor radius starts approaching ℓ the particles begin to diffuse.

Diffusion has two distinctive regimes. Particles that are trapped inside magnetic subdomains (of size $\ell_{\rm Mpc} \equiv \ell/{\rm Mpc}$) follow Kolmogorov diffusion. In such a case, the functional dependence of energy of the difussion coefficient is found to be [114]

$$D(E) \approx 0.0048 \left(\frac{E_{20}\, \ell^2_{\rm Mpc}}{Z\, B_{\rm nG}}\right)^{1/3} \ {\rm Mpc}^2/{\rm Myr}\,. \tag{7}$$

With rising energy, $r_{\rm L} \to \ell$, and there is a transition to Bohm diffusion. The diffusion coefficient in this regime is of order the Larmor radius times velocity ($\sim c$) [115]. In this case the accumulated deflection angle from the direction of the source, can be estimated assuming that the particles make a random walk in the magnetic field [116]

$$\theta(E) \approx 0.54^\circ \, \frac{\ell^{1/2}_{\rm Mpc}\, L^{1/2}_{\rm Mpc}\, Z\, B_{\rm nG}}{E_{20}}\,. \tag{8}$$

Surprisingly little is actually known about the extragalactic magnetic field strength. There are some measurements of diffuse radio emission from the bridge area between Coma and Abell superclusters that under assumptions of equipartition allows an estimate of $0.2 - 0.6$ μG for the magnetic field in this region [117].[4] Such a strong magnetic field (which is compatible with existing upper limits on Faraday rotation measurements [119]) could be possibly understood if the bridge region lies along a filament or sheet of large scale structures [120]. Faraday rotation measurements [119, 121] have thus far served to set upper bounds of $\mathcal{O}(10^{-9} - 10^{-8})$ G on extragalactic magnetic fields on various scales [119, 122], as have the limits on distortion of the CMB [123, 124]. The Faraday rotation measurements sample extragalactic field strengths of any origin out to quasar distances, while the CMB analyses set limits on primordial magnetic fields. Finally, there are some hints suggesting that the extragalactic field strength can be increased in the neighborhood of the Milky Way, $B_{\rm nG} > 10$ [125]. Now, using Eq. (5), one can easily see that because of the large uncertainty on the magnetic field strength, $\mathcal{O}({\rm nG}) - \mathcal{O}(\mu{\rm G})$, all 3 different regimes discussed above are likely to describe UHECR propagation.

[4] Fields of $\mathcal{O}(\mu{\rm G})$ are also indicated in a more extensive study of 16 low redshift clusters [118].

If CRs propagate diffusively, the radius of the sphere for potential proton sources becomes significantly reduced. This is because one expects negligible contribution to the flux from times prior to the arrival time of the diffusion front, and so the average time delay in the low energy region, $\tau_{\rm delay} \approx d^2/[4D(E)]$, must be smaller than the age of the source, or else the age of the universe (if no source within the GZK radius is active today, but such sources have been active in the past). Note that the diffuse propagation of UHE protons requires magnetic fields $\sim 1\mu$G. Therefore, for typical coherence lengths of extragalactic magnetic fields the time delay of CRs with $E \approx 10^{18.7}$ eV cannot exceed $\tau_{\rm delay} \lesssim 14$ Gyr, yielding a radius of $d \sim 30$ Mpc. In the case CR sources are active today, the radius for potential sources is even smaller $d \sim 5$ Mpc.

On the other hand, the sphere of potential nucleus-emitting-sources is severely constrained by the GZK cutoff: straightforward calculation, using the attenuation length given in Fig. 2, shows that less than 1% of iron nuclei (or any surviving fragment of their spallations) can survive more than 3×10^{14} s with an energy $\gtrsim 10^{20.5}$ eV. Therefore, the assumption that UHECRs are heavy nuclei implies ordered extragalactic magnetic fields $B_{\rm nG} \lesssim 15 - 20$, or else nuclei would be trapped inside magnetic subdomains suffering catastrophic spallations.

The large scale structure of the Galactic magnetic field carries substantial uncertainties as well, because the position of the solar system does not allow global measurements. The average field strength can be directly determined from pulsar observations of the rotation and dispersion measures average along the line of sight to the pulsar with a weigh proportional to the local free electron density, $\langle B_{||} \rangle \approx 2\mu$G [126, 127, 128, 129].(We use the standard, though ambiguous notation, in which B refers to either the Galactic or extragalactic magnetic field, depending on the context.) Measurements of polarized synchrotron radiation as well as Faraday rotation of the radiation emitted from pulsars and extragalactic radio sources revealed that the global structure of the magnetic field in the disk of our Galaxy could be well described by spiral fields with 2π (axisymmetric, ASS) or π (bisymmetric, BSS) symmetry [130]. In the direction perpendicular to the Galactic plane the fields are either symmetric (S) or antisymmetric (A). Discrimination between these models is complicated. Field reversals are certainly observed (in the Crux-Scutum arm at 5.5 kpc from the Galactic center, the Carina-Sagittarius arm at 6.5 kpc, the Perseus arm at 10 kpc, and possibly another beyond [131]). However, as discussed by Vallée [132], turbulent dynamo theory can explain field reversals at distances up to ~ 15 kpc within the ASS configuration.

More accurately, the field strength in the Galactic plane ($z = 0$) for the ASS model is generally described by [133, 134]

$$B(\rho, \theta) = B_0(\rho)\, \cos^2[\,\theta - \beta \ln(\rho/\xi_0)]\,, \tag{9}$$

and for the BSS

$$B(\rho,\theta) = B_0(\rho)\,\cos[\,\theta - \beta\ln(\rho/\xi_0)]\,, \tag{10}$$

where θ is the azimuthal coordinate around the Galactic center (clockwise as seen from the north Galactic pole), ρ is the galactocentric radial cylindrical coordinate, and

$$B_0(\rho) = \frac{3r_0}{\rho}\tanh^3(\rho/\rho_1)\ \ \mu\mathrm{G}\,. \tag{11}$$

Here, $\xi_0 = 10.55$ kpc stands for the galactocentric distance of the maximum of the field in our spiral arm, $\beta = 1/\tan p$ (with the pitch angle, $p = -10^\circ$), $r_0 = 8.5$ kpc is the Sun's distance to the Galactic center, and $\rho_1 = 2$ kpc. The θ and ρ coordinates of the field are correspondingly,

$$B_\theta = B(\rho,\,\theta)\,\cos p\ , \qquad B_\rho = B(\rho,\theta)\,\sin p\,. \tag{12}$$

The field strength above and below the Galactic plane (i.e., the dependence on z) has a contribution coming from the disk and another from the halo: *(i)* for A models

$$B_{\rm A}(\rho,\theta,z) = B(\rho,\theta)\ \tanh(z/z_3)\,\left(\frac{1}{2\cosh(z/z_1)} + \frac{1}{2\cosh(z/z_2)}\right)\ , \tag{13}$$

(ii) for S models, $B_{\rm S} = B_{\rm A}(\rho,\theta,z)/\tanh(z/z_3)$; where $z_1 = 0.3$ kpc, $z_2 = 4$ kpc and $z_3 = 20$ pc. With this in mind, the Galactic magnetic field produce significant bending to the CR orbits if $E_{20}/Z = 0.03$ [134].

E. GZK-end of the cosmic ray spectrum?

A first hint of a puzzle surfaced in the highest energy Fly's Eye event [135] which has no apparent progenitor within the Local Supercluster [136]. Subsequent observations with the AGASA experiment [137] carried strong indication that the cutoff was somehow circumvented in the absence of plausible nearby sources.

The big disappointment of 2002 was the CR-flux reported by the HiRes Collaboration [138, 139], which is in sharp disagreement with AGASA data [140]. The discrepancy between the two estimated fluxes is shown in Fig. 3. One can argue correctly that the statistical significance of the discrepancy is small, although such an assesment requires a conspiracy between the two groups to bend their maximal systematic errors in opposite directions. Moreover, an analysis [143] of the combined data reported by the HiRes, the Fly's Eye, and the Yakutsk collaborations is supportive of the existence of the GZK cutoff at the $> 5\sigma$ ($> 3.7\sigma$) level. The deviation from GZK depends on the set of data used as a basis for power law extrapolation from lower energies. An additional input for this analysis was the recent claim [144] that there may be technical

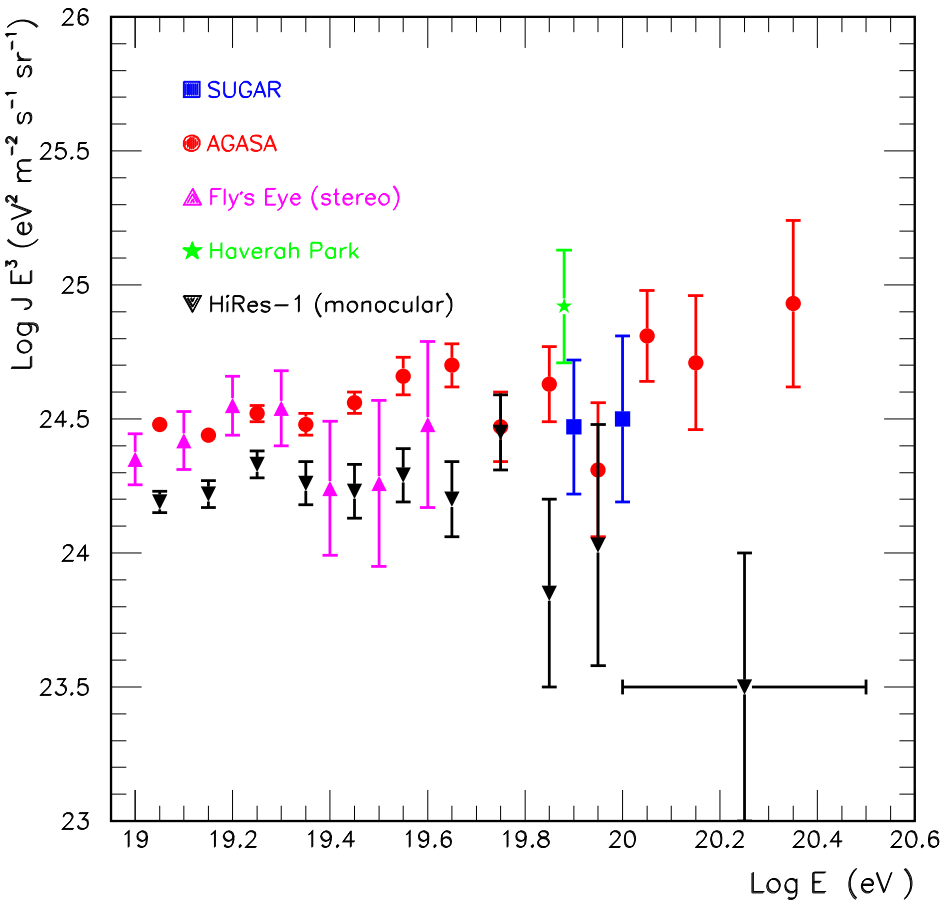

FIG. 3: Upper end of the cosmic ray energy spectrum as observed by AGASA [140], Fly's Eye[141], Haverah Park [142], HiRes [139], and SUGAR [46].

problems with the Yakutsk data collection. More recently, fingerprints of super-GZK CRs have been found [46] by reanalyzing the SUGAR data [16]. However, as one can see in Fig. 3, the number of events is not enough to weight in on one side or the other with respect to the GZK question.

II. VANILLA SKY: UHECR GENERATION WITHIN THE STANDARD LORE

A. A brief low energy perspective

Supernova remnants (SNRs) are thought to be the main source of both CR ions and electrons with energies below the knee. The particle acceleration mechanism in individual SNRs is usually assumed to be diffusive shock acceleration, which naturally

leads to a power-law population of relativistic particles. In the standard version of this mechanism (e.g. [145]), particles are scattered by magnetohydrodynamic waves repeatedly through the shock front. If they encounter an enhancement of molecular density, the pion channel can lead to observable amounts of γ-rays (see Ref. [146] for a review, and references therein for details). Electrons suffer synchrotron losses, producing the non-thermal emission from radio to X-rays usually seen in shell-type SNRs. The maximum energy achieved depends on the shock speed and age as well as on any competing loss processes. In young SNRs, electrons can easily reach energies in excess of 1 TeV, where they produce X-rays by synchrotron mechanism (see, for example, [147, 148]).

CRs of low energies are also expected to be accelerated in OB associations, through turbulent motions and collective effects of star winds (e.g. [149, 150]). The main acceleration region for TeV particles would be in the outer boundary of the supperbubble produced by the core of a given stellar association. If there is a subgroup of stars located at the acceleration region, their winds might be illuminated by the locally accelerated protons, which would have a distribution with a slope close to the canonical value, $\alpha \sim 2$, and produce detectable γ-rays [151]. The HEGRA detection in the vicinity of Cygnus OB2, TeV J2032+4131 [152], could be, judging from multiwavelength observations [153], the result of such a process [151]. A nearby EGRET source (3EG J2033+4118) has also a likely stellar origin [154, 155, 156].

Truth is, as always, bitter. No astrophysical source of UHECRs, nor of CRs with energies below the knee, has been ever confirmed. Out of all SNRs coinciding with non-variable γ-ray sources detected by EGRET [157, 158, 159, 160], the supernova remnant RX J1713.7-3946 is perhaps one the most convincing cases for a hadronic cosmic-ray accelerator detected so far in the Galaxy, although yet subject to confirmation [161, 162, 163, 164, 165]. Other excellent candidates include SN1006 (e.g. [166]) and Cas A (e.g. [167]). Kilometer-scale neutrino telescopes have also been proposed as viable detectors of hadronic CR sources (e.g. [168, 169, 170, 171]), and will be a welcomed addition to the space- and ground-based detectors already existing or planned.

B. Plausible sources of UHECRs and the Hillas' plot

Following the main ideas behind the concept of Fermi's first order acceleration, when $r_{\rm L}$ approaches the accelerator size, it becomes very difficult to magnetically confine the CR to the acceleration region, and thus to continue the accelerating process up to higher energies. If one includes the effect of the characteristic velocity βc of the magnetic

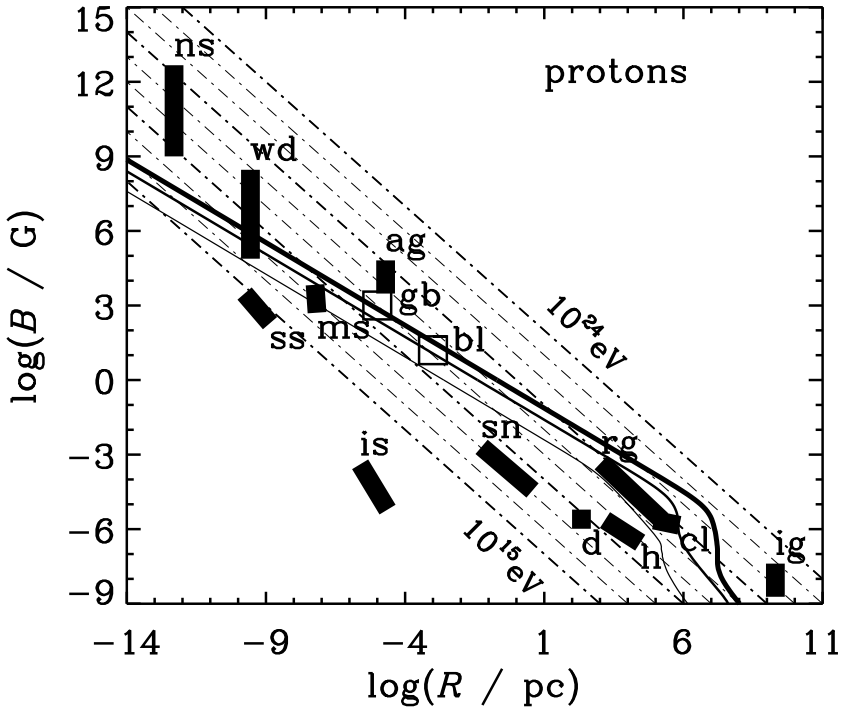

FIG. 4: The Hillas diagram showing (chain curves) magnetic field versus gyroradius for proton momenta 10^{15}, 10^{16}, $\ldots$, 10^{24} eV/c. The solid curves correspond to different shock-waves velocities: the upper solid curve indicates the maximum attainable energy $\beta = 1$, the middle and lower solid curves indicate plausible less effective acceleration processes. Typical size and magnetic field of possible acceleration sites are shown for neutron stars (ns), white dwarfs (wd), sunspots (ss), magnetic stars (ms), active galactic nuclei (ag), interstellar space (is), SNRs (sn), radio galaxy lobes (rg), galactic disk (d) and halo (h), clusters of galaxies (cl) and intergalactic medium (ig). Typical jet-frame parameters of the synchrotron proton blazar model [174] and gamma ray burst model [175] are indicated by open squares labeled "bl" and "gb", respectively [176].

scattering centers[5], the above argument leads to the general condition (sometimes called the "Hillas criterion" [172]),

$$E_{\max} \sim 2\beta\, c\, Ze\, B\, r_{\rm L}\,, \tag{14}$$

for the maximum energy acquired by a particle travelling in a medium with magnetic field B.

[5] The size of the accelerating region containing the magnetic field should be as large as $2r_{\rm L}$. Taking into account a characteristic velocity βc of the scattering centers this transforms into $2r_{\rm L}/\beta$.

In the case of one-shot acceleration scenarios, the maximum reachable energy turns out to have a quite similar expression to the shock acceleration case of Eq. (14). For instance, a dimensional analysis suggests that the maximum energy that can be obtained from a pulsar is [172]

$$E_{\max} = \frac{\omega}{c} Ze\, B_s\, R_s^2\,, \tag{15}$$

where ω is the pulsar angular velocity, B_s the surface magnetic field and R_s the neutron star radius. Therefore, if $B_s \sim 10^{12}$ G, $R_s \sim 10$ km, and $\omega \sim 60\pi$ s^{-1} (as for the Crab pulsar), a circuit connected between pole and equator would see an emf $\sim 10^{18}$ V for an aligned or oblique dipole. When realistic models of acceleration are constructed, however, this ideal dimensional limit is not fully realized, because the large potential drop along the magnetic field lines is significantly short-circuited by electron and positrons moving in opposite directions along the field lines [173].

The dimensional arguments of Eqs. (14) and (15) are conveniently depicted in the "Hillas diagram" [172] shown in Fig. 4. Very few sites can generate particles with energies $> 10^{20}$ eV: either this occurs on highly condensed objects with huge B or enormously extended objects. Some of these potential astrophysical sources are discussed in what follows. For further details on the electrodynamical limitations of CR sources see, e.g. [177, 178].

C. Neutron stars

1. Magnetohydronamic acceleration of iron nuclei in pulsars

Following earlier ideas [179][6], Blasi et al. [182] [7] have shown that young magnetized neutron stars in our own Galaxy may be one such astrophysical system that satisfies the Hillas' criterion.

Neutron stars –endpoints of stellar evolution– begin their life rotating rapidly ($\Omega \sim 3000$ rad s^{-1}) and with large surface magnetic fields ($B_S \gtrsim 10^{13}$ G). The dipole component decreases as the cube of the distance from the star's surface $B(r) = B_S(R_S/r)^3$, where the radius of the star is $R_S \simeq L$. At the light cylinder $R_{lc} = c/\Omega \sim 10^7 \Omega_{3k}^{-1}$ cm, where $\Omega_{3k} \equiv \Omega/3000$ rad s^{-1}, the dipole field cannot be casually maintained, the field is mostly azimuthal, with field lines spiraling outwards [187]. Inside the light cylinder,

[6] Even earlier ideas relating UHECRs with neutron stars can be found in Refs. [180, 181], although these attempts have failed at either reaching the highest energies, or reproducing the spectrum, or reproducing the apparent isotropy of the arrival directions of UHECRs.

[7] See [183, 184], also [185], for related research. See [186] for yet another model of UHECR generation in neutron stars, involving planetoid impacts.

the magnetosphere corotates with the star, and the density of material (mostly iron peak elements formed during the supernova event that were stripped off the surface due to strong electric fields) has the Goldreich-Julian value, $n_{GJ}(r) = B(r)\Omega/(4\pi Zec)$, where c is the speed of light [188]. The behavior of the plasma outside the light cylinder is still not yet fully understood [189, 190, 191, 192], although some analytical and numerical studies show the development of kinetically dominated relativistic winds (see e.g., [190]).

Blasi et al. [182] assumed that the magnetic field in the wind zone decreases as $B(r) \lesssim B_{lc}R_{lc}/r$. For surface fields of $B_S \equiv 10^{13}\, B_{13}$ G, the field at the light cylinder is $B_{lc} = 10^{10}\, B_{13}\Omega_{3k}^3$ G. The maximum energy of particles that can be contained in the wind near the light cylinder is

$$E_{\rm max} = \frac{ZeB_{\rm lc}R_{\rm lc}}{c} \simeq 8 \times 10^{20}\, Z_{26} B_{13}\Omega_{3k}^2\, {\rm eV}\ , \tag{16}$$

where $Z_{26} \equiv Z/26$. The typical energy of the accelerated CRs, $E_{\rm cr}$, can be estimated by considering the magnetic energy per ion at the light cylinder $E_{\rm cr} \simeq B_{lc}^2/8\pi n_{\rm GJ}$. At the light cylinder $n_{\rm GJ} = 1.7 \times 10^{11}\, B_{13}\Omega_{3k}^4/Z\, {\rm cm}^{-3}$ which gives

$$E_{\rm cr} \simeq 4 \times 10^{20}\, Z_{26} B_{13}\Omega_{3k}^2\, {\rm eV}\ . \tag{17}$$

In this model, as the star spins down, the energy of the cosmic ray particles ejected with the wind decreases. The total fluence of UHECRs between energy E and $E + dE$ is

$$N(E)dE = \frac{\dot{\mathcal{N}}}{\dot{\Omega}}\, \frac{d\Omega}{dE}\, dE\ , \tag{18}$$

where the particle luminosity is

$$\dot{\mathcal{N}} = \xi\, n_{GJ}\, \pi R_{lc}^2 c = 6 \times 10^{34} \xi \frac{B_{13}\Omega_{3k}^2}{Z_{26}}\, {\rm s}^{-1} \tag{19}$$

and $\xi < 1$ is the efficiency for accelerating particles at the light cylinder. For a spin down rate dominated by magnetic dipole radiation, given by $I\Omega\dot{\Omega} = -B_S^2 R_S^6 \Omega^4/6c^3$ where $I = 10^{45}$ g cm^2 is the moment of inertia, the time derivative of the spin frequency is $\dot{\Omega} = 1.7 \times 10^{-5} B_{13}^2 \Omega_{3k}^3\, {\rm s}^{-1}$, and Eq. (17) gives

$$\frac{dE}{d\Omega} = 1.7 \times 10^{-3}\ \frac{E}{\Omega_{3k}}\ . \tag{20}$$

Substituting in Eq. (18), the particle spectrum from each neutron star is

$$N(E) = \xi \frac{5.5 \times 10^{31}}{B_{13} E_{20} Z_{26}} {\rm GeV}^{-1}\ . \tag{21}$$

Taking the confining volume for these particles to be V_c and the lifetime for confinement to be t_c, the UHECR density is $n(E) = \epsilon N(E) t_c/\tau V_c$, and the flux at the surface of the Earth is $F(E) = n(E)c/4$. For a characteristic confinement dimension of $R = 10\ R_1$ kpc, $V_c = 4\pi R^3/3$ and $t_c = QR/c$, where $Q > 1$ is a measure of the how well the UHECR are trapped. With this in mind, the predicted UHECR flux at the Earth is [182][8]

$$F(E) = 10^{-24} \frac{\xi \epsilon Q}{\tau_2 R_1^2 B_{13} E_{20} Z_{26}} \, \mathrm{GeV}^{-1} \mathrm{cm}^{-2} \mathrm{s}^{-1} \quad . \tag{22}$$

Here, the fact that neutron stars are produced in our Galaxy at a rate $1/\tau$, where $\tau \equiv 100\, \tau_2$ yr, but that not all them (but rather only a fraction ϵ) have the required magnetic fields, initial spin rates and magnetic field geometry to allow efficient conversion of magnetic energy into kinetic energy of the flow, was taken into account. By comparing with observations, the required efficiency factor, $\xi\epsilon$, can be estimated, and it only needs to be $\xi\epsilon \gtrsim 4 \times 10^{-6} Q^{-1}$.

The condition that a young neutron star could produce the UHECRs[9] is that E_{cr} exceeds the needed energy when the envelope becomes transparent (i.e. before the spinning rate of the neutron star decreases to the level where the star is unable to emit particles of the necessary energy), $E_{cr}(t_{tr}) > 10^{20} E_{20}$ eV. This translates into the following condition [182][10]

$$\Omega_i > \frac{3000\, \mathrm{s}^{-1}}{B_{13}^{1/2} \left[4 Z_{26} E_{20}^{-1} - 0.13 M_1 B_{13} \mathcal{E}_{51}^{-1/2} \right]^{1/2}} \, . \tag{23}$$

Eq. (23) translates in turn into upper bounds on the surface magnetic field strength and the star initial spin period $P_i = 2\pi/\omega_i$,

$$B_{13} < \frac{31\, Z_{26}\, E_{51}^{1/2}}{M_1\, E_{20}} \, , \tag{24}$$

[8] Note that the predicted spectrum of Eq. (22) is very flat, $\gamma = 1$, which would agree only with the lower end of the plausible range of γ observed at ultra-high energies. Propagation effects can produce an energy dependence of the confinement parameter Q and, correspondingly, a steepening of the spectrum toward the middle of the observed range $1 \lesssim \gamma \lesssim 2$.

[9] The gyroradius of these UHECRs in a Galactic field of μG strength is considerably less than the typical distance to a young neutron star (~ 8 kpc). Since the iron arrival distribution at 10^{20} eV probes similar trajectories to protons at a few times 10^{18} eV, Galactic iron nuclei would show a nearly isotropic distribution with a slight correlation with the Galactic center and disk, at higher energies.

[10] A supernova that imparts $E_{SN} = 10^{51} \mathcal{E}_{51}$ erg to the stellar envelope of mass $M_{env} = 10\ M_1\ \mathrm{M}_\odot$ is considered. Also, that the condition for iron nuclei to traverse the supernova envelope without significant losses is that $\Sigma \lesssim 100$ g cm^{-2} [193].

and

$$P_i < 8\pi B_{13}^{1/2}\, Z_{26}\, E_{20}^{-1}\,. \tag{25}$$

For $M_1 = 2$ and $E_{20} = E_{51} = Z_{26} = 1$, Eq (24) gives $B_{13} < 15.4$, whereas Eq. (25) leads to $P_i \lesssim 10$ ms, not very restrictive values for a young neutron star, see for example the Parkes Multibeam Pulsar Survey.[11]

2. Magnetars

Magnetars, neutron stars with surface dipole fields on the order of 10^{15} G [197, 198, 199, 200, 201], were also proposed as plausible sites for the generation of UHECRs [202]. Assuming that they occur in all galaxies which form massive stars (then avoiding the large-distance GZK problem), and that the UHECR are arriving from outside our own Galaxy, the luminous infrared galaxies are preferred sites to search for a magnetar origin of CRs (see [203] and below the discussion in Section II G).

The magnetar model for the acceleration of UHECRs proposed by Arons [202] is a variant of that using neutron stars outlined in the previous Section. The theory predicts an injection of charged particles with maximum energy

$$E_{\rm max} = Ze\Phi_{\rm i} = Ze\frac{B_*\Omega_{\rm i}^2}{R_*^3 c^2} = 3\times 10^{22} Z B_{15}\Omega_4^2 \text{ eV}, \tag{26}$$

where B_* is a magnetar's surface magnetic field, $B_{15} = B_*/(10^{15}$ G), $\Omega_{\rm i} = 10^4\Omega_4$ s^{-1} is the initial angular velocity of the neutron star, R_* is the stellar radius, and c is the speed of light. The initial rotation period is $P_i = 0.64/\Omega_4$ ms (if $Z = 1-2$, one requires $P_{\rm i} < 2-3$ ms for the model to be viable).

The ions actually gain their energy in the relativistic wind electromagnetically expelled from the neutron star at distances r larger than the radii of the star and its magnetosphere. This avoids catastrophic radiation losses; the electric potential in the wind is $rE = rB = \Phi$. As the star spins down, as in the model by Blasi et al., the voltage and the maximum particle energies decline. Summing over the formation and spindown event, one finds a per event injection spectrum proportional to $f(E) = E^{-1}[1 + (E/E_{\rm g})]^{-1}$ for $E < E_{\rm max}$. Here $E_{\rm g}$ measures the importance of gravitational wave losses (calculated for a star with static non-axisymmetric quadrupole

[11] The Parkes multibeam pulsar survey is a large-scale survey of a narrow strip of the inner Galactic plane ($|b| < 5°$, $260° < l < 50°$, see [194] and references therein). It has much greater sensitivity than any previous survey to young and distant pulsars along the Galactic plane, and it has resulted in the detection of many previously unknown young pulsars, potentially counterparts of unidentified γ-ray sources, e.g. [195, 196].

asymmetry) in spinning the star down. When they exert torques larger than the electromagnetic torque, the star spends less time at the fastest rotation rates (i.e. less time accelerating the highest energy particles), thus causing a steepening in the spectral slope at the highest energies. If the star has an internal magnetic field even stronger than the already large surface field, equatorial ellipticities $\epsilon_{\rm e}$ in excess of 10^{-3} can exist, in which case $E_{\rm g}$ would be less than $E_{\rm max}$. Three cases of energy loss due to gravitational radiation (GR) were considered in the model: no GR loss ($\epsilon_{\rm e} = 0, E_{\rm g} = \infty$); moderate GR loss ($\epsilon_{\rm e} = 0.01, E_{\rm g} = 3 \times 10^{20}$ eV); strong GR loss ($\epsilon_{\rm e} = 0.1, E_{\rm g} = 3 \times 10^{18}$ eV). If one assumes that all magnetars have exactly the same starting voltage ($10^{22.5}$ V), then the model predicts that the spectrum $E^3 J(E)$ should rise with E above the energy $E_g = 2.8 \times 10^{20}$ eV, where the GZK loss rate becomes approximately energy independent (unless the gravitational wave losses are large) [202]. This prediction will certainly be testable with the Pierre Auger Observatory.

The total number of particles injected per event is

$$N_{\rm i} \approx 2 \frac{c^2 R_*^3 I}{ZeB_*} \approx \frac{10^{43}}{ZB_{15}}, \tag{27}$$

for a stellar radius of 10 km and a moment of inertia $I = 10^{45}$ cgs. The rate at which galaxies inject UHECR into the universe in this model then is $\dot{n}_{\rm cr} = \nu_{\rm mag}^{\rm fast} N_{\rm i} n_{\rm galaxy}$, where $n_{\rm galaxy} \approx 0.02$ Mpc^{-3} [204], $N_{\rm i}$ is given by Eq. (27), and $\nu_{\rm mag}^{\rm fast}$ is the birth rate of rapidly rotating magnetars per galaxy. Multiplication of the source spectrum $q(E) \propto \dot{n}_{\rm cr} f(E)$ by the energy dependent GZK loss time yields a spectrum received at the Earth in reasonable accord with the existing observations of UHECR if $\nu_{\rm mag}^{\rm fast} \approx 10^{-5}$ yr^{-1} [202]. That fast magnetar birth rate lies between 1% and 10% of the total magnetar birth rate inferred for our galaxy, and about 0.1% of the total core collapse supernova rate in average star forming galaxy, $\sim 10^{-2}$ yr^{-1} [205].

3. UHECRs from a pulsar in Cygnus OB2?

As discussed in Sec. II A, some evidence may be emerging for a CR accelerator in the Cygnus spiral arm. The HEGRA experiment has detected an extended TeV γ-ray source in the Cygnus region with no clear counterpart and a spectrum not easily accommodated with leptonic radiation [152]. The difficulty in accommodating the spectrum by conventional electromagnetic mechanisms has been exacerbated by the failure of Chandra and VLA to detect significant levels of X-rays or radiowaves signaling acceleration of any electrons [153]. Especially intriguing is the possible association of this source with part of Cygnus OB2 itself [151], a cluster of several thousands young, hot OB stars with a total mass of $\sim 10^4 M_\odot$ [206]. At a relatively small distance to Earth, ≈ 1.7 kpc, this is the largest massive Galactic association. It has a diameter of

≈ 60 pc and a core radius of ~ 10 pc. The typical main sequence evolution lifetime of massive O stars is $\mathcal{O}$ (Myr) and a few tens Myr for massive B stars. Since the O-star population should pass through the Wolf-Rayet phase and explode as supernovae, very fast pulsars are expected to be born in explosions of these massive stars at a rate of about one every ten thousand years.

Apart from the mentioned interpretation of a hadronic production of the TeV radiation within the winds of outlying OB stars of Cyg OB2 [151], it was recently put forward that the TeV emission reported by HEGRA and the CR anisotropy observed at about 10^{18} eV in the direction of the Cygnus region can be related to a young pulsar and its pulsar wind nebulae (PWN), born in the Cygnus OB2 association a few ten thousands years ago [207]. The TeV γ-ray emission would originate in the PWN as a result of interactions of high energy hadrons and/or leptons, whereas there would be a directional CR signal due to neutrons that are dissolved from heavy nuclei accelerated by the pulsar.[12] Within this model, however, it is hard to explain the absence of counterparts at lower (EGRET) energies at the location of the TeV source, as well as the absence of a stronger X-ray source.[13] However, disregarding these difficulties, an interesting consequence for CR physics can be inferred.

As already discussed in Sec. II C 1, heavy nuclei can attain ultra high energies through magnetic sling shots inside the neutron star wind zone. The small part of nuclei, which escaped from the pulsar wind nebula, are likely to be captured by strong magnetic fields of dense regions of the OB association. Magnetic field strengths in dense molecular clouds are expected to be ~ 1 mG [209]. Thus, nuclei with $E/Z \sim 1$ EeV propagate attaining Bohm diffusion [207]. The resulting time delay of several thousand years [210] produces a steepening of the characteristic power law injection spectrum, $\propto E^{-2}$, of the pulsar nebula.[14] In their random traversal of the OB association, the nuclei undergo photodisintegration on the far infrared thermal photon population and liberate neutrons.

[12] A similar scenario would explain the anisotropy spot towards the Galactic Center [208].

[13] Indeed, location problems may arise as well: the PWN size (given that the TeV source size is 6 pc if indeed located at 1.7 kpc, and that the source is diffuse) would make the PWN substantially larger than both Vela's PWN ($\sim$0.1 pc at 250 pc) and Crab's ($\sim$1 pc). Additionally, if one were to associate the nearby EGRET source 3EG 2033+4118 with the putative pulsar itself, it is unclear whether the PWN hypothesis for the TeV source would imply that it is only a *one sided PWN* (Y. Butt, private comunication).

[14] Note that once diffusion has been established, additional Rayleigh steps in the Galactic magnetic field do not change the spectral index (~ -3) significantly.

The thermal photon density at the source reads,

$$n_{\rm IR} = \frac{T^3}{\pi^2} \int_{x_1}^{x_2} \frac{x^2\,dx}{e^x - 1} \approx \frac{(4.37\ T)^3}{\pi^2} \int_{x_1}^{x_2} \frac{x^2\,dx}{e^x - 1}\ {\rm cm}^{-3}, \tag{28}$$

where T is the kinetic temperature of the molecular cloud, $x \equiv E_\gamma/T$, and E_γ is the target photon energy in degrees K. The relevant photon energy range is established via standard kinematics of the photodisintegration process,

$$E_\gamma = \frac{E^*\ m_N}{(E_A/A)} = 10\,\frac{E^*_{\rm MeV}}{E_{N,{\rm PeV}}}\,{\rm K}\ , \tag{29}$$

where $5 < E^*_{\rm MeV} < 25$ is the energy region for giant dipole resonance contribution in the nucleus rest frame, and $E_A/A \equiv E_{N,{\rm PeV}}$ is the lab frame energy/nucleon. For $E_{N,{\rm PeV}} \sim 10^3$, Eq. (29) leads to $x_1 = 50/T$ and $x_2 = 250/T$, with T in degree Kelvin. Molecular clouds with HII regions have temperatures between 15 and 100 K [211], thus taking an average photodisintegration cross section of 40 mb,[15] we find that the nucleus mean free path lies between 0.80 and 380 pc. This corresponds to a reaction time between 4 to 1500 yr $\ll$ time delay, allowing sufficient neutron production to explain the anisotropy [65].

The Galactic anisotropy observed by the various collaborations spans the energy range 0.8 to 2.0 EeV. The lower cutoff specifies that only neutrons with EeV energies and above have a boosted $c\tau_n$ sufficiently large to serve as Galactic messengers. The decay mean free path of a neutron is $c\,\Gamma_n\,\overline{\tau}_n = 10\,(E_n/{\rm EeV})$ kpc, the lifetime being boosted from its rest-frame value $\overline{\tau}_n = 886$ seconds to its lab value via $\Gamma_n = E_n/m_n$. Actually, the broad scale anisotropy from the direction of the GP reported by Fly's Eye Collaboration [61] peaks in the energy bin $0.4 - 1.0$ EeV, but persists with statistical significance to energies as low as 0.2 EeV. This implies that if neutrons are the carriers of the anisotropy, there *needs to be* some contribution from at least one source closer than 3 - 4 kpc. Interestingly, the full Fly's Eye data include a directional signal from the Cygnus region which was somewhat lost in unsuccessful attempts [212, 213] to relate it to γ-ray emission from Cygnus X-3. The upper cutoff reflects an important feature of photodisintegration at the source: heavy nuclei with energies in the vicinity of the ankle will fragment to neutrons with energies about an order of magnitude smaller. To account for the largest neutron energies, it may be necessary to populate the heavier nucleus spectrum in the region above the ankle.[16] This is not a problem – one fully expects the emerging harder extragalactic spectrum to overtake and hide

[15] The photoabsorption cross section roughly obeys the Thomas-Reiche-Kuhn sume rule, i.e., $\Sigma_d = 60NZ/A$ mb-MeV [110].

[16] To produce the highest energy neutrons (with energy $\lesssim 10^{18.2}$ eV) via photodisintegration of medium mass (say, $A = 10 - 20$) nuclei, one needs primary particles with energies $\lesssim 10^{19.2}$ eV. For

the steeply falling galactic population. It is not therefore surprising that in order to fit the spectrum in the anisotropy region and maintain continuity to the ankle region without introducing a cutoff, the AGASA Collaboration required a spectrum $\propto E^{-3}$ or steeper [59].

For every surviving neutron at $\sim$ EeV, there are many neutrons at lower energy that decay via $n \rightarrow p + e^- + \overline{\nu}_e$. The proton is bent by the Galactic magnetic field, the electron quickly loses energy via synchrotron radiation, and the $\overline{\nu}_e$ travels along the initial neutron direction, producing a directed TeV energy beam [65]. The sensitivity of forthcoming neutrino telescopes to this signal is discussed in Sec. IV B.

D. Radio Galaxies and Active Galactic Nuclei

1. Definitions

Blazars are active galactic nuclei (AGNs) with a) strong flat spectrum radio emission [the power law index $\alpha > -0.5$, with $S(\nu) \propto \nu^{\alpha}$] and/or b) significant optical polarization, and/or c) significant flux variability in the optical and in other wavelengths. When the optical variability occurs on short timescales, the objects are referred to as optically violently variable –OVV– quasars. The blazar classification also includes BL Lacertae (BL Lac) objects, which present a complete or nearly complete lack of emission lines, and highly polarized quasars (HPQs). It also refers, sometimes, to flat spectrum radio quasars (FSRQs), although these are generally more distant, more luminous, and have stronger emission lines. Within the unification model, the underlying scenario for all AGNs is intrinsically similar. At the very center of the galaxy there is a supermassive black hole ($\sim 10^6$ to $\sim 10^{10}\,\mathrm{M}_\odot$) which accretes galactic matter forming an accretion disk. Broad emission lines are produced in clouds orbiting above the disc at high velocity, the broad line region (BLR) and this central region is surrounded by an extended, dusty, molecular torus. A hot electron corona populates the inner region, probably generating continuum X-ray emission. Narrower emission lines are produced in clouds moving much farther from the central black hole. Two-sided jets of relativistic particles emanate perpendicular to the plane of the accretion disc, the generation of which is still not fully understood. Unification of different AGN classes is achieved

a falling spectrum $\propto E^{-3}$, the medium mass nucleus population at $10^{19.2}$ eV is roughly 3 orders of magnitude smaller than the diffuse flux at $10^{18.2}$ eV. This means that it is about 1.6 orders of magnitude smaller than the reported CR excess (which is about 4% of the diffuse flux, see Sec. I C). However, since each nucleus produces roughly $A-Z$ neutrons, the average number of liberated neutrons is on the same order of magnitude, $1.6 - \log_{10}(A-Z)$, than the obseved neutron population at $\lesssim 10^{18.2}$ eV.

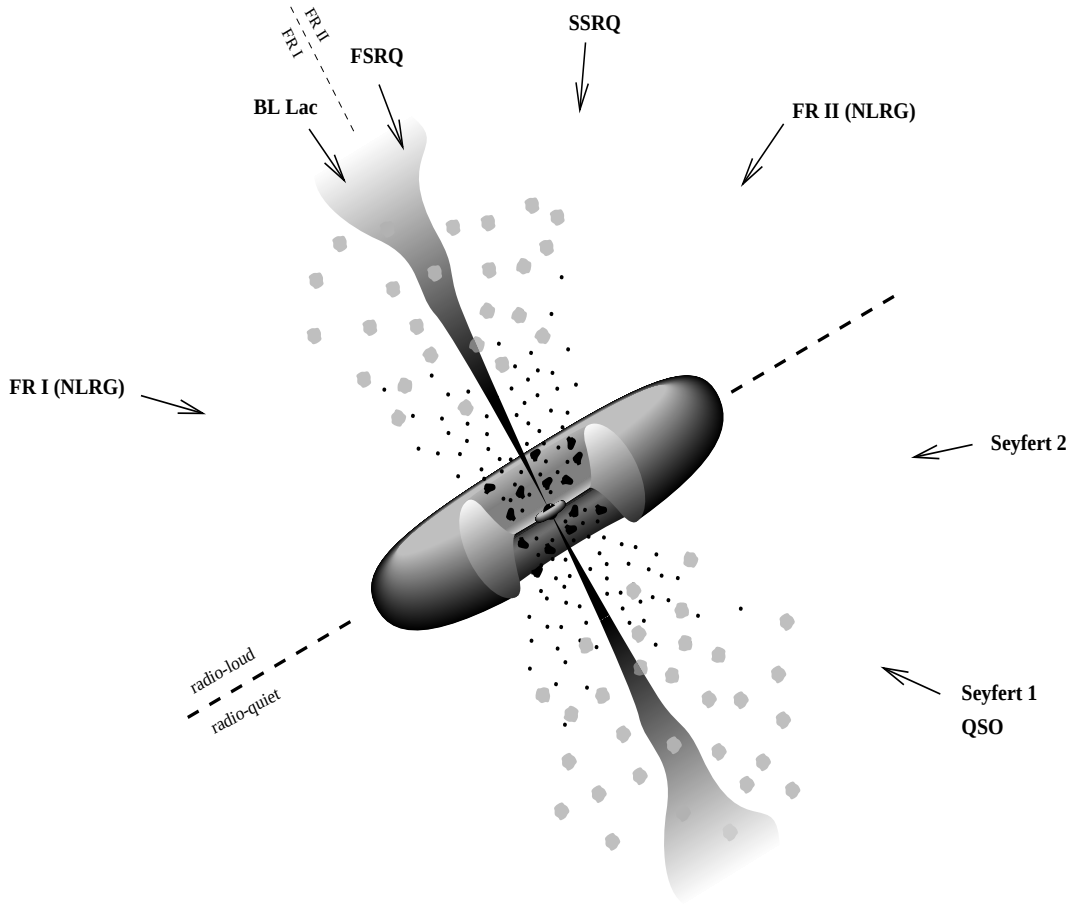

FIG. 5: The unification model for AGNs. The components of the figure are discussed in the text. Blazars are those AGNs for which the jets are close to line of sight. A regular quasar or a Seyfert 1 galaxy is observed if the orientation angle is $\sim 30^{\rm o}$, where the narrow-line and broad-line regions are visible. At larger angular offsets, the broad-line region will be hidden by the torus, the corresponding class being Seyfert 2 galaxies. Perpendicular to the jet axis, the full extent of the jets may be seen particular at low frequencies, giving rise to a morphology typical of radio galaxies. The figure is adapted from Refs. [214, 215, 216, 217].

taking into account the intrinsic anisotropy of the phenomenon, is shown in Fig. 5 (see Refs. [214, 215, 216, 217] for further and more detailed discussions).

For example, Seyfert galaxies possess a dusty torus of gas at distances intermediate between the BLR and NLR (narrow line region). An observer whose line of sight to the black hole intercepts this torus would see a heavily reddened (or completely extinguished) BLR and central continuum radiation but an unreddened NLR. This would be identified with a Seyfert 2 galaxy. If the line-of-sight does not intercept the torus, the central regions of the nucleus can be observed directly, leading to a Seyfert 1 classification. Radio loud quasars are then objects in which the line-of-sight is close

to the jet cone of the source. In the cases in which we are not directly looking into the jet cone –blazars where relativistic effects produce highly variable and continuum dominated emission– emission from the BLR can be observed. Objects with larger inclinations have a less dominant central continuum flux, resulting in Fanaroff-Riley II (FRII) galaxies. If the torus surrounding the black hole obscures the BLR, a narrow line radio galaxy (NLRG) can be observed. It is not clear how FRI radio galaxies fit into such a scheme. Clearly, some (as yet unknown) physical mechanism, probably related to source power, produces different radio morphologies in FRI and FRII sources.[17] Some blazars may be beamed FRI objects, but there is a lack of broad-line FRI radio galaxies [214]. This make the classification within the unified scheme harder to achieve.

2. Radiogalaxies

FRII galaxies [219] are the largest known dissipative objects (non-thermal sources) in the Universe. Localized regions of intense synchrotron emission, known as "hot spots", are observed within their lobes. These regions are presumably produced when the bulk kinetic energy of the jets ejected by a central active nucleus (supermassive black hole + accretion disk) is reconverted into relativistic particles and turbulent fields at a "working surface" in the head of the jets [220]. Specifically, the speed $v_{\rm h}$ with which the head of a jet advances into the intergalactic medium of particle density $n_{\rm e}$ can be obtained by balancing the momentum flux in the jet against the momentum flux of the surrounding medium. Measured in the frame comoving with the advancing head, $v_{\rm h} \approx \ v_{\rm j}\,[1+(n_{\rm e}/n_{\rm j})^{1/2}]^{-1}$, where $n_{\rm j}$ and $v_{\rm j}$ are the particle density and the velocity of the jet flow, respectively. $v_{\rm j} > v_{\rm h}$ for $n_{\rm e} \geq n_{\rm j}$, and the jet will decelerate. The result is the formation of a strong collisionless shock, which is responsible for particle reacceleration and magnetic field amplification [221]. The acceleration of particles up to ultrarelativistic energies in the hot spots is the result of repeated scattering back and forth across the shock front [222]. Dimensional arguments suggest that the energy density per unit of wave number of MHD turbulence is of the Kolmogorov type [223], and so for strong shocks the acceleration time for protons is [224]

$$\tau_{\rm acc} \simeq \frac{40}{\pi}\,\frac{1}{c\,\beta_{\rm jet}^2}\,\frac{1}{u}\,\left(\frac{E}{eB}\right)^{1/3}\,R^{2/3} \tag{30}$$

[17] The Faranoff-Riley classification is based on one parameter, $R_{\rm FR}$, the ratio of the distance between the regions of highest surface brightness on opposite sides of the central galaxy to the total extent of the source. Objects with $R_{\rm FR} < 0.5$ are classified as FRI, whereas those with $R_{\rm FR} > 0.5$ are classified as FRII. It is found that the brighter sources are all FRII class, although the distinction between classes is not clear cut in luminosities (for further details see page 220 of Ref. [218]).

where $\beta_{\rm jet}$ is the jet velocity in units of c, u is the ratio of turbulent to ambient magnetic energy density in the region of the shock (of radius R), and B is the total magnetic field strength. The acceleration process will be efficient as long as the energy losses by synchrotron radiation and photon–proton interactions do not become dominant. The subtleties surrounding the conversion of a particle kinetic energy into radiation provide ample material for discussion [222, 225, 226, 227, 228, 229]. The proton blazar model relates γ-ray emission to the development of electromagnetic cascades triggered by secondary photomeson products that cool instantaneously via synchrotron radiation [222, 225, 226, 227, 228]. The synchrotron loss time for protons is given by [230]

$$\tau_{\rm syn} \sim \frac{6\,\pi\,m_p^3\,c}{\sigma_{\rm T}\,m_e^2\,\Gamma\,B^2}\,, \tag{31}$$

where m_e, m_p, $\sigma_{\rm T}$ and Γ are the electron mass, proton mass, Thomson cross section, and Lorentz factor, respectively. The characteristic single photon energy in synchrotron radiation emitted by an electron is

$$E_\gamma = \left(\frac{3}{2}\right)^{1/2} \frac{h\,e\,E^2\,B}{2\,\pi\,m_e^3\,c^5} \sim 5.4\times10^{-2}\,B_{\mu\rm G}\,E_{20}^2\,{\rm TeV}\quad . \tag{32}$$

For a proton this number is $(m_p/m_e)^3 \sim 6\times10^9$ times smaller. High energy γ-ray production through proton synchrotron radiation requires very large, $\mathcal{O}(100$ G), magnetic fields. Considering an average cross section $\bar\sigma_{\gamma p}$ for the three dominant pion–producing interactions [231], $\gamma p \to p\pi^0\,, \gamma p \to n\pi^+\,, \gamma p \to p\pi^+\pi^-$, the time scale of the energy losses, including synchrotron and photon interaction losses, reads [222]

$$\tau_{\rm loss} \simeq \frac{6\pi\ m_p^4\ c^3}{\sigma_{\rm T}\ m_e^2\ B^2\ (1+Aa)}\ E^{-1}\ = \frac{\tau_{\rm syn}}{1+Aa}\,, \tag{33}$$

where a stands for the ratio of photon to magnetic energy densities and A gives a measure of the relative strength of γp interactions versus the synchrotron emission. Note that the second channel involves the creation of ultrarelativistic neutrons (but $\Gamma_n \lesssim \Gamma_p$) with mean free path in the observer rest frame given by $\lambda_n = \Gamma_n c\tau_n$, where $\tau_n \sim 900$ s, is the neutron lifetime. Since $\lambda_n > \lambda_p$ for $\Gamma_n \lesssim \Gamma_{p\ \rm max}$, such neutrons can readily escape the system, thereby modifying the high end of the proton spectrum. Biermann and Strittmatter [222] have estimated that $A \approx 200$, almost independently of the source parameters. The most energetic protons injected in the intergalactic medium will have an energy that can be obtained by balancing the energy gains and losses [125]

$$E_{20} = 1.4\times10^5\ B_{\mu\rm G}^{-5/4}\ \beta_{\rm jet}^{3/2}\ u^{3/4}\ R_{\rm kpc}^{-1/2}\ (1+Aa)^{-3/4}\ , \tag{34}$$

where $R_{\rm kpc} \equiv R/1\,{\rm kpc}$.

For typical hot-spot conditions ($B \sim 300$ μG, $u \sim 0.5$, and $\beta_{\rm jet} \sim 0.3$) and assuming that the magnetic field of the hot spot is limited to the observable region, one obtains $E < 5 \times 10^{20}$ eV for $a < 0.1$ [232].[18] Particles can also attain ultrahigh energies ($E \gtrsim 10^{20}$ eV) within the jets or the AGNs themselves. For instance, the knot A in the M87 jet, with a length scale $l_{87} \sim 2 \times 10^{20}$ cm, has a magnetic field strength $B_{87} \sim 300$ μG [233]. Typical AGN sizes are $l_{\rm AGN} \sim 10^{15}$ cm, and $B_{\rm AGN} \sim 1$ G [234]. Observational evidence suggests that in the jets $a \ll 1$, whereas $a \sim 1$ for AGNs [222].

3. Cen A: The source of most UHECRs observed at Earth?

Centaurus A (Cen A) is the nearest active galaxy, ~ 3.4 Mpc [235]. It is a complex FRI radio-loud source identified at optical frequencies with the galaxy NGC 5128. Different multi-wavelength studies have revealed that it is comprised of a compact core, a jet also visible at X-ray frequencies, a weak counterjet, two inner lobes, a kpc-scale middle lobe, and two giant outer lobes. The jet would be responsible for the formation of the northern inner and middle lobes when interacting with the interstellar and intergalactic media, respectively. There appears to be a compact structure in the northern lobe, at the extrapolated end of the jet. This structure resembles the hot spots such as those existing at the extremities of FRII galaxies. However, at Cen A, it lies at the side of the lobe rather than at the most distant northern edge, and the brightness contrast (hot spot to lobe) is not as extreme [236].

Low resolution polarization measurements in the region of the suspected hot spot give magnetic fields as high as 25 μG [236]. However, in certain regions where measurements at both high and low resolution are available, the B-field amplitude at high resolution can be seen to be twice that at low resolution. The higher resolution can reveal amplification in the post-shock region [237], yielding B-fields possibly as high as $50 - 60$ μG [238, 239]. The radio-visible size of the hot spot can be directly measured from the large scale map [240], giving $R_{\rm HS} \simeq 2$ kpc. The actual size can be larger by a factor ~ 2 because of uncertainties in the angular projection of this region along the line of sight.[19] Then, if the magnetic field of the hot spot is confined to the visible region, the limiting energy imposed by the Hillas' criterion is $E_{\rm max} \sim 10^{20.6}$ eV.

Estimates of the radio spectral index of synchrotron emission in the hot spot and

[18] The shock structure in hot spots is likely to be much more extended than the visible region in the non-thermal radioemission, as suggested by magnetohydrodynamical modeling [232].

[19] For example, an explanation of the apparent absence of a counterjet in Cen A via relativistic beaming suggests that the angle of the visible jet axis with respect to the line of sight is at most 36° [236], which could lead to a doubling of the hot spot radius. It should be remarked that for a distance of 3.4 Mpc, the extent of the entire source has a reasonable size even with this small angle.

the observed degree of linear polarization in the same region suggests that the ratio of turbulent to ambient magnetic energy density in the region of the shock is $u \sim 0.4$ [241]. The jet velocity is model dependent: possible values range from $\sim$ 500 km s^{-1} to $0.99\,c$ [236]. For FRI galaxies, the ratio of photon to magnetic energy densities, a, is expected to be $\ll 1$. Now, by replacing these numbers into Eq. (34), one can easily see that Cen A can accelerate particles to energies $\gtrsim 10^{20}$ eV, with a maximum attainable energy set by the Hillas' criterion.[20]

Recent observations of the γ ray flux for energies > 100 MeV by EGRET [243] allow an estimate $L_\gamma \sim 10^{41}$ erg s^{-1} for the source.[21] This value of L_γ is consistent with an earlier observation of photons in the TeV-range during a period of elevated activity [244], and is considerably smaller than the estimated bolometric luminosity $L_{\rm bol} \sim 10^{43}$erg s^{-1}[235]. Data across the entire γ ray bandwidth of Cen A is given in Ref.[245], reaching energies as high as 150 TeV [246], though data at this energy await confirmation. For values of B in the μG range, substantial proton synchrotron cooling is suppressed, allowing the production of high energy electrons through photomeson processes. The average energy of synchrotron photons scales as $\overline{E}_\gamma \simeq 0.29 E_\gamma$ [247]. With this in mind, it is straightforward to see that to account for TeV photons, Cen A should harbor a population of ultra-relativistic electrons with $E \sim 6 \times 10^{18}$ eV. We further note that this would require the presence of protons with energies between one and two orders of magnitude larger, since the electrons are produced as secondaries.[22]

There are plausible physical arguments [228, 248] as well as some observational reasons [249] to believe that when proton acceleration is being limited by energy losses, the CR luminosity $L_{\rm CR} \approx L_\gamma$. Defining ϵ, the efficiency of UHECR production compared to high energy γ production – from the above, $\epsilon \simeq 1$ – and using equal power per decade over the interval $(E_{\rm min},\ E_{\rm max})$, the source luminosity is found to be [250]

$$\frac{E^2\, dN_0^{p+n}}{dE\, dt} \approx \frac{6.3\, \epsilon L_{41}\, 10^{52}{\rm eV/s}}{\ln(E_{\rm max}/E_{\rm min})}\,, \tag{35}$$

where $L_{41} \equiv$ luminosity of Cen A$/10^{41}$erg s^{-1} and the subscript "0" refers to quantities at the source.

For fiducial values, $B = 0.5$ μG, $\ell = 0.5$ Mpc, the diffusive distance traveled by CRs with $E = 10^{19}$ eV, is $c\tau_D = 50$ Mpc $\gg d = 3.4$ Mpc. Moreover, one can easily check

[20] It was recently suggested [242] that the 25 kpc jet (with $B \approx 10$ μG) of Cen A could be another promising region for proton acceleration to ultra high energies.

[21] Note that the received radiation is negligibly affected by interactions with the various radiation backgrounds [229].

[22] Consecutive factors of ~ 2 energy loss occur in the processes $p\gamma \to N\pi^0,\ \pi^0 \to \gamma\gamma,\ \gamma \to e^+e^-$. Eq.(32) then implies proton energies of $\sim 10^{20}$ eV for 100 TeV photons.

that for 3.4 Mpc the diffusion time of any proton with energy above the photopion production threshold is always less than the GZK-time, and consequently energy losses can be safely neglected. This implies that the density of protons at the present time t of energy E at a distance r from Cen A (which is assumed to be continuously emitting at a constant spectral rate $dN_0^{p+n}/dE\,dt$ from time $t_{\rm on}$ until the present) can be obtained by solving the Kolmogorov-diffusive-equation, and is found to be [251]

$$\frac{dn(r,t)}{dE} = \frac{dN_0^{p+n}}{dE\,dt}\frac{1}{[4\pi D(E)]^{3/2}}\int_{t_{\rm on}}^{t} dt'\,\frac{e^{-r^2/4D(t-t')}}{(t-t')^{3/2}} = \frac{dN_0^{p+n}}{dE\,dt}\frac{1}{4\pi D(E) r}\;I(x)\,, \qquad (36)$$

where $D(E)$ is the diffusion coefficient given in Eq. (7), $x = 4DT_{\rm on}/r^2 \equiv T_{\rm on}/\tau_D$, $T_{\rm on} = t - t_{\rm on}$, and

$$I(x) = \frac{1}{\sqrt{\pi}}\int_{1/x}^{\infty}\frac{du}{\sqrt{u}}\;e^{-u} \quad . \qquad (37)$$

For $T_{\rm on} \to \infty$, the density approaches its time-independent equilibrium value $n_{\rm eq}$, while for $T_{\rm on} = \tau_D$, $n/n_{\rm eq} = 0.16$.

To estimate the power of Cen A, one can evaluate the energy-weighted approximately isotropic proton flux at 1.5×10^{19} eV, which lies in the center of the flat "low" energy region of the spectrum,

$$E^3 J_p(E) = \frac{Ec}{(4\pi)^2 d\,D(E)}\frac{E^2\,dN_0^{p+n}}{dE\,dt}\,I(t/\tau_D) \approx 7.6\times 10^{24}\,\epsilon L_{41}\,I\ {\rm eV}^2\,{\rm m}^{-2}\,{\rm s}^{-1}\,{\rm sr}^{-1}. \quad (38)$$

In Eq. (38) we have used the fiducial values of B and ℓ as given in the previous paragraph, and set $E_{\rm min} = 1\times 10^{19}$ eV, $E_{\rm max} = 4\times 10^{20}$ eV. As noted by Farrar and Piran [250], by stretching the source parameters the "low" energy flux from Cen A could be comparable to that of all other sources in the Universe. To this end, first fix $\epsilon\,L_{41}\,I = 0.40$, after comparing Eq. (38) to the observed CR-flux by AGASA: $E^3 J_{\rm obs}(E) = 10^{24.5}$ eV^2 m^{-2} s^{-1} sr^{-1} [74]. Next, $\epsilon L_{41} \simeq 1$, determines $I \simeq 0.40$, and consequently the required age of the source $T_{\rm on}$ to be about 400 Myr, which appears plausible [221, 249]. To maintain flux at the "ankle" for the same $T_{\rm on}$, one requires an approximate doubling of $L_{\rm CR}$ at 5×10^{18} eV. Because of the larger diffusive time delay at this energy, this translates into an increased luminosity in the early phase of Cen A. From Eq. (32), the associated synchrotron photons are emitted at energies < 30 MeV. The increase in radiation luminosity in this region is not inconsistent with the flattening of the spectrum observed at lower energies[252, 253].

Having identified Cen A to plausibly be a powerful source of UHECRs, we now explore whether B-field deflections provide correct directional properties, i.e., sufficient isotropy. This can be found by computing the incoming current flux density $D\nabla n$ as viewed by an observer on Earth, and one finds for a continuously-emitting source a

distribution $\sim (1 + \alpha \cos\theta)$ about the direction of the source, where θ is the angle to the zenith and

$$\alpha = \frac{2D(E)}{cr}\,\frac{I'}{I}\,, \qquad\qquad I'(x) = \frac{1}{\sqrt{\pi}}\int_{1/x}^{\infty} du\ \sqrt{u}\ e^{-u}, \tag{39}$$

with $x = T_{\rm on}/\tau_D$, and I as defined in Eq. (37) [251]. For our choices of B and ℓ, and $T_{\rm on} = 400$ Myr, we find for $E = 10^{19}$ eV ($E = 10^{20}$ eV) that $\alpha = 0.04$ ($\alpha = 0.07$). This is in complete agreement with the upper bounds on dipole anisotropies recently reported by HiRes Collaboration [73]. One caveat is that the large deflection angle of the highest energy Fly's Eye event with respect to the line of sight to Cen A must be explained as a 2σ fluctuation [254]. Additionally, Monte Carlo simulations [255] show the predicted auto-correlation function is not consistent with the clustering at small scale reported by AGASA Collaboration [74]. Therefore, if the hypothesis of CR pairing proposed by AGASA Collaboration is confirmed by future data, it will constitute a serious objection to the model outlined above. On the other hand, an interesting observational feature for a Cen A origin of UHECRs is the possible detection of neutrons, which at the highest energies could survive decay and produce a spike in the direction of the source [251]. The estimated event rate at PAO is about 2 direct events per year, against negligible background. Thus, in a few years of running, the hypothesis of Cen A as the source of most UHECRs observed at Earth can be directly tested.

4. M87: The end of all roads?

M87 is a giant radio galaxy for which there has been a recent report of a TeV excess at a level of 4σ [256]. It is also expected to be a source for GLAST, having an EGRET upper limit of 2.8×10^{-8} photons cm^{-2} s^{-1} above 100 MeV (Reimer, private communication, see also the limit imposed in Ref. [257]), and comparable theoretical flux predictions [258, 259].

M87 was thought as a high-energy CR emitter since quite long ago [260, 261]. At a distance of 16.3 Mpc [262], it is the dominant radio galaxy in the Virgo cluster ($l = 282°$, $b = 74°$) [263]. The emission of synchrotron radiation with a steep cutoff at frequencies about 3×10^{14} Hz from its radiojets and hot spots [264, 265] implies an initial turbulence injection scale having the Larmor radius of protons at 10^{21} eV.

The major difficulty with a M87 generation of UHECRs is the observation of the nearly isotropic distribution of the CR arrival directions. One can again argue that the orbits are bent. However, the bending cannot add substantially to the travel time, otherwise the energy would be GZK-degraded. An interesting explanation to overcome this difficulty relies on a Galactic wind, akin the solar wind, that would bend all the orbits of the highest energy CRs towards M87 [266, 267]. Indeed, it has long been

expected that such a kind of wind is active in our Galaxy [268, 269, 270]. In the analysis of [266], it was assumed that the magnetic field in the Galactic wind has a dominant azimuthal component, with the same sign everywhere. This is because in a spherical wind the polar component of the magnetic field becomes negligible rather quickly, decaying like $1/r^2$, and thus the azimuthal part of the magnetic field quickly becomes dominant, with $B_\phi \sim \sin\theta/r$ in polar coordinates [271]. Under these considerations one is left with two degrees of freedom: the strength of the azimuthal component at the location of the Sun, and the distance to which this wind extends. Recent estimates suggest that the magnetic field strength near the Sun is ~ 7 μG [130]. The second parameter is more uncertain. Our Galaxy dominates its near environment well past our neighbor, M31, the Andromeda galaxy, and might well extend its sphere of influence to half way to M81. This implies an outer halo wind of ~ 1.5 Mpc. With this in mind, the mean flight time of the protons in the Galaxy is $\sim 5.05 \times 10^6$ yr $\ll \tau_s$, the time for straight line propagation from M87 (Medina Tanco, private communication). The directions where the 13 highest energy CR events point towards when they leave the halo wind of our Galaxy is consistent with an origin in the Virgo region [266]: *(i)* for CR protons, except for the two highest energy events, all other events can be traced back to within less than about 20° from Virgo; *(ii)* if one assumes that the two highest events are helium nuclei, all 13 events point within 20° of Virgo. Arguably, the super-Galactic plane sheet can focus UHECRs along the sheet. Hence, the particles would arrive at the boundary of our Galactic wind with the arrival directions described by an elongated ellipse along the super-Galactic plane sheet [272]. This would allow a bending of 20° to be accomodated.

Additionally, in order to account for most of the CRs observed above the ankle, the power requirement of Virgo cluster [273] needs a fine-tuning of the source direction relative to the symmetry axis of the wind, so as to turn on magnetic lensing effects [274]. In such a case, M87 could be as high as $> 10^2$ times more powerful than if unlensed at energies below $E/Z \sim 1.3 \times 10^{20}$ eV. Criticisms of this model [275] have been addressed in [276].

5. Other powerful nearby radiogalaxies

Apart from Cen A (which would provide the most energetic particles detectable on Earth), the CR-sky above PAO, if populated by radiogaxies, should be dominated by Pictor A (a strong source with a flat radio spectrum) which would contribute with the larger CR flux [232], and PKS 1333-33 [277]. Other two southern candidates would be Fornax A ($z = 0.057$) and PKS 2152-69 ($z = 0.027$), which could provide contributions to the CR flux above the cutoff. For other powerful sources and their properties see [232, 278].

There are two additional EGRET sources, one of them at high latitude, for which a possible radio galaxy counterpart has been suggested. One such source is 3EG J1621+8203 ($l = 115.5^{\rm o}, b = 31.8^{\rm o}$) [279]. 3EG J1621+8203 observations in individual viewing periods yielded near-threshold detections by EGRET, as for Cen A. However, in the cumulative exposure, it was clearly detected and the measured flux above 100 MeV was 1.1×10^{-7} photon cm^{-2} s^{-1}. The photon spectral index for this source is 2.27±0.53, steeper than the usual blazar-like spectrum. Mukherjee et al. [279] analyzed the X-ray and radio field coincident with 3EG J1621+8203 and concluded that NGC 6251, a bright FRI radio galaxy [214] at a redshift of 0.0234 (implying a distance 91 Mpc for $H_0 = 75$ km s^{-1} Mpc^{-1}), and the parent galaxy of a radio jet making an angle of 45$^{\rm o}$ with the line of sight [280], is the most likely counterpart of the EGRET source. With this identification, the implied γ-ray luminosity is also a factor of 10^{-5} below that typical of blazars. Compared with Cen A, the greater distance to NGC 6251 could, perhaps, be compensated by the smaller angle between the jet and the line of sight.

Combi et al. [281] have also recently reported the discovery of a new radio galaxy, J1737−15, within the location error box of the low-latitude γ-ray source 3EG J1735−1500, whose photon index is $\Gamma = 3.24 \pm 0.47$. The radio galaxy morphology at 1.4 GHz is typical of the double-sided FRII. The integrated radio flux is 55.6 ± 1.5 mJy at 1.4 GHz, the source is non-thermal and it is not detected at 4.8 GHz. Using the relation between approaching and receding jets: $S_{\rm appr}/S_{\rm rec} = (1 + \beta\cos\theta/1 - \beta\cos\theta)^{2-\alpha}$, as well as the radio fluxes of each jet component, a viewing angle in the range $79^{\rm o} - 86^{\rm o}$ for a velocity $\beta = v/c$ between 0.3 and 0.9 and $\alpha = -1$ is derived. Depending on the jet and ambient medium parameters, most double-sided radio sources have sizes below ~ 300 kpc [221]. In the case of J1737−15, and using standard Friedmann-Robertson-Walker models, this size translates into a possible distance smaller than 350 Mpc. If 3EG J1735−1500 is indeed the result of γ-ray emission in J1737−15, the intrinsic luminosity at $E > 100$ MeV, at the distance quoted, should then be less than 2×10^{44} erg s^{-1}, also several orders of magnitude smaller than that of blazars. If both radiogalaxies are closer than 100 Mpc, they could also be relevant acceleration sites of the observed UHECRs.

6. Correlations of UHECRs with QSOs, BL LACs, and EGRET sources

Since an alignment beyond random expectations between UHECRs and QSOs would certainly constitute a great discovery, the possible correlation between UHECRs and QSOs was subject to a great deal of scrutiny. In the spring of 1998, Farrar and Biermann pointed out the existence of a directional correlation between compact radio-QSOs and UHECRs: all events at the high end of the spectrum observed by that time, with energy at least 1σ above $10^{19.9}$ eV, were aligned with high redshifted quasars, a

phenomenon with a chance probability of occurrence less than 0.5% [57]. Since then, this correlation has been analyzed several times. Hoffman stated that one of the 5 events used in the Farrar and Biermann's study, the highest energy event observed by the Fly's Eye experiment, should not be included in the UHECR sample under analysis, because this very same event was considered to introduce the hypothesis [282]. Without this event, the positive alignment with random background probability is increased to $< 3\%$, in any case small enough as to be plausibly significant [111]. Using an updated event list (twice the size of the previous) from the Haverah Park [43] and the AGASA [74] experiments, Sigl et al. [283] showed that the statistical significance of the alignment is lowered to 27%. Other authors, however, favored the earlier alignment [284], but their correlation signal comes from events with large uncertainty both in energy and in position: they considered events from the SUGAR experiment, although it is not clear whether all these events are above the GZK cutoff. Notwithstanding, after the Haverah Park energy estimates have been re-assessed [142], the original correlation has to be dropped altogether: for the cosmic rays in question, the energy of the 2 events observed by this array with incident zenith angle $< 45°$, that was previously quoted as $> 10^{19.9}$ eV at 1σ, is now shifted $\approx 30\%$ downwards, below the energy cut chosen by Farrar and Biermann. Hence, independently of the statistical test used, when considering only the highest energy ($> 10^{19.9}$ eV at 1σ) events the correlation between UHECRs and QSOs is consistent with a random distribution at the 1σ level.

Tinyakov and Tkachev [285, 286, 287] reported a correlation between the arrival directions of UHECRs and BL Lacs. Specifically, the (22) BL Lacs chosen were those identified as such in the (9th-Edition) Veron-Cetty and Veron (2000) [288] catalogue of Quasars and Active Galactic Nuclei, with redshift $z > 0.1$ or unknown, magnitude $m < 18$, and radio flux at 6 GHz $F_6 > 0.17$ Jy. This analysis proposed no energy buffer against contamination by mis-measured protons piled up at the GZK energy limit.[23] The evidence supporting their claim is based on 6 events reported by the AGASA Collaboration (all with average energy $< 10^{19.9}$ eV), and 2 events recorded with the Yakutsk experiment (both with average energy $< 10^{19.6}$ eV), which were found to be within 2.5° of 5 BL Lacs contained in the restricted sample of 22 sources. The chance probability for this coincidence set-up was claim to be 2×10^{-5}. Here also the data set used to make the initial assertion is also being used in the hypothesis testing phase. What is further subject to critique, is that the imposed cuts on the BL Lac catalogue were chosen so as to maximize the signal-to-noise ratio, compensating *a posteriori* the

[23] The CR sample of Tinyakov and Tkachev consists of 26 events measured by the Yakutsk experiment with energy $> 10^{19.38}$ eV [289], and 39 events measured by the AGASA experiment with energy $> 10^{19.68}$ eV [74].

different cut adjustments by inclusion of a penalty factor [290]. Without such arbitrary cuts, the significance of the correlation signal is reduced at the 1σ level. Not to anyone's surprise, even in acceptance of this approach, the estimated value of the penalty factor is subject to debate [287, 290].

Recently, in order to test the *hypothetical* correlation between UHECRs and BL Lacs, Torres et al. [291] performed a blind analysis using the Haverah Park [292] and Volcano Ranch [293] data samples. Such an analysis shows no positional coincidences between these two samples up to an angular bin $> 5^\circ$, an angular scale that is well beyond the error in arrival determination of these experiments ($\approx 3^\circ$) [77]. On the basis of the strongly correlated sample analyzed by Tinyakov and Tkachev, one expects the distribution describing the correlation between the set of BL Lacs and any UHECR data-set with 33 entries to be Poisson with mean ≈ 4.06. This implies a 2σ deviation effect. Alternatively, the 95% CL interval of the distribution which samples the correlation between the BL Lacs and CRs recorded by Volcano Ranch + Haverah Park is (0, 3.09) [294], so that the probability to measure the expected mean value ≈ 4.06 is $\ll 5\%$. With this in mind, Torres et al. [291] conclude that the 8 coincidences found in the Tinyakov and Tkachev's analysis do not represent a statistically significant effect.

Additionally, Gorbunov et al. [295] claimed that a set of γ-ray loud BL Lacs can be selected by intersecting the EGRET, the UHECR, and the BL Lac catalogs (all conveniently cut). The only requirement Gorbunov et al. considered for an object (here, a BL Lac) to be physically associated with an EGRET source is that the angular distance between the best estimated position of the pair does not exceed $2 \times R_{95}$, where R_{95} is the 95% confidence level contour of the EGRET detection. Torres et al. [291] pointed out that identifying EGRET sources with BL Lacs (or any other object) just by positional pairing within twice the EGRET error grossly underestimates the goodness of existing γ-ray data. At this stage, it is worth recalling the reader that the typical R_{95} radius for EGRET sources is 0.5–1°. One can then argue that if the confidence contours have any significance at all, a source should appear beyond the 95% contour only a few percent of the time. Working with 114 EGRET sources above $|b| > 10^o$, Punsly [296] have estimated the number of random coincidences as a function of the field radius: $\sim$ 2 (10) quasars with more than 1 Jy of 5 GHz flux are expected to correlate by random chance if the size of the typical EGRET angular uncertainty is 0.7^o (1.7^o), see Fig. 6.

In our opinion, available statistics on the arrival directions of the UHECRs reveals no significant correlations above random with BL Lacs nor with any other type of quasars, including EGRET blazars.

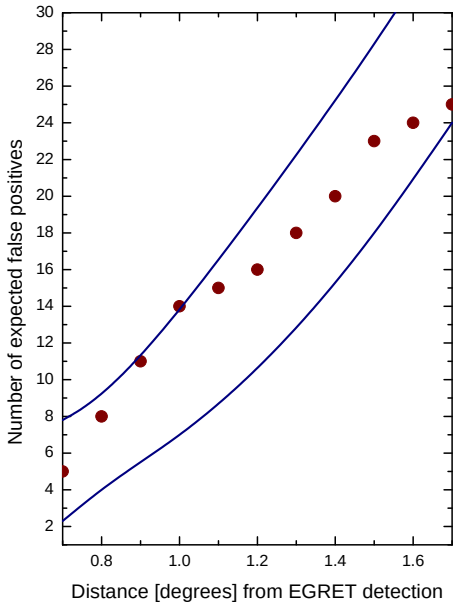

FIG. 6: The expected distribution of radio-loud quasars (louder than 0.5 Jy at 5 GHz) to occur by random chance as a function of the distance from the center of the field for a sample of 114 EGRET detections. Points represent the number of γ-ray detections for which the counterparts are beyond the 95% confidence contour. The dotted curve are the boundaries of the 68% confidence band for the hypothesis that the radio sources are randomly distributed in the EGRET detection fields. Adapted from Punsly (1997). The number of sources whose possible counterpart are beyond the 95% confidence contour is compatible with the chance expectation.

E. Remnants of quasars

1. What is a quasar remnant and how would they accelerate particles?

Interestingly, the absence of powerful radio emitting objects in the direction of several UHECRs led some colleagues to think that dead, faint objects, yet ones sufficiently active as to accelerate particles up to relativistic energies, are responsible for the UHECRs observed. Such is the idea behind the concept of quasar remnants (QRs) as UHECR emitters [297, 298]: a spinning supermassive black hole, threaded by magnetic fields generated by currents flowing in a disc or torus, induces an emf which, if vaccum breakdown is prevented and in the absence of severe energy losses, accelerate a particle near the full voltage.

Although in the present epoch there is a paucity of luminous quasars ($L \gtrsim 10^{47}$ ergs s^{-1}), those which appear at large redshifts, the expected local number of dead quasars associated with the same parent population is expected to be large [299, 300, 301].

Supermassive black holes are now to be found in the relatively dormant nuclei of giant elliptical galaxies, generally regarded as QRs.[24] The compact dynamo model has been proposed as a natural mechanism for accelerating CRs in such environments [297]. In this model [303], if B is the ordered poloidal field near the hole, $V \sim aB$, where a is the hole's specific angular momentum (e.g., $a = M$ for an extreme Kerr hole of mass M). In an appropriate astrophysical scaling [304]

$$V \sim 9 \times 10^{20}(a/M)B_4 M_9 \text{ V}, \tag{40}$$

where $B_4 \equiv B/(10^4\text{G})$ and $M_9 \equiv M/(10^9\text{M}_\odot)$. Assuming that the energy density of the magnetic field near the event horizon is in equipartition with the rest mass energy density of accreting matter [305], it is possible to introduce the accretion rate in the voltage expression. In terms of an Advection Dominated Accretion Flow (ADAF) model (e.g., Ref. [306]), for example,

$$B_4 \sim 1.4\, {M_9}^{-1}\dot{M}^{1/2}, \tag{41}$$

where $\dot{M}$ is the accretion rate dM/dt in $\text{M}_\odot$ yr^{-1}, and then, the maximum emf ($a/M \sim 1$) is

$$V \sim 1.2 \times 10^{21}\dot{M}^{1/2} \text{ V}. \tag{42}$$

This potential is not, however, the maximum obtainable energy.

The rate of energy loss through curvature radiation by a particle of energy $E = mc^2\Gamma$ can then be expressed as

$$P = \frac{2}{3}\frac{e^2 c\Gamma^4}{\rho^2}, \tag{43}$$

see [307] for a detailed explanation. Here, ρ is the average curvature radius of an accelerating ion, assumed to be independent of the ion energy. The energy change per unit length of an accelerating ion having charge Z and mass $m_i = \mu m_p$ is given by

$$d\epsilon/ds = eZ\Delta V/h - P/c, \tag{44}$$

where h is the gap height. After integration from $s = 0$ to h, the maximum acceleration energy is obtained

$$E_{\max} = 3 \times 10^{19}\mu Z^{1/4} M_9^{1/2} B_4^{1/4}(\rho^2 h/R_g^3)^{1/4} \quad \text{eV}. \tag{45}$$

Consequently, only a fraction

$$\eta = 0.1\mu M_9^{-1/2}(ZB_4)^{-3/4}(\rho/R_g)^{1/2}(h/R_g)^{-7/4}; \quad \eta \leq 1, \tag{46}$$

[24] Indeed, the term "quasar remnants" was introduced by Chokshi and Turner [302] to describe the present-epoch population of dead quasars harboring supermassive black hole nuclei.

of the potential energy available will be released as UHECRs; the rest will be radiated in the form of curvature photons.

For a proton, the suppression ratio is $E/[e(V)] \approx [(50M_9)^{-1/2}{B_4}^{-3/4}]r^{1/2}$, where r denotes the magnetic field curvature in units of the Schwarzschild radius ($h \sim R_g$) [298]. For $r \approx 1$ and $\dot{M} \approx (0.1 - 10)$ $M_\odot$ yr^{-1}, and using the previous equations,

$$E_{\rm max} = (1.0 - 1.8) \times 10^{20} {M_9}^{1/4} \text{ eV}. \quad (47)$$

Heavier nuclei would reach higher energies, but are subject to photo-disintegration. For highly energetic protons, energy losses due to photo-pion production in collisions with ambient photons also becomes a relatively important effect. A lower limit to the radiation length ($\Lambda_{\rm min}$) for the proton energy loss associated with photo-pion production is estimated by considering the population of target photons within the source region [$R(\text{source radius}) \geq 2GM/c^2$] at radio frequencies $\nu \geq 360(\Gamma/10^{11})^{-1}$ GHz is given by [298]

$$\begin{aligned} \Lambda/R &= c\pi R/(\langle K\sigma_{p\gamma}\rangle Q) \quad (48) \\ &= (278/\langle K\sigma_{p\gamma,\mu\rm b}\rangle)(R/R_S)M_9(Q/10^{53}\ \text{s}^{-1})^{-1}, \end{aligned}$$

where $\sigma_{p\gamma,\mu\rm b} \equiv \sigma_{p\gamma}/10^{-30}$ cm^2, R_S is the Schwarzschild radius (twice the gravitational radius $R_g = GM$), $K \equiv \langle E(\text{loss})\rangle/E(\text{initial})$ is the inelasticity in a single collision [308] and Q is the core emission rate (photons s^{-1}) for electromagnetic radiation at $\nu > 360$ GHz, given by $Q = h^{-1}\int \nu^{-1}L_\nu d\nu$ where h is the Planck constant and $L_\nu = 4\pi D^2 F_\nu$ for a source of spectral density F_ν at distance D. A useful approximation is that [298] $\langle K\sigma_{p\gamma,\mu\rm b}\rangle \equiv \left[\int (K\sigma_{p\gamma,\mu\rm b}(dQ/d\nu)d\nu\right]/Q < 120$ μb. Those quasar remnants with $\Lambda_{\rm min} > R$ are expected to successfully accelerate protons up to $\sim E_{\rm max}$. Noteworthy, the observed flux of CRs would apparently drain only a negligible amount of energy from the black hole dynamo, since replenishing the particles ejected at high energies ($> 10^{20}$ eV) would only require a minimal mass input: a CR luminosity of 10^{42} ergs/s in such particles (if protons) corresponds to a rest mass loss rate of less than $10^{-5}M_\odot$ in a Hubble time.

2. Correlations of UHECRs with QRs

The first analysis of possible correlations between UHECRs and QRs was carried out in Ref. [309], where, imposing very restrictive selection criteria –those necessary for obtaining candidate objects providing the most favorable setting for a black hole based compact dynamo model of UHECR production– a group of galaxies from the Nearby Optical Galaxy (NOG) catalog of Giuricin et al. [310] was a priori selected as

individual plausible sources of CRs.[25] It was found that nearby QR candidates present an above-random positional correlation with the sample of UHECRs. Surprisingly, this correlation appears on closer angular scales than that expected when taking into account the deflection caused by typically assumed intergalactic or Galactic magnetic fields.[26]

As one can see using Eq. (8), scattering in large scale magnetic irregularities $\mathcal{O}$ (nG) are enough to bend the orbits of super-GZK protons by about 4 deg in a 50 Mpc traversal (see, however, Ref. [311]). The CR angular offsets observed for the quasar remnants in Ref. [309] are much smaller than θ whereas, for a variety of assumed magnetic field scenarios, θ is often substantially larger than the estimated AGASA measurement error of 1.6 degrees. Should the apparent clustering of correlated pairs be supported by future data, perhaps a viable scenario under which this could occur is that in which the intergalactic medium between Earth and the three apparently 'clustered' quasar remnants is sufficiently different from the intergalactic medium in front of the remaining nine objects that are much more uniformly distributed on the accessible sky. This appears at least plausible judging from the 100 micron map of the region shown in Fig. 7.

For the deflection of an energetic (60 EeV) proton in traversing 34 Mpc (the mean of the QRs distances in Table 3 of [309]) to be less than a degree, the magnetic field must fulfill $B < 2 \times 10^{-10}\ \ell^{-1/2}$ G, which appears to be not drastically different from the canonical nG B field and the usually assumed coherence length ~ 1 Mpc. Also, in some directions, the magnetic field of our own galaxy could well lead to a deflection of up to several degrees for primaries with energies below 60 EeV; see, for instance, Table 1 of Ref. [133]. A recent study of this issue was presented by Alvarez-Muñiz et al. [312]. However, a possible filamentary topology of the Galaxy's magnetic field would likely allow some directional windows, albeit narrow, where the deflection of an UHECR could be much less than typical.

In a very recent paper, Isola et al. [313] have studied predictions for large and small scale UHECR arrival direction anisotropies in a scenario where the particles are injected with a mono-energetic spectrum (all particles coming from a source are emitted with the maximal energy of acceleration for that source as derived in that same paper) by a distribution of QRs. They find that the sample of (37) QRs they considered is distributed too anisotropically to explain the isotropic ultra high energy CR flux except in the case where extragalactic magnetic fields of $\simeq 0.1\mu$G extend

[25] The latter catalog is a complete magnitude-limited (corrected blue total magnitude $B \leq 14$), distance-limited (redshift $z \leq 0.02$) sample of several thousand galaxies of latitude $|b| > 20^\circ$.

[26] Deflections due to the magnetic fields would of course be avoided if the primary were a photon, generated in the neighborhood of the QR via an accelerated charged particle interaction.

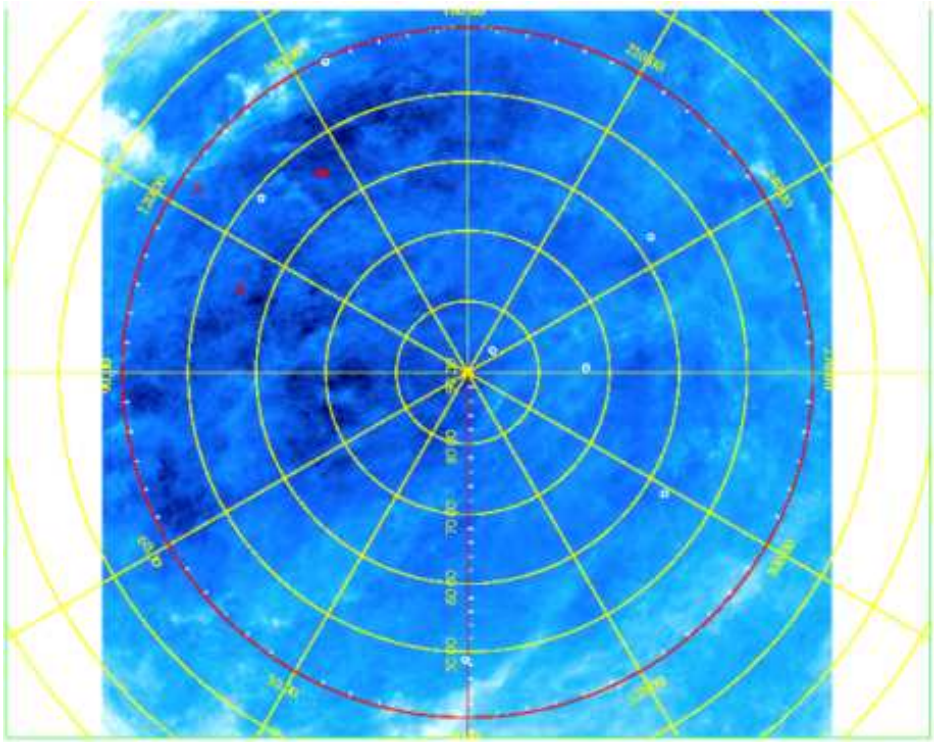

FIG. 7: IRAS 100 micron view of the North Galactic Pole (white=high flux, dark blue=low flux), towards the region of several QRs that appear coinciding with UHECRs. Small circles mark the 12 galaxies (candidate quasar remnants) in the sample of Ref. [309]. Red circles mark galaxies perhaps associated with UHECRs; white circles mark galaxies without associated UHECRs. Note that the palusible UHECR sources tend to be found in directions of lower 100 micron flux, [UHECR-coinciding source directions present IRAS fluxes 0.614 ± 0.022 MJy/sr whereas the directions towards those galaxies non-coinciding with UHECRs presnet 1.68 ± 0.63 MJy/sr.] To the extent that the 100 micron flux traces the Galactic dust and magnetic field, then CRs are likely to be better aligned with their sources in directions of low flux. Figure courtesy of Tim Hamilton.

over many Mpc. As statistical quantities for this analysis spherical multi-poles and the autocorrelation function were used. For a weak magnetic field, of order 1 nG, the predictions appear to be inconsistent with the observed distribution of arrival directions of UHECRs, because the magnetic field is too weak to isotropize the distribution coming from a limited number of non-uniformly distributed sources, as already pointed out in Ref. [255]. Isola et al. also found that the contribution from the farthest sources is completely negligible even for this weak magnetic field. None of the objects that were found close to UHECR positions in the Torres et al. previous set were included in the Isola et al. sample. Little further progress regarding possible correlation of sources can be made until a much more larger set of UHECRs is recorded, something that will

have to wait to the operation of PAO.

3. TeV emission from QRs

A concomitant effect of UHECR emission from QRs is that, as shown by Levinson [314], the dominant fraction of the rotational energy extracted from the black hole is radiated in the TeV band. He showed that the spectrum produced by the curvature radiation of a single ion will peak at an energy

$$E_{\gamma\,\max} = 1.5\Gamma^3\hbar c/\rho \quad (49)$$

$$= 1.6\times10^{-7}E_{\max}\mu^{-1}(ZB_4)^{1/2}(h/R_g)^{1/2} \quad (50)$$

$$= 5M_9^{1/2}(ZB_4)^{3/4}(\rho^2h^3/R_g^5)^{1/4}\mathrm{TeV}, \quad (51)$$

and is a power law $I(E_\gamma)\propto(E_\gamma)^{1/3}$ below the cutoff. The overall spectrum of curvature photons would depend on the energy distribution of the accelerating particles, and is expected to be somewhat softer below the peak. For $E_{\max}=3\times10^{20}$ eV and $h\sim R_g$, $E_{\gamma\,\max}\simeq50\mu^{-1}(ZB_4)^{1/2}$ TeV. Then, provided that vaccum breakdown does not occur, and that TeV photons can escape the system, QRs should emit γ-rays.

Indeed, it was recently noted by Neronov et al. [315] that the concomitant TeV radiation would be at a level sufficiently high as to be (for many combination of the system parameters) ruled out by bounds imposed by HEGRA/AIROBICC.

Recent numerical simulations additionally suggest that the accretion process and magnetic field structure in the vicinity of the horizon can be non-stationary, owing to rapid magnetic field reconnection [316]. This would probably lead to appreciable complications of the model, as the location of the gap, the injection of seed particles into the gap, and, perhaps, the voltage drop across it might change with time. How should this affect the picture described above is unclear at present.

F. Starbursts

1. What are they?

Starbursts are galaxies (sometimes, the term also refers only to particular regions of galaxies) undergoing a large-scale star formation episode. They feature strong infrared emission originating in the high levels of interstellar extinction, strong HII-region-type emission-line spectrum (due to a large number of O and B-type stars), and considerable radio emission produced by recent SNRs. Typically, starburst regions are located close to the galactic center, in the central kiloparsec. This region alone can be orders of magnitude brighter than the center of normal spiral galaxies. From such an active

region, a galactic-scale superwind is driven by the collective effect of supernovae and particular massive star winds. The enhanced supernova explosion rate creates a cavity of hot gas ($\sim 10^8$ K) whose cooling time is much greater than the expansion time scale. Since the wind is sufficiently powerful, it can blow out the interstellar medium of the galaxy, preventing it from remaining trapped as a hot bubble. As the cavity expands, a strong shock front is formed on the contact surface with the cool interstellar medium. The shock velocity can reach several thousands of kilometers per second and ions like iron nuclei can be efficiently accelerated in this scenario, up to ultrahigh energies, by Fermi's mechanism [317]. If the super-GZK particles are heavy nuclei from outside our Galaxy, then the nearby ($\sim$ 3 Mpc [318]) starburst galaxies M82 ($l = 141°, b = 41°$) and NGC 253 ($l = 89°, b = -88°$) are prime candidates for their origin.

2. M82 and NGC253

M82 is probably the best studied starburst galaxy, located at only 3.2 Mpc. The total star formation rate in the central parts is at least ~ 10 $M_\odot$ yr^{-1} [319]. The far infrared luminosity of the inner region within 300 pc of the nucleus is $\sim 4 \times 10^{10}$ $L_\odot$ [320]. There are $\sim 1 \times 10^7$ $M_\odot$ of ionized gas and $\sim 2 \times 10^8$ $M_\odot$ of neutral gas in the IR source [320, 321]. The total dynamical mass in this region is $\sim (1-2) \times 10^9$ $M_\odot$ [321]. The main observational features of the starburst can be modelled with a Salpeter IMF extending from 0.1 to 100 $M_\odot$. The age of the starburst is estimated in $\sim (1-3) \times 10^7$ yr [320]. Around $\sim 2.5 \times 10^8$ $M_\odot$ (i.e. ~ 36 % of the dynamical mass) is in the form of new stars in the burst [321]. The central region, then, can be packed with large numbers of early-type stars.

NGC 253 has been extensively studied from radio to γ-rays (e.g. [322, 323, 324]). A TeV detection was reported by CANGAROO [325], but has been yet unconfirmed by other experiments. More than 60 individual compact radio sources have been detected within the central 200 pc [326], most of which are supernova remnants (SNRs) of only a few hundred years old. The supernova rate is estimated to be as high as $0.2 - 0.3$ yr^{-1}, comparable to the massive star formation rate, $\sim 0.1 M_\odot$ yr^{-1} [326, 327]. The central region of this starburst is packed with massive stars. Four young globular clusters near the center of NGC 253 can account for a mass well in excess of $1.5 \times 10^6 M_\odot$ [328, 329]. Assuming that the star formation rate has been continuous in the central region for the last 10^9 yrs, and a Salpeter IMF for 0.08-100 $M_\odot$, the bolometric luminosity of NGC 253 is consistent with $1.5 \times 10^8 M_\odot$ of young stars [328]. Based on this evidence, it appears likely that there are at least tens of millions of young stars in the central region of the starburst. These stars can also contribute to the γ-ray luminosity at high energies [151, 330]. Physical, morphological, and kinematic evidence for the existence of a galactic superwind has been found for NGC 253 [331]. Shock interactions with

low and high density clouds can produce X-ray continuum and optical line emission, respectively, both of which have been directly observed.

A region about 1 kpc of the M82 galactic center appears to be a fossil starburst, presenting a main sequence stellar cutoff corresponding to an age of 100-200 Myr and a current average extinction of 0.6 mag (compare with the extinction of the central and current starburst region, 2.2 mag) whereas, nearby globular glusters age estimations are between 2×10^8 and 10^9 yr [332]. It appears possible for this galaxy, then, that a starburst (known as M82 "B") of similar amplitude than the current one was active in the past.

3. Two-step acceleration-process in starbursts

The acceleration of particles in starburst galaxies is thought to be a two-stage process [317]. First, ions are thought to be diffusively accelerated at single SNRs within the nuclear region of the galaxy. Energies up to $\sim 10^{14-15}$ eV can be achieved in this step (see, e.g. [333]). Due to the nature of the central region, and the presence of the superwind, the escape of the iron nuclei from the central region of the galaxy is expected to be dominated by convection.[27] Collective plasma motions of several thousands of km per second and the coupling of the magnetic field to the hot plasma forces the CR gas to stream along from the starburst region. Most of the nuclei then escape through the disk in opposite directions along the symmetry axis of the system, being the total path travelled substantially shorter than the mean free path.

Once the nuclei escape from the central region of the galaxy they are injected into the galactic-scale wind and experience further acceleration at its terminal shock. CR acceleration at superwind shocks was first proposed in Ref. [335] in the context of our own Galaxy. The scale length of this second shock is of the order of several tens of kpc (see Ref. [318]), so it can be considered as locally planar for calculations. The shock velocity $v_{\rm sh}$ can be estimated from the empirically determined superwind kinetic energy flux $\dot{E}_{\rm sw}$ and the mass flux $\dot{M}$ generated by the starburst through: $\dot{E}_{\rm sw} = 1/2 \dot{M} v_{\rm sh}^2$. The shock radius can be approximated by $r \approx v_{\rm sh}\tau$, where τ is the starburst age.

[27] The relative importance of convection and diffusion in the escape of the CRs from a region of disk scale height h is given by the dimensionless parameter, $q = V_0\, h/\kappa_0$, where V_0 is the convection velocity and κ_0 is the CR diffusion coefficient inside the starburst [334]. When $q \lesssim 1$, the CR outflow is difussion dominated, whereas when $q \gtrsim 1$ it is convection dominated. For the central region of NGC 253 a convection velocity of the order of the expanding SNR shells ~ 10000 km s^{-1}, a scale height $h \sim 35$ pc, and a reasonable value for the diffusion coefficient $\kappa_0 \sim 5 \times 10^{26}$ cm^2 s^{-1} [193], lead to $q \sim 216$. Thus, convection dominates the escape of the particles. The residence time of the iron nuclei in the starburst results $t_{\rm RES} \sim h/V_0 \approx 1 \times 10^{11}$ s.

Since the age is about a few tens of million years, the maximum energy attainable in this configuration is constrained by the limited acceleration time arising from the finite shock's lifetime. For this second step in the acceleration process, the photon field energy density drops to values of the order of the cosmic background radiation (we are now far from the starburst region), and consequently, iron nuclei are safe from photodissociation while energy increases to $\sim 10^{20}$ eV.

To estimate the maximum energy that can be reached by the nuclei, consider the superwind terminal shock propagating in a homogeneous medium with an average magnetic field B. If we work in the frame where the shock is at rest, the upstream flow velocity will be $\mathbf{v_1}$ ($|\mathbf{v_1}| = v_{\rm sh}$) and the downstream velocity, $\mathbf{v_2}$. The magnetic field turbulence is assumed to lead to isotropization and consequent diffusion of energetic particles which then propagate according to the standard transport theory [336]. The acceleration time scale is then [337]: $t_{\rm acc} = \frac{4\kappa}{v_1^2}$ where κ is the upstream diffusion coefficient which can be written in terms of perpendicular and parallel components to the magnetic field, and the angle θ between the (upstream) magnetic field and the direction of the shock propagation: $\kappa = \kappa_\parallel \cos^2\theta + \kappa_\perp \sin^2\theta$. Since strong turbulence is expected from the shock we can take the Bohm limit for the upstream diffusion coefficient parallel to the field, i.e. $\kappa_\parallel = \frac{1}{3}E/ZeB_1$, where B_1 is the strength of the pre-shock magnetic field and E is the energy of the Z-ion. For the $\kappa_\perp$ component we shall assume, following Biermann [338], that the mean free path perpendicular to the magnetic field is independent of the energy and has the scale of the thickness of the shocked layer ($r/3$). Then, $\kappa_\perp = 1/3\ r(v_1 - v_2)$ or, in the strong shock limit, $\kappa_\perp = rv_1^2/12$. The upstream time scale is $t_{\rm acc} \sim r/(3v_1)$, $r/3v_1 = 4/v_1^2\left(E/(3ZeB_1)\cos^2\theta + rv_1^2/12\sin^2\theta\right)$. Thus, using $r = v_1\tau$ and transforming to the observer's frame one obtains

$$E_{\rm max} \approx \frac{1}{4}ZeBv_{\rm sh}^2\tau \approx \frac{1}{2}ZeB\frac{\dot{E}_{\rm sw}}{\dot{M}}\tau. \qquad (52)$$

The predicted kinetic energy and mass fluxes of the starburst of NGC 253 derived from the measured IR luminosity are 2×10^{42} erg s^{-1} and 1.2 M$_\odot$ yr^{-1}, respectively [318]. The starburst age is estimated from numerical models that use theoretical evolutionary tracks for individual stars and make sums over the entire stellar population at each time in order to produce the galaxy luminosity as a function of time [320]. Fitting the observational data these models provide a range of suitable ages for the starburst phase that, in the case of NGC 253, goes from 5×10^7 to 1.6×10^8 yr (also valid for M82) [320]. These models must assume a given initial mass function (IMF), which usually is taken to be a power-law with a variety of slopes. Recent studies has shown that the same IMF can account for the properties of both NGC 253 and M82 [339]. Finally, the radio and γ-ray emission from NGC 253 are well matched by models with $B \sim 50\mu$ G [323]. With these figures, already assuming a conservative age $\tau = 50$ Myr, one obtains a maximum energy for iron nuclei of $E_{\rm max}^{\rm Fe} > 3.4 \times 10^{20}$ eV.

4. The starburst hypothesis: UHECR-luminosity and correlations

For an extragalactic, smooth, magnetic field of $\approx 15-20$ nG, diffusive propagation of nuclei below 10^{20} eV evolves to nearly complete isotropy in the CR arrival directions [340, 341]. Thus, we could use the rates at which starbursts inject mass, metals and energy into superwinds to get an estimate of the CR-injection spectra. Generalizing the procedure discussed in Sec. II D 3 –using equal power per decade over the interval $10^{18.5}\,\mathrm{eV} < E < 10^{20.6}\,\mathrm{eV}$ – we obtain a source CR-luminosity

$$\frac{E^2\,dN_0}{dE\,dt} \approx 3.5\,\varepsilon\,10^{53}\mathrm{eV/s} \tag{53}$$

where ε is the efficiency of ultra high energy CR production by the superwind kinetic energy flux. With this in mind, the energy-weighted, approximately isotropic nucleus flux at 10^{19} eV is given by [340]

$$E^3J(E) = \frac{Ec}{(4\pi)^2 d\,D(E)}\frac{E^2\,dN_0}{dE\,dt}\,I_\star \approx 2.3\times10^{26}\,\epsilon\,I_\star\,\mathrm{eV^2\,m^{-2}\,s^{-1}\,sr^{-1}}, \tag{54}$$

where $I_\star = I_{\rm M82} + I_{\rm NGC\ 253}$. To estimate the diffusion coefficient we used $B_{\rm nG} = 15$, $\ell_{\rm Mpc} = 0.5$, and an average $Z = 20$. We fix

$$\epsilon\,I_\star = 0.013, \tag{55}$$

after comparing Eq.(54) to the observed CR-flux. Note that the contribution of $I_{\rm M82}$ and $I_{\rm NGC\ 253}$ to $I_\star$ critically depends on the age of the starburst. The relation "starburst-age/superwind-efficiency" derived from Eq. (55), leads to $\epsilon \approx 10\%$, if both M82 and NGC 253 were active for 115 Myr. The power requirements may be reduced assuming contributions from M82 "B" [340].

Above $> 10^{20.2}$ eV iron nuclei do not propagate diffusively. Moreover, the CR-energies get attenuated by photodisintegration on the CMB and the intergalactic infrared background photons. However, the energy-weighted flux beyond the GZK-energy due to a single M82 flare

$$E^3J(E) = \frac{E}{(4\pi d)^2}\frac{E_0^2\,dN_0}{dE_0\,dt}\,e^{-Rt/56} \approx 2.7\times10^{25}E_{20}\epsilon\,e^{-Rt/56}\,\mathrm{eV^2\,m^{-2}\,s^{-1}\,sr^{-1}}, \tag{56}$$

is easily consistent with observation [340]. Here, R is the effective nucleon loss rate of the nucleus on the CBM [107].

In the non-diffusive regime (i.e., $10^{20.3}$ eV $\lesssim E \lesssim 10^{20.5}$ eV), the accumulated deflection angle from the direction of the source in the extragalactic B-field is roughly $10^\circ \lesssim \theta \lesssim 20^\circ$ [341]. The nuclei suffer additional deflection in the Galactic magnetic field. In particular, if the Galactic field is of the ASS type, the arrival direction of

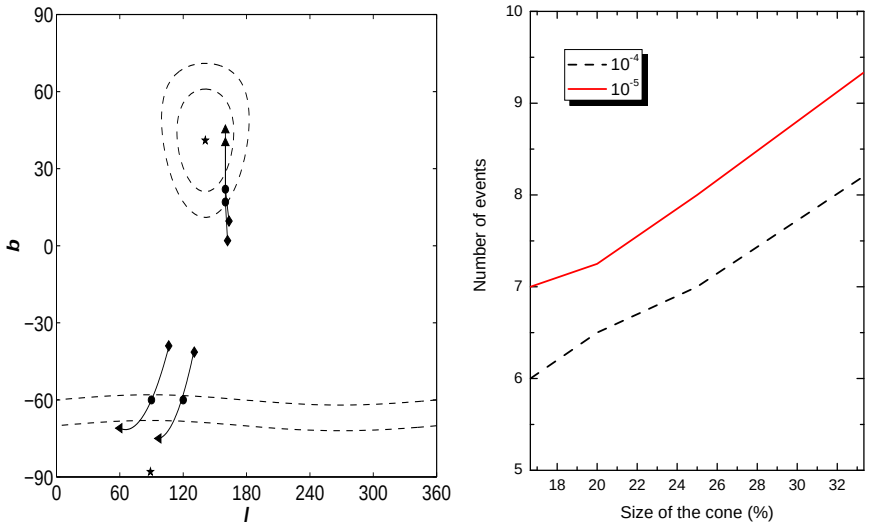

FIG. 8: Left: Directions in Galactic coordinates of the four highest energy CRs at the boundary of the Galactic halo. The diamonds represent the observed incoming directions. The circles and arrows show the directions of neon and iron nuclei, respectively, before deflection by the Galactic magnetic field. The solid line is the locus of incoming directions at the halo for other species with intermediate atomic number. The stars denote the positions of M82 and NGC253. The dashed lines are projections in the (l, b) coordinates of angular directions within 20° and 30° of the starbursts. Right: Curves of constant probabilities in the two-dimensional parameter space defined by the size of the cone and the minimum number of events originating within the resulting effective solid angle [342].

the 4 highest energy CRs can be traced backwards to one of the starbursts [342]. Figure 8 shows the extent to which the observed arrival directions of the highest energy CRs deviate from their incoming directions at the Galactic halo because of bending in the magnetic field given in Eq. (13). The incoming CR trajectories are traced backwards up to distances of 20 kpc away from the Galactic center, where the effect of the magnetic field is negligible. The diamond at the head of each solid line denotes the observed arrival direction, and the points along these lines indicate the direction from which different nuclear species (with increasing mass) entered the Galactic halo. In particular, the tip of the arrows correspond to incoming directions at the halo for iron nuclei, whereas the circles correspond to nuclei of neon. Regions within the dashed lines comprise directions lying within 20° and 30° degrees of the starbursts. It is seen that trajectories for CR nuclei with $Z \geq 10$ can be further traced back to one of the starbursts, within the uncertainty of the extragalactic deviation.

The effects of the BSS configuration are completely different. Because of the averaging over the frequent field reversals, the resulting deviations of the CR trajectories

are markedly smaller, and in the wrong direction for correlation of current data with the starburst sources. We note that the energy-ordered 2D correlation distribution of the AGASA data is in disagreement with expectations for positively charged particles and the BSS configuration [312].

We now attempt to assess to what extent these correlations are consistent with chance coincidence. We arrive at the effective angular size of the source in a two-step process. Before correcting for bias due to the coherent structure of the Galactic magnetic field, the deflections in the extragalactic and Galactic fields (regular and random components) may be assumed to add in quadrature, so that the angular sizes of the two sources are initially taken as cones with opening half-angles between 40° and 60°, which for the purpose of our numerical estimate we approximate to 50°. However, the global structure of the field will introduce a strong bias in the CR trajectories, substantially diminishing the effective solid angle. The combined deflections in the l and b coordinates mentioned above concentrate the effective angular size of the source to a considerably smaller solid angle. As a conservative estimate, we retain 25% of this cone as the effective source size. A clear prediction of this consideration is then that the incoming flux shows a strong dipole anisotropy in the harmonic decomposition.

Now, by randomly generating four CR positions in the portion of the sky accessible to the existing experiments (declination range $\delta > -10°$), an expected number of random coincidences can be obtained. The term "coincidence" is herein used to label a synthetic CR whose position in the sky lies within an effective solid angle $\Omega_{\rm eff}$ of either starburst. $\Omega_{\rm eff}$ is characterized by a cone with opening half-angle reduced from 50° to 24° to account for the 75% reduction in effective source size due to the magnetic biasing discussed above. Cosmic ray positional errors were considered as circles of 1.6° radius for AGASA. For the other experiments the asymmetric directional uncertainty was represented by a circle with radius equal to the average experimental error. The random prediction for the mean number of coincidences is 0.81 ± 0.01. The Poisson probability [28] for the real result to be no more than the tail of the random distribution is 1%. Alternatively, we may analyze this in terms of confidence intervals. For the 4 observed events, with zero background, the Poisson signal mean 99% confidence interval is $0.82 - 12.23$ [294]. Thus our observed mean for random events, 0.81 ± 0.01, falls at the lower edge of this interval, yielding a 1% probability for a chance occurrence. Of course, this is not compelling enough to definitively rule out chance probability as generating the correlation of the observed events with the candidate sources, but it is suggestive enough to deserve serious attention in analyses of future data.

Assuming an extrapolation of AGASA flux ($E^3 J_{\rm obs}(E)$) up to $10^{20.5}$ eV, the event

[28] Because of constraints inherent in partitioning events among clusters, the distributions are very close to, but not precisely Poisson [76].

rate at Pampa Amarilla[29] is given by

$$\frac{dN}{dt} = A \int_{E_1}^{E_2} E^3 J(E) \frac{dE}{E^3} \approx \frac{A}{2} \langle E^3 J(E) \rangle \left[\frac{1}{E_1^2} - \frac{1}{E_2^2} \right] \approx 5.3 \text{ yr}^{-1} , \qquad (57)$$

where $E_1 = 10^{20.3}$ eV and $E_2 = 10^{20.5}$ eV. Considering a 5-year sample of 25 events and that for this energy range the aperture of PAO is mostly receptive to cosmic rays from NGC253, we allow for different possibilities of the effective reduction of the cone size because of the Galactic magnetic field biasing previously discussed. In Fig. 8 we plot contours of constant probabilities ($P = 10^{-4},\ 10^{-5}$) in the two-dimensional parameter space of the size of the cone (as a fraction of the full 50° circle) and the minimum number of events originating within the resulting effective solid angle. The model predicts that after 5 years of operation, all of the highest energy events would be observed in the aperture described above. Even if 7 or 8 are observed, this is sufficient to rule out a random fluctuation at the 10^{-5} level. Thus, a clean test of the starburst hypothesis can be achieved at a very small cost: $< 10^{-5}$ out of a total 10^{-3} PAO probability budget [343].

G. Luminous Infrared Galaxies

1. Definition

In carrying to the extreme the concept of a starburst, we find the powerful luminous infrared galaxies (LIGs). At luminosities above 10^{11} $L_\odot$, LIGs ($L_{\rm FIR} > 10^{11}$ $L_\odot$) are the dominant extragalactic objects in the local universe ($z < 0.3$) with such high luminosities. Some, having $L_{\rm FIR} > 10^{12}$ $L_\odot$, are the most luminous local objects (see [344] for a review). These galaxies possess very large amounts of molecular material (e.g., [345, 346, 347, 348, 349]). They present large CO luminosities, but also a high value for the ratio $L_{\rm FIR}/L_{\rm CO}$, both being about one order of magnitude greater than for spirals, implying a higher star formation rate per solar mass of gas.[30] LIGs are generally regarded as recent galaxy mergers in which much of the gas of the colliding objects has fallen into a common center (typically less than 1 kpc in extent), triggering a huge starburst phenomenon [344]. There is evidence for the existence of even more

[29] The Southern Site of PAO has been christened Pampa Amarilla. Recall that it has an aperture $A \approx 7000$ km^2 sr for showers with incident zenith angle less than 60°.

[30] For stars to form, a large mass fraction at high density, $dM/d(\log n)$, is required. The Milky Way has an order of magnitude more gas at less than 300 cm^{-3} than what it has at 10^4 cm^{-3}, contrary to LIGs, which have nearly equal mass per decade of density between 10^2 and 10^4 cm^{-3} (see, e.g., Ref. [348, 349])

extreme enviroments within LIGs (see, e.g., [345]): These, larger than giant molecular clouds but with densities found only in small cloud cores, appear to be the most outstanding star formation places in the universe. They are well traced by HCN emission, i.e., they produce a substantial fraction of the whole HCN emission observed for the whole galaxy [345], see also [350, 351]. The CR enhancement factor in these small but massive regions can well exceed the average value for the galaxy. In Arp 220, for instance, two such regions were discovered to contain about 2×10^9 $M_\odot$ [345]. If the CR enhancement in these regions is significantly larger than the starburst average, these extreme environments could be the main origin for any γ-ray emission observed from this galaxy [352].

2. Propagation and further studies

Using the PSCz catalogue [353], Smialkowski et al. [354] constructed all-sky maps of UHE proton intensities plausibly originating in LIGs, taking into account effects of particle propagation through the extragalactic medium and the possible influence of the regular galactic magnetic field. The PSCz catalogue consists of almost 15000 IR galaxies with known redshifts, covering 84% of the sky. Finding correlations with such an overdistributed sample might be thought as a risky business. There are, however, some phenomenological reasons —apart of LIGs being super-starbursts— to search for a possible UHECR origin in LIGs.

Arp 299, one of the the brightest infrared source within 70 Mpc and a system of colliding galaxies showing intense starburst, appeared earlier as VV 118 in the list of candidates for the AGASA triplet presented by in Ref. [74, 137, 140]. Indeed, for Arp 299, even when a hidden AGN was observed, it can not account for the whole FIR luminosity [355] and a strong starburst activity is required to explain it. It might be considered as a prime candidate for the origin of the triplet [354], if such is not a statistical fluctuation.

Equatorial maps of the expected intensity of the UHE protons originating in LIGs for the energy region 40-80 EeV with sky coverage and declination dependent exposure for the AGASA experiment were presented in Ref. [354]. Expected proton intensities for 40-80 EeV appear to show good correlation with the distribution of the experimental events from AGASA, especially, from the region of the sky near Arp 299 and the AGASA triplet of events (RA$\approx$ 170°, $\delta \approx$ 60°). No correlation of the data events above 80 EeV with the expected CR intensities was reported.

The latter result was confirmed in Ref. [203], where application of the Kolmogorov-Smirnov (KS) to the 11 highest AGASA events above 10^{20} eV yields a KS probability of $< 0.5\%$, rejecting the possible association at $> 99.5\%$ significance level. This was used to argue that the existing CR events above 10^{20} eV do not owe their origin to

long burst GRBs, rapidly rotating magnetars, or any other events associated with core collapse supernovae (although it would yet be too early to completely rule out such a possibility, based only in a 2σ deviation).[31]

A more sensitive approach to study a possible LIG origin of UHECRs, perhaps, is not to look for possible correlations between the whole PSCz calatog and UHECRs, but rather to select *a priori* which LIGs are most likely to be detectable by their possible UHECR emission. There are several LIGs for which reasonable values of CR enhancements, comparable to, or lower than, the ratio between their SFR and the Milky Way's, can provide a γ-ray flux above GLAST sensitivity, and if the CR spectrum is sufficiently hard, also above the sensitivities of the new Čerenkov telescopes. These LIGs are then most likely to appear as new point-like γ-ray sources. Even when it is natural to expect that a LIG will emit γ-rays, only the more gaseous, nearby, and CR-enhanced galaxies are the ones which could be detected as γ-ray point sources [352].

Out of the HCN just presented in Refs. [350, 351][32] and the larger Pico dos Dias Survey (PDS, [358])[33], the most likely γ-ray sources are listed in Table I, together with EGRET fluxes upper limits, obtained in [352]. In our opinion, this group, as well as the HCN and the PDS should be separately taken into account when searching for

[31] Following [203], the core collapse supernova rate per galaxy, summed over all galaxy types, is $\dot{S}_{\rm sn} \approx 0.011$ SN per galaxy-year [205], which yields a volume averaged rate of supernovae of $\dot{S}_{\rm sn} n_{\rm g} \approx 2.2 \times 10^{-4}$ SN/Mpc^3-year. The supernova rate for galaxies with far infrared emission is $\dot{S}_{\rm sn}^{\rm fir} = 2.5 \times 10^{-4} L_{10}$ SN/(FIR galaxy)-year [356]. Integrating this supernova rate over the FIR galaxy luminosity function yields $\dot{S}_{\rm sn}^{\rm fir} n_{\rm firg} \approx 0.7 \times 10^{-4} K_{\rm obsc} (L_{10}^{\rm max}/300)$ SN/Mpc^3-year. $K_{\rm obsc}$, the correction for supernovae missed in the existing optical and near infrared supernova detection surveys, might be as large as 10, and probably is at least as large as 3 [356]. Thus, the luminous infrared galaxies contribute at least 28% ($K_{\rm obsc} = 1$) of the total supernova rate, with a total space density only 25% that of all normal galaxies. Furthermore, since the brightest infrared galaxies ($L_{\rm FIR} > 10^{12}\ L_\odot$) dominate the contribution from all FIR galaxies, and these are quite rare, with space density $\sim 4 \times 10^{-8}$ Mpc^{-3} [357], correlations of UHECR arrival directions with the sky positions of the luminous IRAS galaxies offers a promising opportunity to test the hypothesis that UHECR acceleration has something to do with core collapse supernovae, as is implied by the GRB shock and magnetar unipolar inductor models for the acceleration sites.

[32] This survey is a systematic observation (essentially, all galaxies with strong CO and IR emission were chosen for HCN survey observations) of 53 IR-bright galaxies, including 20 LIGs with $L_{\rm FIR} > 10^{11} {\rm L}_\odot$, 7 with $L_{\rm FIR} > 10^{12} {\rm L}_\odot$, and more than a dozen of the nearest normal spiral galaxies. It also includes a literature compilation of data for another 9 IR-bright objects. This is the largest and most sensitive HCN survey (and thus of dense interstellar mass) of galaxies to date.

[33] The PDS survey consists of relatively nearby and luminous starbursts galaxies selected in the FIR. PDS galaxies have a lower mean IR luminosity $\log({\rm L_{IR}/L_\odot}) = 10.3 \pm 0.5$, redshifts smaller than 0.1, and form a complete sample limited in flux in the FIR at 2×10^{-10} erg cm^{-2} s^{-1}.

TABLE I: Powerful local LIGs (all with interferometric measurements) likely to be detected by GLAST, with EGRET upper limits. The luminosity distance in an standard universe ($D_L = c/H_0 {q_0}^2[1 - q_0 + q_0 z + (q_0 - 1)(2q_0 z + 1)^{1/2}]$, H_0 ($\sim$75 km s^{-1} Mpc^{-1}) is the Hubble parameter, q_0 ($\sim$0.5) is the deceleration parameter, and z is the redshift), the central-sphere radius from which the line emission was detected, the FIR luminosity and gas mass are also given. The minimum average value of CR enhancement k for which the γ-ray flux above 100 MeV is above 2.4 $\times 10^{-9}$ photons cm^{-2} s^{-1}, i.e. GLAST sensitivity is given. The smaller the value of $\langle k \rangle$, the higher the possibility for these Galaxies to appear as γ-ray sources.

Name	D_L [Mpc]	R [pc]	$\log(L_{\rm FIR}/{\rm L}_\odot)$	$\log M({\rm H}_2/{\rm M}_\odot)$	$\langle k \rangle$	$F^{\rm EGRET}_{>100\,{\rm MeV}}$ [10^{-8} photons cm^{-2} s^{-1}]
NGC3079	15	0.26	10.52	9.56	62	<4.4
NGC1068	15	0.10	10.74	9.46	78	<3.6
NGC2146	20	0.33	10.78	9.43	149	<9.7
NGC4038/9	22	0.49	10.65	9.07	412	<3.7
NGC520	29	0.38	10.58	9.47	285	<4.6
IC694	41	0.30	11.41	9.59	432	<2.2
Zw049.057	52	0.40	10.95	9.67	578	<6.9
NGC1614	64	0.60	11.25	9.78	680	<5.0
NGC7469	65	0.82	11.26	9.89	544	<3.2
NGC828	72	0.92	11.03	10.09	421	<6.1
Arp220	72	0.16	11.91	10.43	193	<6.1
VV114	80	0.93	11.35	10.03	597	<3.9
Arp193	94	0.25	11.34	10.22	532	<5.2
NGC6240	98	1.65	11.52	10.03	896	<6.4
Mrk273	152	0.13	11.85	10.33	1081	<2.3
IRAS 17208−0014	173	0.75	12.13	10.67	640	<7.5
VIIZw31	217	1.27	11.66	10.70	940	<3.2

possible UHECR correlations with new sets of data. [34]

[34] A stacking procedure with EGRET data is to be reported by Cillis et al. [359].

H. Gamma-ray bursts

1. Basic phenomenology

Gamma ray bursts (GRBs) are flashes of high energy radiation that can be brighter, during their brief existence, than any other gamma ray source in the sky. The bursts present an amazing variety of temporal profiles, spectra, and timescales that have puzzled astrophysicists for almost three decades [360]. In recent years, our observational insight of this phenomenon has been dramatically improved by the huge amount of data collected by the Burst and Transient Source Experiment (BATSE): several thousand GRB observations were obtained. New breakthrough results are the expected outcome of HETE-2 and Swift.

The temporal distribution of the bursts is one of the most striking signatures of the GRB phenomenon. There are at least four classes of distributions, from single-peaked bursts, including the fast rise and exponential decaying (FREDs) and their inverse (anti-FREDs), to chaotic structures (e.g. [361, 362]). Burst timescales go through the 30 ms scale to hundreds of seconds.

The GRB photon spectrum is well fitted in the BATSE detectors range, 20 keV to 2 MeV [360], by a combination of two power-laws, $dn_\gamma/d\epsilon_\gamma \propto \epsilon_\gamma^{(\alpha-1)}$ (α is the flux density spectral index, $F_\nu \propto \nu^{+\alpha}$) with different values of α at low and high energy [363]. Here, $dn_\gamma/d\epsilon_\gamma$ is the number of photons per unit photon energy. The break energy (where α changes) in the observer frame is typically $\epsilon_{\gamma b} \sim 1$ MeV, with $\alpha \simeq 0$ at energies below the break and $\alpha \simeq -1$ above the break. In several cases, the spectrum has been observed to extend to energies > 100 MeV [360, 364].

The angular distribution of these bursts is isotropic, and the paucity of comparatively faint bursts implies that we are seeing to near the edge of the source population [365]. Both effects, isotropy and non-homogeneity in the distribution, strongly suggest a cosmological origin of the phenomenon, confirmed by the detection of afterglows, delayed low energy emission of GRBs that allowed the measurement of the distance to the burst via a redshift determination of several GRB host-galaxies (e.g. [366, 367]).

2. The fireball model

The most popular interpretation of the GRB-phenomenology is that the observable effects are due to the dissipation of the kinetic energy of a relativistic expanding plasma wind, a "fireball", whose primal cause is not yet known [368, 369, 370, 371, 372, 373, 374] (see [375] for a detailed review). The rapid rise time and short duration, ~ 1 ms of the burst imply that the sources are compact, with a linear scale comparable to a light-ms, $r_0 \sim 10^7$ cm. If the sources are so distant, the energy necessary to produce

the observed events by an intrinsic mechanism is astonishing: about 10^{52} erg of γ rays must be released in less than 1 second. Compactness and high γ-ray luminosity implied by cosmological distances result in a very high optical depth to pair creation, since the energy of observed γ-ray photons is above the threshold for pair production. The number density of photons at the source n_γ is

$$L_\gamma = 4\pi r_0^2 c n_\gamma \epsilon, \tag{58}$$

where $\epsilon \simeq 1$MeV is the characteristic photon energy. Using $r_0 \sim 10^7$cm, the optical depth for pair production at the source is

$$\tau_{\gamma\gamma} \sim r_0 n_\gamma \sigma_T \sim \frac{\sigma_T L_\gamma}{4\pi r_0 c \epsilon} \sim 10^{15}\,. \tag{59}$$

The high optical depth creates the fireball: a thermal plasma of photons, electrons, and positrons. The radiation pressure on the optically thick source drives relativistic expansion, converting internal energy into the kinetic energy of the inflating shell [369, 370]. As the source expands, the optical depth is reduced. If the source expands with a Lorentz factor Γ, the energy of photons in the source frame is smaller by a factor Γ compared to that in the observer frame, and most photons may therefore be below the pair production threshold.

Baryonic pollution in this expanding flow can trap the radiation until most of the initial energy has gone into bulk motion with Lorentz factors of $\Gamma \geq 10^2 - 10^3$ [375, 376]. The kinetic energy, however, can be partially converted into heat when the shell collides with the interstellar medium or when shocks within the expanding source collide with one another. The randomized energy can then be radiated by synchrotron radiation and inverse Compton scattering yielding non-thermal bursts with timescales of seconds, at large radius $r = r_d > 10^{12}$cm, beyond the Thompson sphere. Relativistic random motions are likely to give rise to a turbulent build up of magnetic fields, and therefore to Fermi acceleration of charged particles.

Coburn and Boggs [377] recently reported the detection of polarization, a particular orientation of the electric-field vector, in the γ-rays observed from a burst. The radiation released through synchrotron emission is highly polarized, unlike in other previously suggested mechanisms such as thermal emission or energy loss by relativistic electrons in intense radiation fields. Thus, polarization in the γ-rays from a burst provides direct evidence in support of synchrotron emission as the mechanism of γ-ray production (see also [378]).

3. Fermi acceleration in dissipative wind models of GRBs

Following Hillas' criterion, the Larmor radius $r_{\rm L}$ should be smaller than the largest scale $l_{\rm GRB}$ over which the magnetic field fluctuates, since otherwise Fermi acceleration

will not be efficient. One may estimate $l_{\rm GRB}$ as follows. The comoving time, i.e., the time measured in the fireball rest frame, is $t = r/\Gamma c$. Hence, the plasma wind properties fluctuate over comoving scale length up to $l_{\rm GRB} \sim r/\Gamma$, because regions separated by a comoving distance larger than r/Γ are causally disconnected. Moreover, the internal energy is decreasing because of the expansion and thus it is available for proton acceleration (as well as for γ-ray production) only over a comoving time t. The typical acceleration time scale is then [248]

$$\tau_{\rm acc}^{\rm GRB} \sim \frac{r_{\rm L}}{c\beta^2}\,, \tag{60}$$

where βc is the Alfvén velocity. In the GRB scenario $\beta \sim 1$, so Eq. (60) sets a lower limit on the required comoving magnetic field strength, and the Larmor radius $r_{\rm L} = E'/eB = E/\Gamma eB$, where $E' = E/\Gamma$ is the proton energy measured in the fireball frame.

This condition sets a lower limit for the required comoving magnetic field strength [248],

$$\left(\frac{B}{B_{e.p.}}\right)^2 > 0.15\Gamma_{300}^2 E_{20}^2 L_{51}^{-1}, \tag{61}$$

where $E = 10^{20}E_{20}$eV, $\Gamma = 300\Gamma_{300}$, $L = 10^{51}L_{51}$erg s^{-1} is the wind luminosity, and $B_{e.p.}$ is the equipartition field, i.e. a field with comoving energy density similar to that associated with the random energy of the baryons.

The dominant energy loss process in this case is synchrotron cooling. Therefore, the condition that the synchrotron loss time of Eq. (31) be smaller than the acceleration time sets the upper limit on the magnetic field strength

$$B < 3 \times 10^5 \Gamma_{300}^2 E_{20}^{-2}{\rm G}. \tag{62}$$

Since the equipartition field is inversely proportional to the radius r, this condition may be satisfied simultaneously with (61) provided that the dissipation radius is large enough, i.e.

$$r_d > 10^{12}\Gamma_{300}^{-2}E_{20}^3{\rm cm}. \tag{63}$$

The high energy protons lose energy also in interaction with the wind photons (mainly through pion production). It can be shown, however, that this energy loss is less important than the synchrotron energy loss [248].

A dissipative ultra-relativistic wind, with luminosity and variability time implied by GRB observations, satisfies the constraints necessary to accelerate protons to energy $> 10^{20}$ eV, provided that $\Gamma > 100$, and the magnetic field is close to equipartition with electrons. We stress that the latter must be satisfied to account for both γ-ray emission and afterglow observations [376]. At this stage, it is worthwhile to point out

that for the acceleration process at shocks with large Γ the particle distributions are extremely anisotropic in shock, with the particle angular distribution opening angles $\sim \Gamma^{-1}$ in the upstream plasma rest frame. Therefore, when transmitted downstream the shock particles have a limitted chance to be scattered efficiently to re-eneter the shock [379]. However, in this particular case, the energy gain by any "successful" CR can be comparable to its original energy, i.e., $\langle \Delta E \rangle / E \sim 1$.

4. UHECRs and GRBs: connections

In the GRB model for UHECR production described above[35], the high energy CRs are protons accelerated by Fermi's mechanism in sources that are distributed throughout the universe [248, 387]. It is therefore possible to compare the UHECR spectrum with the prediction from a homogeneous cosmological distribution of sources, each generating a power law differential spectrum $\propto E^{-2.2}$ of high energy protons as typically expected from Fermi acceleration. Under the assumption that the GRB rate evolution is similar to the star-formation rate evolution, the local GRB rate is ~ 0.5 Gpc^{-3} yr^{-1} [388], implying a local γ-ray energy generation rate of $\approx 10^{44}$ erg Mpc^{-3} yr^{-1}.[36]

The energy observed in γ-rays reflects the fireball energy in accelerated electrons. If accelerated electrons and protons (as indicated by afterglow observations [389]) carry similar energy, then the GRB production rate of high energy protons is

$$\epsilon_p^2 (d\dot{n}_p / d\epsilon_p)_{z=0} \approx 10^{44} \text{ erg Mpc}^{-3} \text{ yr}^{-1}. \quad (64)$$

The generation rate (Eq. 64) of high energy protons is remarkably similar to that required to account for the flux of $> 10^{19}$ eV CRs, whereas in this model, the suppression of model flux above $10^{19.7}$ eV is due to the GZK cutoff. Stecker and Scully [390, 391] have raised doubts on the possibility of this generating a very strong cutoff at the highest CR energies, since if the GRB redshift distribution follows that of the star formation rate in the universe, a rate which is higher at larger redshift, most of the GRBs would be just too far and CR with energies above 3×10^{19} eV would be strongly attenuated by the CMB. For a HiRes-shape spectrum, a common origin between GRBs

[35] An alternative model for the GRB phenomenon has been recently put forward [380]. In such a model, the GRB explosion occurs when a massive star collapses into an electromagnetic black hole which readily discharges due to the annihilation of pairs produced by vacuum polarization [381]. The model explains the time variability, the spectra, and the GRB afterglows to a very high level of accuracy [382, 383, 384]. Interestingly, within this set up one is able to accelerate the ionized hydrogen atoms sorrounding the death star to ultra high energies [385] (see also [386]).

[36] The local ($z = 0$) energy production rate in γ-rays by GRBs is roughly given by the product of the characteristic GRB γ-ray energy, $E \approx 2 \times 10^{53}$ erg, and the local GRB rate.

and ultrahigh energy CRs [392] is favored.[37] For appraisals of this and other general criticisms made to the GRB-UHECR connection see [393, 394].

Two of the highest energy CRs come from directions that are within the error boxes of two remarkable GRBs detected by BATSE with a delay of $\mathcal{O}(10)$ months after the bursts [395]. However, a rigorous analysis shows no correlation between the arrival direction of UHECRs and GRBs from the third BATSE catalog [396]. No correlations were found either between a pre-CGRO burst catalog and the Haverah Park shower set that covered approximately the same period of time. These analysis, however, could have been distorted by the angular resolution ($\Delta\theta \sim 3^\circ$) of the GRB measurements. A sensitive anisotropy analysis between UHECRs and GRBs will be possible in the near future, using PAO, HETE-2 and Swift. Preliminary results (if one assumes that GRBs are most likely to happen in infrared luminous galaxies) do not seem to indicate any strong correlation (see above Section II G).

5. A GRB origin for CRs below the ankle?

Wick, Dermer and Atoyan [397] have recently proposed a model for the origin of all CRs above $\sim 10^{14}$ eV/nucleon. In this model, GRBs are assumed to inject CR protons and ions into the interstellar medium of star-forming galaxies –including ours– with a power-law spectrum extending to a maximum energy $\sim 10^{20}$ eV. In addition to the more energetic, extragalactic spectrum of CR, the CR spectrum near the knee was also shown to be plausibly fitted with CRs trapped in the Galactic halo that were accelerated and injected by an earlier Galactic GRB.[38] For power-law CR proton injection spectra $\propto E^{-2.2}$ and low and high-energy cutoffs, normalization to the local time- and space-averaged GRB luminosity density implies that if this model is correct, the nonthermal content in GRB blast waves is hadronically dominated by a factor $\approx$ 60-200, limited in its upper value by energetic and spectral considerations. Neutrinos to be detected in kilometer-scale neutrino detectors such as IceCube (See Sec. IV) provide a clean signal of this model [400].

The last GRB in the Galaxy has been also proposed as the possible progenitor of

[37] In addition, dispersion of magnetic fields in the intergalactic medium can make the number of UHECR-contributing GRBs to grow above the burst rate within the GZK sphere. The latter, within 100 Mpc from Earth, is in the range of 10^{-2} to 10^{-3} yr^{-1}. Assuming a dispersion tiemscale, $\Delta t \sim 10^7$ yr, the number of sources contributing to the flux at any given time may be as large as $\sim 10^4$ [248].

[38] Arguably, from the evidence for beaming and the association of GRBs with star-forming galaxies like the Milky Way, GRB events are estimated to occur once every $10^4 - 10^6$ yrs in the inner Galaxy [398, 399].

the CR anisotropy observed in the direction of the GC [401]. In order to estimate the remaining traces of any CR activity produced by the last GRB in the galaxy, one has to take into account several considerations:

(i) The UHECRs escaping the GRB fireball

$$N_0(E > 10^{18}\ \mathrm{eV}) \sim 10^{-2}\ N_0(E > E_{\min}) \tag{65}$$

are mostly neutrons, because protons are captive in the magnetic field and suffer extensive adiabatic losses on the way out [402].[39] Some of these neutrons will decay into protons within the GC thin disk-like ($r \sim 3$ kpc) region of high interestellar medium density and high star formation rate. The population of secondary protons would then be captured by the strong B-field near the GC, attaining diffusion with a residence time scale of about $T \sim 10^5$ yr. At the end of this time, about 1/300 protons are able to avoid leakeage. The trapped protons,

$$N_T(E > 10^{18}\ \mathrm{eV}) = N_0(E > 10^{18}\ \mathrm{eV})\ \left(1 - e^{-\frac{r\, m_n}{E\, \overline{\tau}}}\right)/300\ , \tag{66}$$

can then be turned back into neutrons by interaction with nuclei in the interstellar medium with probability of 5×10^{-2}. Here, m_n and $\overline{\tau}$ are the neutron mass and lifetime, respectively.

(ii) The formation of the $n \to p$ reservoir depends on the GRB rate in the inner Galaxy (taken here as $10^6\ \mathrm{yr}^{-1}$) times the probability that a GRB jet points more o less along the direction of the GP. The latter is estimated to be about 50%.

(iii) The total CR production by a single GRB is $\approx 10^{51}$ erg [403].

Now, recalling that the CR excess observed by AGASA represents a luminosity of particles beyond 10^{18} eV of about 4×10^{30} erg/s [59], straightforward calculation shows that the observed anisotropy in the direction of the GC can be easily fitted by the neutrons produced in the GRB reservoir, that ultimately travel unscathed to Earth [401].

III. FULL THROTTLE: UHECR GENERATION BEYOND THE STANDARD LORE

The astrophysical models discussed present difficulties in providing a completely satisfactory explanation of the super-GZK events, if there are any. This may simply reflect our present lack of statistics, our present ignorance of the true conditions of processes in some highly energetic regions of the universe, or, perhaps, may imply

[39] We remind the reader that the differential injection spectrum of GRBs $\propto E^{-2.2}$.

that exotic mechanisms are at play. Physics from the most favored theories beyond the standard model (SM) like string/M theory, supersymmetry (SUSY), grand unified theories (GUTs), and TeV-scale gravity have been invoked to explain the possible flux above the GZK energy limit. This review is not mainly concerned with beyond–SM scenarios (for more comprehensive surveys see e.g. [1, 82, 404, 405, 406]), but for the sake of completeness, we provide here a brief account of some of the most relevant exotic explanations.

The most economical among hybrid proposals involves a familiar extension of the SM, namely, neutrino masses. It was noted many years ago that ν's arriving at Earth from cosmologically distant sources have an annihilation probability on the relic neutrino background of roughly $3\,h_{65}^{-1}\%$ [407]. Inspired on this analysis, Weiler [408] and Fargion et al. [409] noted that neutrinos within a few Z widths of the right energy,

$$E_\nu^{RZ} = \frac{M_Z^2}{2m_{\nu_i}} = 4\,\left(\frac{\rm eV}{m_{\nu_i}}\right) \times 10^{21}\ {\rm eV}\,, \tag{67}$$

to annihilate with the relic neutrinos at the Z-pole with large cross section,

$$\langle\sigma_{\rm ann}\rangle^Z \equiv \int \frac{ds}{M_Z^2}\,\sigma_{\rm ann}(s) = 2\,\pi\,\sqrt{2}\,G_F \sim 40.4\,{\rm nb}\ , \tag{68}$$

may produce a "local" flux of nucleons and photons.[40] Remarkably, the energy of the neutrino annihilating at the peak of the Z-pole has to be well above the GZK limit. The mean energies of the ~ 2 nucleons and ~ 20 γ-rays in each process can be estimated by distributing the resonant energy among the mean multiplicity of 30 secondaries. The proton energy is given by

$$\langle E_p\rangle \sim \frac{M_Z^2}{60\,m_{\nu_j}} \sim 1.3\,\left(\frac{\rm eV}{m_{\nu_j}}\right) \times 10^{20}\ {\rm eV}, \tag{69}$$

whereas the γ-ray energy is given by

$$\langle E_\gamma\rangle \sim \frac{M_Z^2}{120\,m_{\nu_j}} \sim 0.7\,\left(\frac{\rm eV}{m_{\nu_j}}\right) \times 10^{20}\ {\rm eV}. \tag{70}$$

The latter is a factor of 2 smaller to account for the photon origin in two body π^0 decay. This implies that the highly boosted decay products of the Z could be observed as super-GZK primaries.[41] However, to reproduce the observed spectrum, the Z-burst mechanism requires very luminous sources of extremely high energy neutrinos

[40] $G_F = 1.16639(1) \times 10^{-5}$ GeV^{-2} is the Fermi coupling constant.
[41] Similarly, gravi-burst fragmentation jets can contribute to the super-GZK spectrum [410].

throughout the universe [411, 412, 413]. The present limits on these sources are near the threshold of sensitivity to the required flux [414].

In 1931, Georges Lemaître [415] – a forerunner of the Big Bang hypothesis – introduced the idea that the entire material filling the universe, as well as the universe's expansion, originated in the super-radioactive disintegration of a "Primeval Atom", which progressively decayed into atoms of smaller and smaller atomic weight. The CRs were introduced in this picture as the energetic particles emitted in intermediate stages of the decay-chain. Echoing Lemaître, in the so-called "top-down models", charged and neutral primaries arise in the quantum mechanical decay of supermassive elementary X particles [416, 417, 418, 419, 420, 421, 422, 423, 424, 425, 426, 427, 428, 429, 430].

To maintain an appreciable decay rate today, it is necessary to tune the X lifetime to be longer (but not too much longer) than the age of the universe, or else "store" short-lived X particles in topological vestiges of early universe phase transitions (such as magnetic monopoles, superconducting cosmic strings, vortons, cosmic necklaces, etc.). Discrete gauged symmetries [431, 432, 433] or hidden sectors [434, 435] are generally introduced to stabilize the X particles. Higher dimensional operators, wormholes, and instantons are then invoked to break the new symmetry super-softly to maintain the long lifetime [423, 424] (collissional annihilation has been considered too [436]). Arguably, these metastable super-heavy relics (MSRs) may constitute (a fraction of) the dark matter in galactic haloes.

Of course, the precise decay modes of the X's and the detailed dynamics of the first generation of secondaries depend on the exact nature of the X particles under consideration. However, in minimal extensions of the SM, where there are no new mass scales between $M_{\rm SUSY} \sim 1$ TeV and m_X, the squark and sleptons would behave like their corresponding supersymmetric partners, enabling one to infer from the "known" evolution of quarks and leptons the gross features of the X particle decay: the strongly interacting quarks would fragment into jets of hadrons containing mainly pions together with a 3% admixture of nucleons [437, 438, 439].[42] This implies that the injection spectrum is a rather hard fragmentation-type shape (with an upper limit usually fixed by the GUT scale) and dominated by γ-rays and neutrinos produced via pion decay. Therefore, the photon/proton ratio can be used as a diagnostic tool in determining the CR origin [442]. In light of the mounting evidence that UHECRs are not γ-rays, one may try to force a proton dominance at ultrahigh energies by postulating efficient absorption of the dominant ultrahigh energy photon flux on the universal and/or galactic radio background.[43] However, the neutrino flux accompanying a nor-

[42] In light of this, the sensitivity of future CR experiments to test the SUSY parameter space has been estimated [440, 441].

[43] Of course, this is not the case in traditional scenarios (for an exception see [443]) of decaying massive

malized proton flux is inevitably increased to a level where it should be within reach of operating experiments [444].

It is clear that because of the wide variety of top down models the ratio of the volume density of the X-particle to its decay time is model dependent. However, if a top down scenario is to explain the origin of UHECRs, the injection spectrum should be normalized to account for the super-GZK events without violating any observational flux measurements or limits at higher or lower energies [445]. In particular, neutrino and γ-ray fluxes depend on the energy released integrated over redshift, and thus on the specific top down model. Note that the electromagnetic energy injected into the Universe above the pair production threshold on the CMB is recycled into a generic cascade spectrum below this threshold on a short time scale compared with the Hubble time. Therefore, it can have several potential observable effects, such as modified light element abundances due to ^{4}He photodisintegration, or induce spectral distortions of universal γ-ray and neutrino backgrounds [446, 447]. Additionally, measurements of the diffuse GeV γ-ray flux [448], to which the generic cascade spectrum would contribute directly, limit significantly the parameter space in which X's can generate the flux of the UHECRs [449, 450, 451], especially if there is already a significant contribution to this background from conventional sources such as unresolved γ-ray blazars. Recently, a possible lower extragalactic contribution to the diffuse γ-ray background measured by EGRET has been pointed out [452, 453]. The $\sim 50\%$ smaller EGRET flux practically rules out extragalactic top down and Z-burst scenarios [454].

If MSRs are the progenitors of the observable UHECRs, then the flux will be dominated by the decay or annihilation products of X's in the Galactic halo, i.e., by sources at distances smaller than all relevant interaction lengths. A clean signal of this scenario is the predicted anisotropy due to the non-central position of the Sun in our galaxy [455, 456].[44] Although it was noted that the predicted anisotropy is consistent with AGASA and Haverah Park data [70], recent analyses [458, 459] of SUGAR data excludes the MSR hypothesis at the 5σ level if all events above $10^{19.6}$ eV are due to metastable X clustered in the halo. (For the extreme case where the population of MSRs is responsible only for CRs with energies $\gtrsim 10^{19.8}$ eV, the annihilation scenario is disfavored at least at the 99% CL, whereas decaying MSRs still have a probability $\sim 10\%$ to reproduce SUGAR data.)

A more exotic explanation postulates that the X's themselves constitute the primaries: magnetic monopoles easily pick up energy from the magnetic fields permeating

dark matter in the Galactic halo, which due to the lack of absorption, predict compositions directly given by the fragmentation function, i.e., domination by γ-rays.

[44] Additionally, the arrival directions of UHECRs can show significant deviations from a random distribution due to an anisotropic spectrum of relics in the early universe [457].

the universe and can traverse unscathed through the primeval radiation, providing an interesting candidate to generate extensive air showers [460]. In particular, a baryonic monopole encountering the atmosphere will diffuse like a proton, producing a composite heavy-particle-like cascade after the first interaction [461] with a great number of muons among all the charged particles [462]. Although this feature was observed in a poorly understood super-GZK event [463, 464], it seems unlikely that a complete explanation for the UHECR data sample would be in terms of magnetic monopoles alone. Moreover, any confirmed directional pairing of events would appear difficult to achieve with the monopole hypothesis.

A novel beyond–SM–model proposal to break the GZK barrier is to assume that UHECRs are not known particles but rather a new species, generally referred to as the uhecron, U [465, 466, 467]. The meager information we have about super-GZK particles allows a naïve description of the properties of the U. The muonic content in the atmospheric cascades suggests U's should interact strongly. At the same time, if U's are produced at cosmological distances, they must be stable, or at least remarkably long lived, with mean-lifetime $\tau \gtrsim 10^6\,(m_U/3\text{ GeV})\,(d/\text{Gpc})\,\text{s}$, where d is the distance to the source and m_U, the uhecron's mass. Additionally, since the threshold energy increases linearly with m_U, to avoid photopion production on the CMB $m_U \gtrsim 1.5$ GeV. In recent years, direct searches of supersymmetric hadrons [468, 469, 470, 471] have severely eroded the attractiveness of the U scenario. However, adequate fine-tunings leave a small window still open [472, 473].

On a similar track, it was recently put forward [474] that strangelets (stable lumps of quark matter with roughly equal numbers of up, down, and strange quarks) can circumvent the acceleration problem in a natural way (due to a high mass and charged, but low charge-to-mass ratio) and move the expected cutoff to much higher energies.

Another possibility in which super-GZK CRs can reach us from very distant sources may arise out of photons that mix with light axions in extragalactic magnetic fields [475]. These axions would be sufficiently weakly coupled to travel large distances unhindered through space, and so they can convert back into high energy photons close to the Earth.[45] An even more radical proposal postulates a tiny violation of local Lorentz invariance, such that some processes become kinematically forbidden [477]. In particular, photon-photon pair production and photopion production may be affected by Lorentz invariance violation.[46] Hence, the absence of the GZK-cutoff would result from the fact that the threshold for photopion production "disappears" and the process becomes kinematically not allowed. This implies that future PAO observations of

[45] See also [476] for a SUSY inspired related scenario.

[46] Existing limits on the violation of Lorentz invariance come from multi–TeV γ-ray observations of Mrk 501 [478].

faraway sources could provide constraints on, or even a measurement of, the violation of Lorentz symmetry, yielding essential insights into the nature of gravity-induced wave dispersion in the vacuum [479, 480, 481, 482, 483, 484, 485, 486, 487, 488].

In summary, future UHECR data may not only provide clues to the particle sources, but could enhance our understanding of fundamental particle physics. We are entering this new High Energy Physics era with the Pierre Auger Observatory [489, 490, 491].

IV. MINORITY REPORT: NEUTRINO SHOWERS

Extraterrestrial neutrinos provide a unique window to probe the deepest reaches of stars, quasars, and exotic structures in the cosmos. In contrast to all other SM particles, they can escape from dense astrophysical environments and propagate to the Earth unscathed, arriving aligned with their source. Even at the highest energies the $\nu\bar{\nu}$ annihilation mean free path on the cosmic neutrino background,

$$\lambda_\nu = (n_\nu \, \sigma_{\nu\bar{\nu}})^{-1} \approx 4 \times 10^{28} \text{ cm} \ , \tag{71}$$

is somewhat above the present size of the horizon (recall that $H_0^{-1} \sim 10^{28}$ cm) [492].

In addition, the fluxes of ultra-high energy cosmic neutrinos offer clues to the properties of neutrinos themselves and provide an important probe of new ideas in particle physics. Namely, their known interactions are so weak that new physics may easily alter neutrino properties. This is especially relevant for extraterrestrial neutrinos with energies $\gtrsim 10^6$ GeV that interact with nucleons in the Earth atmosphere with center-of-mass energies above the electroweak scale, where the SM is expected to be modified by new physics.

In summary, ultra high energy extraterrestrial neutrinos are inextricably linked with the physics processes discussed throughout this review. This chapter will therefore focus on the main features of high energy neutrino astronomy. For comprehensive reviews on cosmic neutrinos the reader is referred to [493, 494, 495, 496].

A. Bounds on the energy spectrum

The basic operational system of neutrino telescopes is an array of strings with photomultiplier tubes (PMTs) distributed throughout a natural Čerenkov medium such as ice or water. The largest pilot experiments (~ 0.1 km in size) are: the now defunct DUMAND (Deep Underwater Muon and Neutrino Detector) experiment [497] in the deep sea near Hawaii, the underwater experiment in Lake Baikal [498], and AMANDA (Antarctic Muon And Neutrino Detector Array) [499] in the South Pole ice. Next generation neutrino telescopes aim towards an active volume in the range of 1 km^3

of water. Projects under construction or in the proposal stage are: two deep sea experiments in the Mediterranean, the French ANTARES (Astronomy with a Neutrino telescope Abyss environment RESearch) [500] and NESTOR (Neutrino Experiment SouthwesT Of GReece [501]), and IceCube [502], a scaled up version of the AMANDA detector.

The traditional technique to observe cosmic neutrinos is to look for muons (along with a visible hadronic shower if the ν is of sufficient energy) generated via charged-current interactions, $(\nu_\mu, \bar{\nu}_\mu)N \rightarrow (\mu^-, \mu^+)+$ anything, in the rock below the detector. The Čerenkov light emitted by these muons is picked up by the PMTs, and is used for track reconstruction. The muon energy threshold is typically in the range of $10-100$ GeV. However, besides the desired extraterrestrial neutrinos, below $\sim 10^3$ GeV there is a significant background of leptons (produced by CRs interacting in the atmosphere) [503, 504] and so the task of developing diagnostics for neutrino sources becomes complicated. With rising energy ($\gtrsim 10^6$ GeV) the three neutrino flavors can be identified [505].

The spectacular neutrino fireworks (in the 10 MeV range) from supernova 1987A constitute the only extragalactic source so far observed [506, 507]. The Fréjus [508], Baikal [509], MACRO [510], and AMANDA [511] collaborations reported no excess of neutrinos above the expected atmospheric background, enabling significant limts to be set on the diffuse neutrino flux.[47] These limits are shown in Fig. 9.

Upward going neutrinos with energies $\gtrsim 10^8$ GeV are typically blocked by the Earth. This shadowing severely restricts the high energy event rates in underground detectors. However, neutrinos may also induce extensive air showers, so current and future air shower experiments might also function as neutrino detectors. The neutrino interaction length is far larger than the Earth's atmospheric depth, which is only 0.36 km water equivalent (kmwe) even when traversed horizontally. Neutrinos therefore shower uniformly at all atmospheric depths. As a result, the most promising signal of neutrino-induced cascades are quasi-horizontal showers initiated deep in the atmosphere. For showers with large enough zenith angles, the likelihood of interaction is maximized and the background from hadronic cosmic rays is eliminated, since the latter shower high in the atmosphere. These ν-showers will appear as hadronic vertical showers, with large electromagnetic components, curved fronts (a radius of curvature of a few km), and signals well spread over time (on the order of microseconds).

[47] The Frejus experiment, located in an underground laboratory, measured the energy of muons produced by neutrino interactions in the rock above the detector. The detector itself comprised a calorimeter made from a vertical sandwich of over 900 iron slabs interspersed with flash chambers. Geiger tubes embedded in the structure provided the trigger [512]. The extensive air shower array on top of the Gran Sasso Laboratory (EAS-TOP) [513] and MACRO [514] used similar techniques.

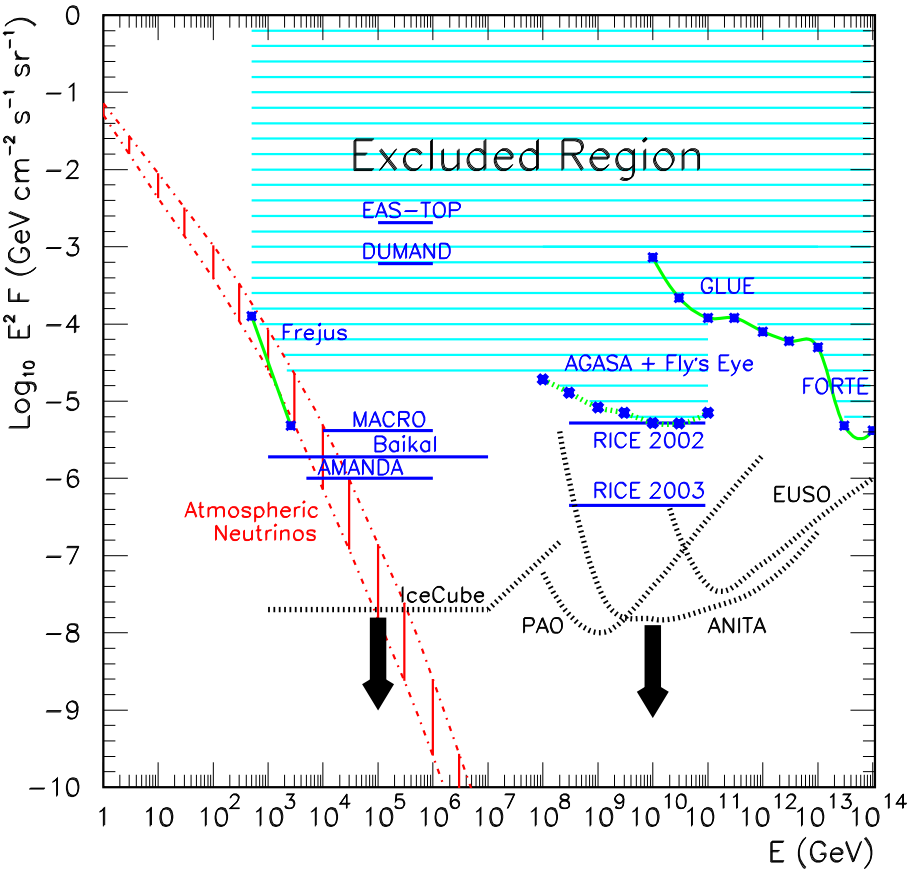

FIG. 9: The horizontal solid lines indicate current 90% CL upper limits on the neutrino fluxes $\propto E^{-2}$ as reported by the EAS-TOP [515], DUMAND [516], Baikal [509], MACRO [510], AMANDA [511], and RICE [517, 518] collaborations. The $*-*-*$ lines indicate model independent bounds on the neutrino flux ($d\Phi_{\langle\nu_i+\bar{\nu}_i\rangle}/dE$, with $i = e, \mu, \tau$) from AGASA + Fly's Eye data [519] (95% CL), Frejus [508], GLUE [414, 520], and FORTE searches in the Greenland ice sheet [521]. The horizontal and diagonal thick dotted lines indicate the expected 90% CL sensitivity of IceCube in 1 yr of operation [522]. Also shown (non-horizontal thick dotted lines) are the projected sensitivities of PAO (1 yr running) [523], EUSO (1 yr running) [524] and ANITA (45 days running) [524] corresponding to 1 event per decade. The region between the falling dashed-dotted lines indicates the flux of atmospheric neutrinos.

The event rate for quasi-horizontal deep showers from ultra-high energy neutrinos is [519]

$$N = \sum_{i,X} \int dE_i \, N_A \, \frac{d\Phi_i}{dE_i} \, \sigma_{iN\to X}(E_i) \, \mathcal{E}(E_i) \ , \tag{72}$$

where the sum is over all neutrino species $i = \nu_e, \bar{\nu}_e, \nu_\mu, \bar{\nu}_\mu, \nu_\tau, \bar{\nu}_\tau$, and all final states X. $N_A = 6.022 \times 10^{23}$ is Avogadro's number, and $d\Phi_i/dE_i$ is the source flux of neutrino

species i, σ as usual denotes the cross section, and $\mathcal{E}$ is the exposure measured in cm^3 w.e. sr time. The Fly's Eye and the AGASA Collaborations have searched for quasi-horizontal showers that are deeply-penetrating, with depth at shower maximum $X_{\max} > 2500$ g/cm^2 (see e.g. [525, 526]). There is only 1 event that unambiguously passes this cut with 1.72 events expected from hadronic background, implying an upper bound of 3.5 events at 95%CL from neutrino fluxes. Note that if the number of events integrated over energy is bounded by 3.5, then the same limit is certainly applicable bin by bin in energy. Thus, using Eq. (72) one obtains

$$\sum_{i,X} \int_{\Delta} dE_i \, N_A \, \frac{d\Phi_i}{dE_i} \, \sigma_{iN\to X}(E_i) \, \mathcal{E}(E_i) \; < 3.5 \; , \tag{73}$$

at 95% CL for some energy interval Δ. Here, the sum over X takes into account charge and neutral current processes. In a logarithmic interval Δ where a single power law approximation

$$\frac{d\Phi_i}{dE_i} \, \sigma_{iN\to X}(E_i) \, \mathcal{E}(E_i) \sim E_i^{\alpha} \tag{74}$$

is valid, a straightforward calculation shows that

$$\int_{\langle E\rangle e^{-\Delta/2}}^{\langle E\rangle e^{\Delta/2}} \frac{dE_i}{E_i} \, E_i \, \frac{d\Phi_i}{dE_i} \, \sigma_{iN\to X} \, \mathcal{E} = \langle \sigma_{iN\to X} \, \mathcal{E} \, E_i \, d\Phi_i/dE_i \rangle \, \frac{\sinh\delta}{\delta} \, \Delta \, , \tag{75}$$

where $\delta = (\alpha+1)\Delta/2$ and $\langle A\rangle$ denotes the quantity A evaluated at the center of the logarithmic interval. The parameter $\alpha = 0.363 + \beta - \gamma$, where 0.363 is the power law index of the SM neutrino cross sections [527] and β and $-\gamma$ are the power law indices (in the interval Δ) of the exposure and flux $d\Phi_i/dE_i$, respectively. Since $\sinh\delta/\delta > 1$, a conservative bound may be obtained from Eqs. (73) and (75):

$$N_A \sum_{i,X} \langle \sigma_{iN\to X}(E_i)\rangle \, \langle \mathcal{E}(E_i)\rangle \, \langle E_i d\Phi_i/dE_i\rangle < 3.5/\Delta \; . \tag{76}$$

By taking $\Delta = 1$ as a likely interval in which the single power law behavior is valid (this corresponds to one e-folding of energy), and setting $\langle E_i d\Phi_i/dE_i\rangle = \frac{1}{6}\langle E_\nu d\Phi_\nu/dE_\nu\rangle$ ($\Phi_\nu \equiv$ total neutrino flux) from Eq. (76) it is straightforward to obtain 95%CL upper limits on the neutrino flux. The limits are shown in Fig. 9.

These bounds will be improved in the near future. In particular, each site of PAO will observe ~ 15 km^{3}we sr of target mass around 10^{19} eV [528]. Moreover, the study of radio pulses from electromagnetic showers created by neutrino interactions in ice would provide an increase in the effective area up to 10^4 km^2. A prototype of this technique is the Radio Ice Čerenkov Experiment (RICE) [529]. Similar concepts are used by

the Goldstone Lunar ultrahigh energy neutrino Experiment (GLUE),[48] the ANtartic Impulse Transient Array (ANITA),[49] and the Fast On-orbit Recording of Transient Events (FORTE).[50] Existing limits on ν-fluxes from RICE, GLUE and FORTE, as well as the projected sensitivities of forthcoming experiments are collected in Fig. 9.

B. Astronomy on Ice

IceCube is, perhaps, the most promising route for neutrino detection [522]. This telescope will consist of 80 kilometer-length strings, each instrumented with 60 10-inch photomultipliers spaced by 1.7 m. The deepest module is 2.4 km below the ice surface. The strings are arranged at the apexes of equilateral triangles 125 m on a side. The instrumented detector volume is a cubic kilometer.[51] A surface air shower detector, IceTop, consisting of 160 Auger-style Čerenkov detectors deployed over 1 km^2 above IceCube, augments the deep-ice component by providing a tool for calibration, background rejection and air-shower physics. Muons can be observed from 10^{11} eV to 10^{18} eV. Cascades, generated by ν_e, $\overline{\nu}_e$, ν_τ, and $\overline{\nu}_\tau$ can be observed above 10^{11} eV and reconstructed at energies somewhat above 10^{13} eV. The angular resolution is $\approx 0.7^\circ$ at TeV energies.

A variety of neutrino-emitting-sources have been proposed, such as supernovae [531] (see also [532] for a detailed study on directionality), GRB fireballs [400, 533, 534, 535], microquasars [536], X-ray binaries [169], AGN [537], FRI radio galaxies [538], etc. As an example of the IceCube potential, in what follows we briefly discuss its sensitivity to probe the neutron hypothesis of UHECRs via observation of the antineutrino beam $n \to p + e^- + \overline{\nu}_e$, expected from the Cygnus direction [65]. To this end, we first estimate the background signal. As discussed in Sec. II A, the TeV γ-ray flux,

$$\frac{dF_\gamma}{dE_\gamma} = 4.7(\pm 2.1_{\rm stat} \pm 1.3_{\rm sys}) \times 10^{-13} \left(\frac{E}{1\ {\rm TeV}}\right)^{-1.9(\pm 0.3_{\rm stat} \pm 0.3_{\rm sys})} \ {\rm ph\,cm^{-2}s^{-1}TeV^{-1}}\ , \tag{77}$$

reported by HEGRA Collaboration [152] in the vicinity of Cygnus OB2 is likely due to hadronic processes. Since π^0's, π^+'s, and π^-'s are produced in equal numbers,

[48] This experiment observes microwave Čerenkov pulses from electromagnetic showers induced by neutrinos interacting in the Moon's rim [520]

[49] A balloon-borne payload that will circle the continent of Antartica at 35,000 meters, scanning the vast expanses of ice for telltale pulses of radio emission generated by the neutrino collisions [`http://www.ps.uci.edu~anita/`].

[50] The FORTE satellite records bursts of electromagnetic waves arising from near the Earth's surface in the radio frequency range 30 to 300 MHz with a dual polarization antena [521].

[51] Extension of these aperture is in the proposal stage [530].

we expect two photons, two ν_e's, and four ν_μ's per π^0. On average, the photons carry one-half of the energy of the pion, and the neutrinos carry one-quarter. For $dF_\pi/dE_\pi \propto E_\pi^{-2}$, the energy-bins dE scale with these fractions, and we arrive at

$$\begin{aligned}
\frac{dF_\gamma}{dE_\gamma}(E_\gamma = E_\pi/2) &= 4\,\frac{dF_\pi}{dE_\pi}(E_\pi) \\
\frac{dF_{\nu_e}}{dE_{\nu_e}}(E_{\nu_e} = E_\pi/4) &= 4\,\frac{dF_\pi}{dE_\pi}(E_\pi)\,, \\
\frac{dF_{\nu_\mu}}{dE_{\nu_\mu}}(E_{\nu_\mu} = E_\pi/4) &= 8\,\frac{dF_\pi}{dE_\pi}(E_\pi)\,,
\end{aligned} \tag{78}$$

for the fluxes at the source, where π denotes any one of the three pion charge-states. Terrestrial experiments (see e.g. [539]) have shown that ν_μ and ν_τ are maximally mixed with a mass-squared difference $\sim 10^{-3}\mathrm{eV}^2$. This together with the known smallness of $|\langle\nu_e|\nu_3\rangle|^2$, implies that the ν_μ's will partition themselves equally between ν_μ's and ν_τ's on lengths large compared to the oscillation length $\lambda_{\rm osc} \sim 1.5\times 10^{-3}\,(E_\nu/\mathrm{PeV})$ pc. Here $\nu_3 \simeq (\nu_\mu + \nu_\tau)/\sqrt{2}$ is the third neutrino eigenstate. From these remarks, one finds a nearly identical flux for each of the three neutrino flavors ($j = e, \mu, \tau$), which is equal to [168]

$$\frac{dF_{\nu_j}}{dE_{\nu_j}}(E_{\nu_j} = E_\gamma/2) = 2\,\frac{dF_\gamma}{dE_\gamma}(E_\gamma)\,. \tag{79}$$

Although TeV neutrinos are copiously produced, because they are weakly interacting the detection probability on Earth is tiny, about 10^{-6} [493]. In particular, the expected ν event rate at IceCube associated with the unidentified HEGRA source is $< 1\ \mathrm{yr}^{-1}$ (D. Hooper, private communication). Such an event rate is even smaller than the atmospheric neutrino background.[52] Moreover, existing limits on TeV γ-ray fluxes in this region of the sky are near the HEGRA sensitivity.[53] In light of this, we take as background the atmospheric neutrino event rate, and so Poisson statistics implies that a signal ≥ 3.7 events is significant at the 95% CL.

Antineutrinos take only a very small part of the energy of the parent neutron, typically $\sim 10^{-3}$. Hence, to estimate the event rate of TeV antineutrinos at IceCube, the

[52] For a year of running at IceCube the expected background from atmospheric neutrinos (with energy ≥ 1 TeV) within 1° circle centered in the Cygnus direction (about 40° below the horizon) is < 1.5 events.

[53] Specifically, the CASA-MIA experiment observed the Cygnus region over a 5 year period (1990-1995) and the collected data place a bound $F_\gamma(E_\gamma > 115\ \mathrm{TeV}) < 6.3\times 10^{-15}\,\mathrm{ph\,cm^{-2}\,s^{-1}}$, at the 90%CL [540]. Extrapolation down to lower energies, assuming a spectrum $\propto E_\gamma^{-2}$, leads to $F_\gamma(E_\gamma > 1\mathrm{TeV}) < 7.2\times 10^{-13}\,\mathrm{ph\,cm^{-2}\,s^{-1}}$. This is within a factor of 2 of the HEGRA measurements [152, 541], $F_\gamma(E_\gamma > 1\mathrm{TeV}) \approx 4.5\times 10^{-13}\,\mathrm{ph\,cm^{-2}\,s^{-1}}$.

relevant nucleus population at the source has an energy per nucleon $E_{N,\rm PeV} \sim 1$ PeV. Nuclei with Lorentz factor $\sim 10^6$ are synthesized in all supernovae. Hadronic interactions with the HII population (density < 30 cm^{-3} [153]) and photodisintegration processes provide the flux of PeV neutrons. In this energy regime, the target photons at photodisintegration threshold energies are in the ultraviolet, ~ 5 eV. This includes the entire emission spectrum of the O stars and about 60% of photons from B stars (with average temperature 28,000 K). From the photon emission rate $F_{\rm UV}$ the number density $n_{\rm UV}$ at the surface of a sphere of radius R from the core center is given by

$$\frac{1}{4} n_{\rm UV}\ c = \frac{F_{\rm UV}}{4\pi R^2}\ . \tag{80}$$

For the O-star population, the photon emission rate in the Lyman region is found to be $F_{\rm L} \approx 10^{51}$ photons s^{-1} [206]. The Lyman emission corresponds to 60% of the entire O star spectrum. Furthermore, as mentioned above, 60% of the B star spectrum is also active for photodisintegration in this energy region, and the B star population is about 20 times greater than that of the O stars [206]. Now, from the H-R diagram [542] one can infer that the energy luminosity of a B-star is about 0.1 that of an O star. Additionally, the B star temperature is about 0.5 the O star temperature, giving a number luminosity ratio of about 0.2. All in all, for photodisintegration resulting in PeV nucleons, the relevant photon density in the core of the Cygnus OB2 association is $n_{\rm UV} \sim 230$ cm^{-3}. The nucleus mean free path is ≈ 35 kpc, corresponding to a collision time $\tau = 10^5$ yr. Thus, the collision rate for photodisintegration in the core region is comparable to the hadronic interaction rate.[54]

Since one is interested in neutrinos, it is still necessary to compare the production rate for charged pions in the hadronic case to the overall rate for generating neutrons. To assess this ratio, we made use of available high energy event simulations showing spectator nucleon and pion spectra for Fe-N/p-N collisions at 10^{15} and 10^{16} eV [543] (summarized in [544]). The pion rapidity spectra in the central plateau are roughly energy independent, except for the widening of the plateau with energy –see [39]–, whereas there is a slow increase of spectator neutrons as one reaches the region of interest ($E_N \approx 1$ PeV). Allowing for sizeable differences in hadronic interaction models, the secondary populations are roughly 35% $\pi^\pm$, 45% γ, 10% nucleons, and 10% K [544]. In the energy range yielding PeV neutrons, only about 30% of the rapidity plateau contributes charged pions above 2 TeV. Since only half the nucleons are neutrons, we arrive at a ratio

$$\frac{\pi^\pm(>2\ {\rm TeV})}{n(\sim\ {\rm PeV})} \approx 3 \tag{81}$$

[54] This estimate takes into account a hadronic cross section, $\sigma_{{\rm Fe}p} \sim A^{0.75}\,\sigma_{pp} \approx 6 \times 10^{-25}$ cm^2, and the generous upper limit [151] of the nucleon density ~ 30 cm^{-3} [153].

in the hadronic interactions.

However, photodisintegration also takes place in the outer regions of the OB association as long as: *(i)* the density of the optical photons propagating out from the core allows a reaction time which is smaller than the age of the cluster ~ 2.5 Myr [545] and *(ii)* the diffusion front of the nuclei has passed the region in question. From Eq. (80) we estimate an average photon density $n_{\rm UV} \gtrsim 25$ cm^{-3} out to 30 pc, which gives a reaction time of $\approx 10^6$ yr. The diffusion time (~ 1.2 Myr) is a bit smaller than the age of the cluster, and somewhat higher than the reaction time, allowing about 90% of the nuclei to interact during the lifetime of the source. Thus, the production rate of neutrons via photodisintegration is amplified by a volume factor of 27 over the rate in the 10 pc core. The net result of all this consideration is that the PeV neutron population is about an order of magnitude greater than that of the TeV charged pions [65].

With this in mind, we now discuss the prospects for a new multi-particle astronomy: neutrons as directional pointers + antineutrinos as inheritors of directionality. The basic formula that relates the neutron flux at the source (dF_n/dE_n) to the antineutrino flux observed at Earth ($dF_{\overline{\nu}}/dE_{\overline{\nu}}$) is [65]:

$$\frac{dF_{\overline{\nu}}}{dE_{\overline{\nu}}}(E_{\overline{\nu}}) \;=\; \int dE_n \, \frac{dF_n}{dE_n}(E_n) \left(1 - e^{-\frac{D\, m_n}{E_n\, \overline{\tau}_n}}\right) \int_0^Q d\epsilon_{\overline{\nu}} \, \frac{dP}{d\epsilon_{\overline{\nu}}}(\epsilon_{\overline{\nu}}) \\ \times \int_{-1}^{1} \frac{d\cos\overline{\theta}_{\overline{\nu}}}{2} \, \delta\left[E_{\overline{\nu}} - E_n \, \epsilon_{\overline{\nu}} \, (1 + \cos\overline{\theta}_{\overline{\nu}})/m_n\right] \, . \qquad (82)$$

The variables appearing in Eq. (82) are the antineutrino and neutron energies in the lab ($E_{\overline{\nu}}$ and E_n), the antineutrino angle with respect to the direction of the neutron momentum, in the neutron rest-frame ($\overline{\theta}_{\overline{\nu}}$), and the antineutrino energy in the neutron rest-frame ($\epsilon_{\overline{\nu}}$). The last three variables are not observed by a laboratory neutrino-detector, and so are integrated over. The observable $E_{\overline{\nu}}$ is held fixed. The delta-function relates the neutrino energy in the lab to the three integration variables.[55] The parameters appearing in Eq. (82) are the neutron mass and rest-frame lifetime (m_n and $\overline{\tau}_n$), and the distance to the neutron source (D). dF_n/dE_n is the neutron flux at the source, or equivalently, the neutron flux that would be observed from the Cygnus region in the absence of neutron decay. Finally, $dP/d\epsilon_{\overline{\nu}}$ is the normalized probability that the decaying neutron in its rest-frame produces a $\overline{\nu}_e$ with energy $\epsilon_{\overline{\nu}}$. Setting the beta-decay neutrino energy $\epsilon_{\overline{\nu}}$ equal to its mean value $\equiv \epsilon_0 \sim (m_n - m_p)[1 - m_e^2/(m_n - m_p)^2]/2 \approx 0.55$ MeV, we have $dP/d\epsilon_{\overline{\nu}} = \delta(\epsilon_{\overline{\nu}} - \epsilon_0)$.[56] Here, the maximum neutrino energy in the neutron rest frame is $Q \equiv m_n - m_p - m_e = 0.71$ MeV, and the minimum neutrino energy

[55] Note that $E_{\bar{\nu}} = \Gamma_n(\epsilon_{\bar{\nu}} + \beta\epsilon_{\bar{\nu}}\cos\overline{\theta}_{\bar{\nu}}) = E_n\epsilon_{\bar{\nu}}(1 + \cos\overline{\theta}_{\bar{\nu}})/m_n$, where $\Gamma_n = E_n/m_n$ is the Lorentz factor, and (as usual) $\beta \approx 1$ is the particle's velocity in units of c.

[56] The delta-function in the neutron frame gives rise to a flat spectrum for the neutrino energy in the

is zero in the massless limit.[57] The expression in parentheses in Eq. (82) is the decay probability for a neutron with lab energy E_n, traveling a distance D. In principle, one should consider a source distribution, and integrate over the volume $\int d^3D$. Instead, we will take D to be the 1.7 kpc distance from Earth to Cygnus OB2; for the purpose of generating the associated neutrino flux, this cannot be in error by too much.

Putting all this together, normalization to the observed "neutron" excess at $\sim 10^{18}$ eV leads to about 20 antineutrino events at IceCube per year [65]. Note that anti-neutrino flux at 1 TeV may also originate in the decay of 1 PeV neutrons from sources whose spectrum cuts off at that energy, and hence are not subject to normalization by the anisotropy. Thus, this estimate may be regarded as very conservative. A direct TeV $\overline{\nu}_e$ event in IceCube will make a showering event, which, even if seen, provides little angular resolution. In the energy region below 1 PeV, IceCube will resolve directionality only for ν_μ and $\bar{\nu}_\mu$. Fortunately, neutrino oscillations rescue the signal. Since the distance to the Cygnus region greatly exceeds the $\overline{\nu}_e$ oscillation length $\lambda_{\rm osc} \sim 10^{-2}(E_{\bar{\nu}}/{\rm PeV})$ pc (taking the solar oscillation scale $\delta m^2 \sim 10^{-5}{\rm eV}^2$), the antineutrinos decohere in transit. The arriving antineutrinos are distributed over flavors, with the muon antineutrino flux $F_{\bar{\nu}_\mu}$ given by the factor $\frac{1}{4}\sin^2(2\,\theta_\odot) \simeq 0.20$ times the original $F_{\bar{\nu}_e}$ flux. The $\bar{\nu}_\tau$ flux is the same, and the $\bar{\nu}_e$ flux is 0.6 times the original flux. Here we have utilized for the solar mixing angle the most recent SNO result $\theta_\odot \simeq 32.5^\circ$ [546], along with maximal mixing for atmospheric ν_μ-ν_τ neutrinos and a negligible ν_e component in the third neutrino eigenstate. All in all, for a year of running at IceCube, one conservatively expects 4 $\overline{\nu}_\mu$ showers with energies $\gtrsim 1$ TeV to cluster within 1° of the source direction, comfortably above the stated CL [65].

IceCube is not sensitive to TeV neutrinos from the Galactic Center, as these are above the IceCube horizon, where atmospheric muons will dominate over any signal. However, other kilometer-scale neutrino detectors, such as those planned for the Mediterranean Sea, may see the Galactic Center flux.

In summary, in a few years of observation, IceCube will attain 5σ sensitivity for discovery of the Fe$\rightarrow n \rightarrow \overline{\nu}_e \rightarrow \overline{\nu}_\mu$ cosmic beam, providing the "smoking ice" for the Galactic Plane neutron hypothesis.

---

lab for fixed neutron lab-energy $E_n = \Gamma_n\, m_n$:

$$\frac{dP}{dE_{\overline{\nu}}} = \int_{-1}^{1} \frac{d\cos\overline{\theta}_{\overline{\nu}}}{2} \left(\frac{d\epsilon_{\overline{\nu}}}{dE_{\overline{\nu}}}\right) \left(\frac{dP}{d\epsilon_{\overline{\nu}}}\right) = \frac{1}{2\,\Gamma_n\,\epsilon_0}\,,$$

with $0 \le E_{\overline{\nu}} \le 2\,\Gamma_n\,\epsilon_0$.

[57] The massless-neutrino approximation seems justifiable here: even an eV-mass neutrino produced at rest in the neutron rest-frame would have a lab energy of $m_\nu\,\Gamma_n \lesssim$ GeV, below threshold for neutrino telescopes.

C. Probes of new physics beyond the electroweak scale

It is intriguing – and at the same time suggestive – that the observed flux of CRs beyond the GZK-energy is well matched by the flux predicted for cosmogenic neutrinos [547, 548, 549, 550]. Of course, this is not a simple coincidence: any proton flux beyond $E^{\rm th}_{p\gamma_{\rm CMB}}$ is degraded in energy by photoproducing π^0 and $\pi^\pm$, with the latter in turn decaying to produce cosmogenic neutrinos. The number of neutrinos produced in the GZK chain reaction compensates for their lesser energy, with the result that the cosmogenic flux matches well the observed CR flux beyond 10^{20} eV. Recently, the prospect of an enhanced neutrino cross section has been explored in the context of theories with large compact dimensions.[58] In these theories, the extra spatial dimensions are responsible for the extraordinary weakness of the gravitational force, or, in other words, the extreme size of the Planck mass [552, 553]. For example, if spacetime is taken as a direct product of a non-compact 4-dimensional manifold and a flat spatial n-torus T^n (of common linear size $2\pi r_c$), one obtains a definite representation of this picture in which the effective 4-dimensional Planck scale, $M_{\rm Pl} \sim 10^{19}$ GeV, is related to the fundamental scale of gravity, M_D, according to $M^2_{\rm Pl} = 8\pi\, M_D^{2+n}\, r_c^n$. Within this framework, virtual graviton exchange would disturb high energy neutrino interactions, and in principle, could increase the neutrino interaction cross section in the atmosphere by orders of magnitude beyond the SM value; namely $\sigma_{\nu N} \sim [E_\nu/(10^{10})\ {\rm GeV}]$ mb [554, 555, 556]. However, it is important to stress that a cross section of ~ 100 mb would be necessary to obtain consistency with observed showers which start within the first 50 g/cm^2 of the atmosphere. This is because Kaluza–Klein modes couple to neutral currents and the scattered neutrino carries away 90% of the incident energy per interaction [557]. Moreover, models which postulate strong neutrino interactions at super-GZK energies also predict that moderately penetrating showers should be produced at lower energies, where the neutrino-nucleon cross section reaches a sub-hadronic size. Within TeV scale gravity $\sigma_{\nu N}$ is likely to be sub-hadronic near the energy at which the cosmogenic neutrino flux peaks, and so moderately penetrating showers should be copiously produced [558]. Certainly, the absence of moderately penetrating showers in the CR data sample should be understood as a serious objection to the hypothesis of neutrino progenitors of the super-GZK events.

Large extra dimensions still may lead to significant increases in the neutrino cross section. If this scenario is true, we might hope to observe black hole (BH) production (somewhat more masive than M_D) in elementary particle collisions with center-

[58] A point worth noting at this juncture: the neutrino-nucleon cross section can also be significantly enhanced at center-of-mass energies $\gtrsim 100$ TeV (within the SM) via electroweak instanton-induced processes [551].

of-mass energies $\gtrsim$ TeV [559, 560, 561]. In particular, BHs occurring very deep in the atmosphere (revealed as intermediate states of ultrahigh energy neutrino interactions) could trigger quasi-horizontal showers and be detected by cosmic ray observatories [562, 563, 564, 565, 566]. Additionally, neutrinos that traverse the atmosphere unscathed may produce BHs through interactions in the ice or water and be detected by neutrino telescopes [567, 568]. Interestingly, $\sigma_{\nu N \to \rm BH} \propto M_D^{(-4+2n)/(1+n)}$. Therefore, the non-observation of the almost guaranteed flux of cosmogenic neutrinos can be translated into bounds on the fundamental Planck scale. For $n \geq 5$ extra spatial dimensions compactified on T^n, recent null results from CR detectors lead to $M_D > 1.0 - 1.4$ TeV [569, 570]. These bounds are among the most stringent and conservative to date. In the near future, PAO will provide more sensitive probes of TeV-scale gravity and extra dimensions [571]. Certainly, the lack of observed deeply-penetrating showers can be used to place more general, model-independent, bounds on $\sigma_{\nu N}$ [519, 572, 573, 574].

Up to now we have only discussed how to set bounds on physics beyond the SM. An actual discovery of new physics in cosmic rays is a tall order because of large uncertainties associated with the depth of the first interaction in the atmosphere, and the experimental challenges of reconstructing cosmic air showers from partial information. However, a similar technique to that employed in discriminating between photon and hadron showers can be applied to search for signatures of extra-dimensions. Specifically, if an anomalously large quasi-horizontal deep shower rate is found, it may be ascribed to either an enhancement of the incoming neutrino flux, or an enhancement in the neutrino-nucleon cross section. However, these two possibilities may be distinguished by separately binning events which arrive at very small angles to the horizontal, the so-called "Earth-skimming" events [575, 576]. An enhanced flux will increase both quasi-horizontal and Earth-skimming event rates, whereas a large BH cross section suppresses the latter, because the hadronic decay products of BH evaporation do not escape the Earth's crust [577]. For a more detailed discussion of neutrino interactions in the Earth atmosphere within TeV scale gravity scenarios see e.g. [1].

V. ANY GIVEN SUNDAY: COUNTDOWN TO DISCOVERY

With data now at hand, not only there are several interesting, plausible theoretical models within the standard astrophysical agenda to explain all the CRs detected so far, but there could indeed be too many. Perhaps yet unexpected degeneracy problems will appear, even with the forthcoming data of the Pierre Auger Observatory, a topic which till now has not been a subject of debate. In our view, Occam's razor imposes that *all* standard astrophysical models be eliminated before embarking in the consequences of explanations involving physics beyond the standard scenarios. However, should this be

the case, the prospect for encountering a profound scientific revolution are endless. The puzzle of UHECRs may have something to say about issues as fundamental as local Lorentz invariance: On the one hand, the absence of photo-pion production above the GZK-limit would imply no cosmogenic neutrino flux and possibly undeflected pointing of the primary back to its source. On the other hand, a significant correlation of TeV-antineutrinos with directional signals at EeV energies will validate Special Relativity to an unprecedented boost factor of $\Gamma \approx 10^9$, several orders of magnitude beyond current limits. Additionally, contrasting the observed quasi-horizontal neutrino flux with the expected neutrino flux can help constrain TeV-scale gravity interactions and improve current bounds on the fundamental Planck scale. An optimist might even imagine the discovery of microscopic BHs, the telltale signature of the Universe's unseen dimensions. At the time of writing, new data is being collected at Pampa Amarilla. Whatever happens, in T–2 years we shall witness the lift-off of a new era of cosmic ray physics.

Acknowledgments

During the last few years, we have benefitted from discussions with several colleagues and collaborators, among them, Felix Aharonian, John Bahcall, Paula Benaglia, Peter Biermann, Elihu Boldt, Murat Boratav, Yousaf Butt, Analía Cillis, Jorge Combi, Jim Cronin, Tom Dame, Chuck Dermer, Seth Digel, Eva Domingo, Susan and Gabor Domokos, María Teresa Dova, Luis Epele, Jonathan Feng, Francesc Ferrer, Haim Goldberg, Francis Halzen, Tim Hamilton, Carlos Hojvat, Dan Hooper, Michael Kachelriess, Mike Loewenstein, Tom Mc Cauley, Gustavo Medina Tanco, Pran Nath, Carlos Nuñez, Tom Paul, Santiago Perez Bergliaffa, Brian Punsly, Olaf Reimer, Steve Reucroft, Andreas Ringwald, Gustavo Romero, Esteban Roulet, Subir Sarkar, Sergio Sciutto, Dmitri Semikoz, Al Shapere, Paul Sommers, Guenter Sigl, Todor Stanev, John Swain, Tomasz Taylor, Dave Thompson, Peter Tinyakov, Alan Watson, Tom Weiler, and Allan Widom. We specially thank Frank Scherb for valuable information on the early history of cosmic ray detectors. We would like to thank several of the collegues mentioned above as well as Ray Protheroe for allowing us to use some figures from their papers in this review. We thank Julianna Gianni for inspiration. The work of DFT was performed under the auspices of the U.S. Department of Energy (NNSA) by University of California's LLNL under contract No. W-7405-Eng-48. The work of LAA has been partially supported by the US National Science Foundation (NSF) under grant No. PHY-0140407.

---

[1] L. Anchordoqui, T. Paul, S. Reucroft and J. Swain, Int. J. Mod. Phys. A **18**, 2229 (2003) [arXiv:hep-ph/0206072].

[2] M. Nagano and A. A. Watson, Rev. Mod. Phys. **72**, 689 (2000).
[3] A. A. Watson, Phys. Rept. **333**, 309 (2000).
[4] X. Bertou, M. Boratav and A. Letessier-Selvon, Int. J. Mod. Phys. A **15**, 2181 (2000) [arXiv:astro-ph/0001516].
[5] S. Yoshida and H. Dai, J. Phys. G **24**, 905 (1998) [arXiv:astro-ph/9802294].
[6] P. Sokolsky, P. Sommers and B. R. Dawson, Phys. Rept. **217**, 225 (1992).
[7] G. W. Clark, J. Earl, W. L. Kraushaar, J. Linsley, B. B. Rossi, F. Scherb, and D. W. Scott, Phys. Rev. **122**, 637 (1961).
[8] G. W. Clark, J. Earl, W. L. Kraushaar, J. Linsley, B. B. Rossi, and F. Scherb, Nature **180**, 353 (1957).
[9] G. W. Clark, J. Earl, W. L. Kraushaar, J. Linsley, B. B. Rossi, and F. Scherb, Nuovo Cim. Suppl. **8** Ser. 10, 623 (1958).
[10] J. Linsley, L. Scarsi, and B. Rossi, Phys. Rev. Lett. **6**, 485 (1961).
[11] J. Linsley and L. Scarsi, Phys. Rev. **128**, 2384 (1962).
[12] J. Linsley, Phys. Rev. Lett. **10**, 146 (1963).
[13] M. A. Lawrence, R. J. Reid and A. A. Watson, J. Phys. G **17**, 733 (1991).
[14] G. B. Khristiansen, Proc. of 19th International Cosmic Ray Conference (La Jolla), **9** 487 (1985).
[15] A. A. Ivanov, S. P. Knurenko and I. Y. Sleptsov, Nucl. Phys. Proc. Suppl. **122**, 226 (2003) [arXiv:astro-ph/0305053].
[16] M. M. Winn, J. Ulrichs, L. S. Peak, C. B. Mccusker and L. Horton, J. Phys. G **12**, 653 (1986).
[17] N. Chiba *et al.*, Nucl. Instrum. Meth. A **311**, 338 (1992).
[18] H. Ohoka *et al.,* [AGASA Collaboration], Nucl. Instrum. Meth. A **385**, 268 (1997).
[19] H. E. Bergeson *et al.*, Phys. Rev. Lett. **39**, 847 (1977).
[20] R. M. Baltrusaitis *et al.*, Nucl. Instrum. Meth. A **240**, 410 (1985).
[21] R. M. Baltrusaitis *et al.*, Nucl. Instrum. Meth. A **264**, 87 (1988).
[22] S. C. Corbato *et al.*, Nucl. Phys. Proc. Suppl. **28B**, 36 (1992).
[23] T. Abu-Zayyad *et al.*, Nucl. Instrum. Meth. A **450**, 253 (2000).
[24] P. M. S. Blackett and A. C. B Lovell, Proc. Roy. Soc. (London) Ser. A **177**, 183 (1940).
[25] P. W. Gorham, Astropart. Phys. **15**, 177 (2001) [arXiv:hep-ex/0001041].
[26] P. W. Gorham, AIP Conf. Proc. **579**, 253 (2001).
[27] T. Vinogradova, E. Chapin, P. Gorham and D. Saltzberg, AIP Conf. Proc. **579**, 271 (2001).
[28] J. Abraham *et al.* [AUGER Collaboration], Nucl. Instrum. Meth. A **523**, 50 (2004).
[29] O. Catalano, Nuovo Cim. **24C**, 445 (2001).
[30] L. Scarsi, Nuovo Cim. **24C**, 471 (2001).
[31] J. A. Hinton [The HESS Collaboration], New Astron. Rev. **48**, 331 (2004) [arXiv:astro-ph/0403052].
[32] C. Baixeras *et al.*, Nucl. Instrum. Meth. A **518**, 188 (2004).
[33] M. Mori [CANGAROO Collaboration], Prog. Theor. Phys. Suppl. **151**, 85 (2003).
[34] T. C. Weekes *et al.*, Astropart. Phys. **17**, 221 (2002) [arXiv:astro-ph/0108478].

[35] N. Gehrels [GLAST Collaboration], AIP Conf. Proc. **558**, 3 (2001).
[36] N. Gehrels and P. Michelson, Astropart. Phys. **11**, 277 (1999).
[37] F. Longo *et al.*, Nucl. Phys. Proc. Suppl. **125**, 222 (2003).
[38] L. A. Anchordoqui, M. T. Dova, L. N. Epele and S. J. Sciutto, Phys. Rev. D **59**, 094003 (1999) [arXiv:hep-ph/9810384].
[39] J. Ranft, arXiv:hep-ph/0012171.
[40] J. Alvarez-Muniz, R. Engel, T. K. Gaisser, J. A. Ortiz and T. Stanev, arXiv:astro-ph/0205302.
[41] J. Knapp, D. Heck, S. J. Sciutto, M. T. Dova and M. Risse, Astropart. Phys. **19**, 77 (2003) [arXiv:astro-ph/0206414].
[42] L. Anchordoqui, M. T. Dova, A. Mariazzi, T. McCauley, T. Paul, S. Reucroft and J. Swain, arXiv:hep-ph/0407020.
[43] M. Ave, J. A. Hinton, R. A. Vazquez, A. A. Watson and E. Zas, Phys. Rev. Lett. **85**, 2244 (2000) [arXiv:astro-ph/0007386].
[44] J. Linsley and A. A. Watson, Phys. Rev. Lett. **46**, 459 (1981).
[45] A. M. Hillas, J. D. Hollows, H. W. Hunter, and D. J. Marsden, Proc. 12th International Cosmic Ray Conference (Hobart) **3**, 1007 (1971).
[46] L. Anchordoqui and H. Goldberg, Phys. Lett. B (to be published) [arXiv:hep-ph/0310054].
[47] D. J. Bird *et al.* [HIRES Collaboration], Phys. Rev. Lett. **71**, 3401 (1993).
[48] T. K. Gaisser *et al.* [HIRES Collaboration], Phys. Rev. D **47**, 1919 (1993).
[49] R. Walker and A. A. Watson, J. Phys. G **8**, 1131 (1982).
[50] N. Hayashida *et al.* [Akeno Collaboration], J. Phys. G **21**, 1101 (1995).
[51] T. Wibig and A. W. Wolfendale, J. Phys. G. **25**, 1099 (1999).
[52] M. T. Dova, M. E. Mancenido, A. G. Mariazzi, T. P. McCauley and A. A. Watson, arXiv:astro-ph/0312463.
[53] B. R. Dawson, R. Meyhandan and K. M. Simpson, Astropart. Phys. **9**, 331 (1998) [arXiv:astro-ph/9801260].
[54] M. Ave, L. Cazon, J. A. Hinton, J. Knapp, J. LLoyd-Evans and A. A. Watson, Astropart. Phys. **19**, 61 (2003) [arXiv:astro-ph/0203150].
[55] M. T. Dova, M. E. Mancenido, A. G. Mariazzi, T. P. McCauley and A. A. Watson, arXiv:astro-ph/0305351.
[56] N. Hayashida *et al.*, Phys. Rev. Lett. **77**, 1000 (1996).
[57] G. R. Farrar and P. L. Biermann, Phys. Rev. Lett. **81**, 3579 (1998) [arXiv:astro-ph/9806242].
[58] J. Linsley, Phys. Rev. Lett. **34**, 1530 (1975).
[59] N. Hayashida *et al.* [AGASA Collaboration], Astropart. Phys. **10**, 303 (1999) [arXiv:astro-ph/9807045].
[60] M. Teshima *et al.*, Proc. 27th International Cosmic Ray Conference, (Copernicus Gesellschaft, 2001) p.341.
[61] D. J. Bird *et al.* [HIRES Collaboration], Astrophys. J. **511**, 739 (1999) [arXiv:astro-ph/9806096].

[62] J. A. Bellido, R. W. Clay, B. R. Dawson and M. Johnston-Hollitt, Astropart. Phys. **15**, 167 (2001) [arXiv:astro-ph/0009039].
[63] K. Tsuchiya *et al.* [CANGAROO-II Collaboration], Astrophys. J. **606**, L115 (2004) [arXiv:astro-ph/0403592].
[64] T. Antoni *et al.* [The KASCADE Collaboration], arXiv:astro-ph/0312375.
[65] L. A. Anchordoqui, H. Goldberg, F. Halzen and T. J. Weiler, arXiv:astro-ph/0311002.
[66] D. M. Edge, A. M. Pollock, R. J. Reid, A. A. Watson and J. G. Wilson, J. Phys. G **4**, 133 (1978).
[67] M. M. Winn, J. Ulrichs, L. S. Peak, C. B. Mccusker and L. Horton, J. Phys. G **12**, 675 (1986).
[68] G. L. Cassiday *et al.*, Astrophys. J. **351**, 454 (1990).
[69] M. Takeda *et al.*, Astrophys. J. **522**, 225 (1999) [arXiv:astro-ph/9902239].
[70] N. W. Evans, F. Ferrer and S. Sarkar, Astropart. Phys. **17**, 319 (2002).
[71] J. Wdowczyk and A. W. Wolfendale, J. Phys. G **10**, 1453 (1984).
[72] L. A. Anchordoqui, C. Hojvat, T. P. McCauley, T. C. Paul, S. Reucroft, J. D. Swain and A. Widom, Phys. Rev. D **68**, 083004 (2003) [arXiv:astro-ph/0305158].
[73] R. Abbasi *et al.* [HiRes Collaboration], arXiv:astro-ph/0309457.
[74] N. Hayashida *et. al.* [AGASA Collaboration], arXiv:astro-ph/0008102.
[75] L. A. Anchordoqui, H. Goldberg, S. Reucroft, G. E. Romero, J. Swain and D. F. Torres, Mod. Phys. Lett. A **16**, 2033 (2001) [arXiv:astro-ph/0106501].
[76] H. Goldberg and T. J. Weiler, Phys. Rev. D **64**, 056008 (2001) [arXiv:astro-ph/0009378].
[77] Y. Uchihori, M. Nagano, M. Takeda, M. Teshima, J. Lloyd-Evans and A. A. Watson, Astropart. Phys. **13**, 151 (2000) [arXiv:astro-ph/9908193].
[78] P. G. Tinyakov and I. I. Tkachev, JETP Lett. **74**, 1 (2001) [Pisma Zh. Eksp. Teor. Fiz. **74**, 3 (2001)] [arXiv:astro-ph/0102101].
[79] R. U. Abbasi *et al.* [HiRes Collaboration], arXiv:astro-ph/0404137.
[80] R. U. Abbasi *et al.* [HiRes Collaboration], arXiv:astro-ph/0404366.
[81] C. B. Finley and S. Westerhoff, arXiv:astro-ph/0309159.
[82] P. Bhattacharjee and G. Sigl, Phys. Rept. **327**, 109 (2000) [arXiv:astro-ph/9811011].
[83] G. Sigl, *Prepared for Physics and Astrophysics of Ultrahigh-energy Cosmic Rays,* Meudon, France, 26-29 Jun 2000.
[84] F. W. Stecker, J. Phys. G **29**, R47 (2003) [arXiv:astro-ph/0309027].
[85] L. A. Anchordoqui and M. T. Dova, AUGER Internal Note, GAP-2003-092.
[86] K. Greisen, Phys. Rev. Lett. **16**, 748 (1966).
[87] G. T. Zatsepin and V. A. Kuzmin, JETP Lett. **4**, 78 (1966) [Pisma Zh. Eksp. Teor. Fiz. **4**, 114 (1966)].
[88] O. E. Kalashev, V. A. Kuzmin, D. V. Semikoz and I. I. Tkachev, arXiv:astro-ph/0107130.
[89] F. W. Stecker, Phys. Rev. Lett. **21**, 1016 (1968).
[90] C. T. Hill and D. N. Schramm, Phys. Rev. D **31**, 564 (1985).
[91] V. S. Berezinsky and S. I. Grigor'eva, Astron. Astrophys. **199**, 1 (1988).

[92] F. W. Stecker, Nature **342**, 401 (1989).
[93] F. A. Aharonian, B. L. Kanevsky and V. V. Vardanian, Astrophys. Space. Sci. **167**, 93 (1990).
[94] S. Yoshida and M. Teshima, Prog. Theor. Phys. **89**, 833 (1993).
[95] F. A. Aharonian and J. W. Cronin, Phys. Rev. D **50**, 1892 (1994).
[96] R. J. Protheroe and P. A. Johnson, Astropart. Phys. **4**, 253 (1996) [arXiv:astro-ph/9506119].
[97] L. A. Anchordoqui, M. T. Dova, L. N. Epele and J. D. Swain, Nucl. Phys. Proc. Suppl. **52B**, 249 (1997).
[98] L. A. Anchordoqui, M. T. Dova, L. N. Epele and J. D. Swain, Phys. Rev. D **55**, 7356 (1997) [arXiv:hep-ph/9704387].
[99] S. Lee, Phys. Rev. D **58**, 043004 (1998) [arXiv:astro-ph/9604098].
[100] A. Achterberg, Y. A. Gallant, C. A. Norman and D. B. Melrose, arXiv:astro-ph/9907060.
[101] T. Stanev, R. Engel, A. Mucke, R. J. Protheroe and J. P. Rachen, Phys. Rev. D **62**, 093005 (2000) [arXiv:astro-ph/0003484].
[102] Z. Fodor and S. D. Katz, Phys. Rev. D **63**, 023002 (2001) [arXiv:hep-ph/0007158].
[103] L. A. Anchordoqui and D. F. Torres, Phys. Lett. A **283**, 319 (2001) [arXiv:cond-mat/0009199].
[104] G. R. Blumenthal, Phys. Rev. D **1**, 1596 (1970).
[105] F. W. Stecker, Phys. Rev. **180**, 1264 (1969).
[106] J. L. Puget, F. W. Stecker and J. H. Bredekamp, Astrophys. J. **205**, 638 (1976).
[107] L. A. Anchordoqui, M. T. Dova, L. N. Epele and J. D. Swain, Phys. Rev. D **57**, 7103 (1998) [arXiv:astro-ph/9708082].
[108] L. A. Anchordoqui, *Ph.D. Thesis* [arXiv:astro-ph/9812445].
[109] L. N. Epele and E. Roulet, JHEP **9810**, 009 (1998) [arXiv:astro-ph/9808104].
[110] F. W. Stecker and M. H. Salamon, Astrophys. J. **512**, 521 (1992) [arXiv:astro-ph/9808110].
[111] G. R. Farrar and P. L. Biermann, Phys. Rev. Lett. **83**, 2472 (1999) [arXiv:astro-ph/9901315].
[112] M. Lemoine, G. Sigl and P. Biermann, arXiv:astro-ph/9903124.
[113] G. R. Farrar and T. Piran, Phys. Rev. Lett. **84**, 3527 (2000) [arXiv:astro-ph/9906431].
[114] P. Blasi and A. V. Olinto, Phys. Rev. D **59** (1999) 023001 [arXiv:astro-ph/9806264].
[115] G. Sigl, M. Lemoine and P. Biermann, Astropart. Phys. **10**, 141 (1999) [arXiv:astro-ph/9806283].
[116] E. Waxman and J. Miralda-Escude, Astrophys. J. **472**, L89 (1996) [arXiv:astro-ph/9607059].
[117] K.-T. Kim, P. P. Kronberg, G. Giovannini and T. Venturi, Nature **341**, 720 (1989).
[118] T. E. Clarke, P. P. Kronberg and H. Böhringer, Astrophys. J. **547**, L111 (2001).
[119] P. P. Kronberg, Rept. Prog. Phys. **57**, 325 (1994).
[120] D. Ryu, H. Kang, and P. L. Biermann, Astron. Astrophys. **335**, 19 (1998).
[121] J. P. Vallée, Astrophys. J. **360**, 1 (1990).

[122] P. Blasi, S. Burles and A. V. Olinto, Astrophys. J. **514**, L79 (1999) [arXiv:astro-ph/9812487].
[123] J. D. Barrow, P. G. Ferreira and J. Silk, Phys. Rev. Lett. **78**, 3610 (1997) [arXiv:astro-ph/9701063].
[124] K. Jedamzik, V. Katalinic and A. V. Olinto, Phys. Rev. Lett. **85**, 700 (2000) [arXiv:astro-ph/9911100].
[125] L. A. Anchordoqui and H. Goldberg, Phys. Rev. D **65**, 021302 (2002) [arXiv:hep-ph/0106217].
[126] R. N. Manchester, Astrophys. J. **188**, 637 (1974).
[127] R. C. Thomson and A. H. Nelson, Mont. Not. Roy. Astron. Soc. **191**, 863 (1980).
[128] J. L. Han and G. J. Qiao, Astron. Astrophys. **288**, 759 (1994).
[129] C. Indrani and A. A. Deshpande, New Astron. **4**, 33 (1998).
[130] R. Beck, A. Brandenburg, D. Moss, A. Shukurov, and D. Sokoloff, Ann. Rev. Astron. Astrophys. **34**, 155 (1996).
[131] J. L. Han, R. N. Manchester and G. J. Qiao, Mont. Not. Roy. Astron. Soc. **306**, 371 (1999) [arXiv:astro-ph/9903101].
[132] J. P. Vallée, Astrophys. J. **366**, 450 (1991).
[133] T. Stanev, Astrophys. J. **479**, 290 (1997) [arXiv:astro-ph/9607086].
[134] D. Harari, S. Mollerach and E. Roulet, JHEP **9908**, 022 (1999) [arXiv:astro-ph/9906309].
[135] D. J. Bird *et al.*, Astrophys. J. **441**, 144 (1995).
[136] J. W. Elbert and P. Sommers, Astrophys. J. **441**, 151 (1995) [arXiv:astro-ph/9410069].
[137] M. Takeda *et al.*, Phys. Rev. Lett. **81**, 1163 (1998) [arXiv:astro-ph/9807193].
[138] T. Abu-Zayyad *et al.* [HiRes Collaboration], arXiv:astro-ph/0208243.
[139] T. Abu-Zayyad *et al.* [High Resolution Fly's Eye Collaboration], arXiv:astro-ph/0208301.
[140] M. Takeda *et al.*, Astropart. Phys. **19**, 447 (2003) [arXiv:astro-ph/0209422].
[141] D. J. Bird *et al.* [HIRES Collaboration], Astrophys. J. **424** (1994) 491.
[142] M. Ave, J. Knapp, J. Lloyd-Evans, M. Marchesini and A. A. Watson, Astropart. Phys. **19**, 47 (2003) [arXiv:astro-ph/0112253].
[143] J. N. Bahcall and E. Waxman, Phys. Lett. B **556**, 1 (2003) [arXiv:hep-ph/0206217].
[144] A. A. Watson, Proc. 28th International Cosmic Ray Conference (Tsukuba), 373 (2003).
[145] A. R. Bell, Mon. Not. Roy. Astron. Soc. **182**, 147, (1978).
[146] D. F. Torres, G. E. Romero, T. M. Dame, J. A. Combi, and Y. M. Butt, Phys. Rept. **382**, 303 (2003) [arXiv:astro-ph/0209565].
[147] S. P. Reynolds, Astrophys. J. **459**, L13 (1996).
[148] S. P. Reynolds, Astrophys. J. **493**, 375 (1998).
[149] A. M. Bykov and G. D. Fleishman, Mon. Not. Roy. Astron. Soc. **255**, 269 (1992a).
[150] A. M. Bykov and G. D. Fleishman, Sov. Astron. Lett. **18**, 95 (1992b).
[151] D. F. Torres, E. Domingo-Santamaria and G. E. Romero, Astrophys. J. **601**, L75 (2004) [arXiv:astro-ph/0312128].
[152] F. A. Aharonian, A. Akhperjanian, M. Beilicke, Y. Uchiyama and T. Takahashi, Astron.

Astrophys. **393**, L37 (2002) [arXiv:astro-ph/0207528].
[153] Y. Butt et. al., Astrophys. J. **597**, 494 (2003) [arXiv:astro-ph/0302342].
[154] R. L. White and W. Chen, Astrophys. J. **387** L81 (1992).
[155] W. Chen, R. L. White, and D. Bertsch, Astron. Astrophys. Suppl. **120**, 423 (1996).
[156] P. Benaglia, G. E. Romero, I. R. Stevens and D. F. Torres, Astron. Astrophys. **366**, 605 (2001) [arXiv:astro-ph/0010605].
[157] G. E. Romero, P. Benaglia and D. F. Torres, Astron. Astrophys. **348**, 868 (1999) [arXiv:astro-ph/9904355].
[158] D. F. Torres, G. E. Romero, J. A. Combi, P. Benaglia, H. Andernach and B. Punsly, Astron. Astrophys. **370**, 468 (2001) [arXiv:astro-ph/0007464].
[159] D. F. Torres, M. E. Pessah and G. E. Romero, Astron. Nachr. **322**, 223 (2001) [arXiv:astro-ph/0104351].
[160] P. L. Nolan, W. F. Tompkins, I. A. Grenier and P. F. Michelson, Astrophys. J. **597**, 615 (2003) [arXiv:astro-ph/0307188].
[161] Y. M. Butt, D. F. Torres, J. A. Combi, T. Dame and G. E. Romero, Astrophys. J. **562**, L167 (2001) [arXiv:astro-ph/0109292].
[162] R. Enomoto et. al., Nature **416**, 823 (2002).
[163] O. Reimer, M. Pohl, Y. M. Butt, D. F. Torres and G. E. Romero, Astron. Astrophys. **390**, L43 (2002) [arXiv:astro-ph/0205256].
[164] Y. M. Butt, D. F. Torres, G. E. Romero, T. M. Dame and J. A. Combi, Nature **418**, 499 (2002) [arXiv:astro-ph/0208034].
[165] Y. Uchiyama, F. A. Aharonian and T. Takahashi, Astron. Astrophys. **400**, 567 (2003) [arXiv:astro-ph/0209217].
[166] E. G. Berezhko, L. T. Ksenofontov and H. J. Voelk, Astron. Astrophys. **412**, L11 (2003) [arXiv:astro-ph/0310862].
[167] E. G. Berezhko, G. Puehlhofer and H. J. Voelk, Astron. Astrophys. **400**, 971 (2003) [arXiv:astro-ph/0301205].
[168] J. Alvarez-Muniz and F. Halzen, Astrophys. J. **576**, L33 (2002) [arXiv:astro-ph/0205408].
[169] L. A. Anchordoqui, D. F. Torres, T. P. McCauley, G. E. Romero and F. A. Aharonian, Astrophys. J. **589**, 481 (2003) [arXiv:hep-ph/0211231].
[170] G. E. Romero, D. F. Torres, M. M. K. Bernado and I. F. Mirabel, Astron. Astrophys. **410**, L1 (2003) [arXiv:astro-ph/0309123].
[171] W. Bednarek, Astron. Astrophys. **407**, 1 (2003) [arXiv:astro-ph/0305430].
[172] A. M. Hillas, Ann. Rev. Astron. Astrophys. **22**, 425 (1984).
[173] A. Venkatesan, M. C. Miller and A. V. Olinto, Astrophys. J. **484**, 323 (1997) [arXiv:astro-ph/9612210].
[174] A. Mucke, R. J. Protheroe, R. Engel, J. P. Rachen, T. Stanev, Astropart. Phys. **18**, 593 (2003).
[175] G. Pelletier and E. Kersale, Astron. Astrophys. **361**, 788 (2000) [arXiv:astro-ph/0007096].
[176] R. J. Protheroe, arXiv:astro-ph/0401523.

[177] F. A. Aharonian, A. A. Belyanin, E. V. Derishev, V. V. Kocharovsky and V. V. Kocharovsky, Phys. Rev. D **66**, 023005 (2002) [arXiv:astro-ph/0202229].
[178] M. V. Medvedev, Phys. Rev. E **67**, 045401 (2003) [arXiv:astro-ph/0303271].
[179] A. V. Olinto, R. I. Epstein, and P. Blasi, Proc. 26th International Cosmic Ray Conference (Salt Lake City) 4, 361 (1999).
[180] J. Gunn and J. Ostriker, Phys. Rev. Lett. **22**, 728 (1969).
[181] A. R. Bell, Mon. Not. Roy. Astron. Soc. **257**, 493 (1992).
[182] P. Blasi, R. I. Epstein and A. V. Olinto, Astrophys. J. **533**, L123 (2000) [arXiv:astro-ph/9912240].
[183] M. Giller in the *Eighteenth Texas Symposium on Relativistic Astrophysics and Cosmology, Texas in Chicago, Chicago, 15-20 December 1996"* ., p.444 (edited by Angela V. Olinto, Joshua A. Frieman, and David N. Schramm. River Edge, N. J. : World Scientific, 1998).
[184] W. Bednarek, M. Giller and M. Zielinska, J. Phys. G **28**, 2283 (2002) [arXiv:astro-ph/0205324].
[185] E. M. De Gouveia Dal Pino and A. Lazarian, Astrophys. J. **560**, 358 (2001) [arXiv:astro-ph/0106452].
[186] C. Litwin and R. Rosner, Phys. Rev. Lett. **86**, 4745 (2001) [arXiv:astro-ph/0104090].
[187] F. C. Michel, Theory of Neutron Stars Magnetosphere (The University of Chicago Press:Chicago, 1991).
[188] P. Goldreich and W. H. Julian, Astrophys. J. **157**, 869 (1969).
[189] Y. A. Gallant and J. Arons, Astrophys. J. **435**, 230 (1994).
[190] M. C. Begelman and Z-Y. Li, Astrophys. J. **426**, 269 (1994).
[191] T. Chiueh, Z-Y. Li, and M. C. Begelman, Astrophys. J. **505**, 835 (1998).
[192] A. Melatos and D. B. Melrose, Mon. Not. Roy. Astron. Soc. **279**, 1168 (1996).
[193] V. S. Berezinskii, S. V. Bulanov, V. A. Dogiel, V. L. Ginzburg, and V. S. Ptuskin, *Astrophysics of Cosmic Rays*, (North Holland, Amsterdam, 1990).
[194] M. Kramer *et al.*, Mon. Not. Roy. Astron. Soc. **342**, 1299 (2003) [arXiv:astro-ph/0303473].
[195] D. F. Torres, Y. M. Butt and F. Camilo, Astrophys. J. **560**, L155 (2001) [arXiv:astro-ph/0109228].
[196] D. F. Torres and S. E. Nuza, Astrophys. J. **583**, L25 (2003) [arXiv:astro-ph/0212168].
[197] M. Duncan and C. Thompson, Astrophys. J. **392**, L9 (1992).
[198] B. Paczynski, Acta Astron. **42**, 145 (1992).
[199] C. Kouveliotou et. al., Nature **393**, 235 (1998).
[200] C. Kouveliotou, Proc. Natl. Acad. Sci. **96**, 5351 (1999).
[201] C. Kouveliotou et. al., Astrophys. J. **510**, L115 (1999).
[202] J. Arons, Astrophys. J. **589**, 871 (2003) [arXiv:astro-ph/0208444].
[203] S. Singh, C. P. Ma and J. Arons, arXiv:astro-ph/0308257.
[204] M. R. Blanton, et al., Astron. J. **121**, 2358 (2001).
[205] E. Cappellaro, R. Evans, and M. Turatto, Astron. Astrophys. **351**, 459 (1999).
[206] J. Knodlseder, astro-ph/0007442.

[207] W. Bednarek, Mon. Not. Roy. Astron. Soc. **345**, 847 (2003) [arXiv:astro-ph/0307216].
[208] W. Bednarek, Mon. Not. Roy. Astron. Soc. **331**, 483 (2002) [arXiv:astro-ph/0112008].
[209] M. R. Crutcher and S. -P. Lai, ASP Conf. Proc. **267**, 61 (2002). Edited by Paul A. Crowther, San Francisco, Astronomical Society of the Pacific.
[210] W. Bednarek and R. J. Protheroe, Astropart. Phys. **16**, 397 (2002).
[211] C. D. Wilson, C. E. Walker and M. D. Thornley, arXiv:astro-ph/9701245.
[212] G. L. Cassiday *et al.*, Phys. Rev. Lett. **62**, 383 (1989).
[213] M. Teshima *et al.*, Phys. Rev. Lett. **64**, 1628 (1990).
[214] C. M. Urry and P. Padovani, ASP Conf. Proc. **107**, 803 (1995).
[215] P. Padovani, (1997), astro-ph/9701074.
[216] W. Collmar, Mem. Soc. Astron. Ital. **73**, 99 (2002).
[217] D. F. Torres, (2004). To appear in the book "Cosmic Gamma-ray Sources", edited by K.S. Cheng and G.E. Romero, to be published by Kluwer Academic Press, arXiv:astro-ph/0308069.
[218] A. Kembhavi and J. V. Narlikar, Quasars and Active Galactic Nuclei, Cambridge University Press, Cambridge, 1999
[219] B. L. Fannaroff and J. M. Riley, Mon. Not. Roy. Astron. Soc. **167**, 31 (1974).
[220] R. D. Blandford and M. J. Rees, Mon. Not. Roy. Astron. Soc. **169**, 395 (1974).
[221] M. C. Begelman, R. D. Blandford and M. J. Rees, Rev. Mod. Phys. **56**, 255 (1984).
[222] P. L. Biermann and P. A. Strittmatter, Astrophys. J. **322**, 643 (1987).
[223] A. N. Kolmogorov, C. R. Acad. URSS **30**, 201 (1941).
[224] L. O. 'C. Drury, Rep. Prog. Phys. **46**, 973 (1983).
[225] K. Mannheim, Space Sci. Rev. **75**, 331 (1996).
[226] K. Mannheim, Science **279**, 684 (1998) [arXiv:astro-ph/9803241].
[227] K. Mannheim, Rev. Mod. Astron. **12**, 101 (1999) [arXiv:astro-ph/9902185].
[228] K. Mannheim, Astron. Astrophys. **269**, 67 (1993) [arXiv:astro-ph/9302006].
[229] F. A. Aharonian, New Astron. **5**, 377 (2000) [arXiv:astro-ph/0003159].
[230] G. B. Rybicki and A. P. Lightman, *Radiative Processes in Astrophysics* (New York: Wiley-Interscience, 1979).
[231] T. A. Armstrong et. al., Phys. Rev. D **5** (1972) 1640.
[232] J. P. Rachen and P. L. Biermann, Astron. Astrophys. **272**, 161 (1993) [arXiv:astro-ph/9301010].
[233] J. T. Stocke, G. H. Rieke, and M. J. Lebofsky, Nature **294**, 319 (1981).
[234] J. R. P. Angel and H. S. Stockman, Ann. Rev. Astron. Astrophys. **18**, 321 (1980).
[235] F. P. Israel, Astron. Astrophys. Rev. **8**, 237 (1998).
[236] J. O. Burns, E. D. Feigelson, and E. J. Schreier, Astrophys. J. **273**, 128 (1983).
[237] L. Landau and E. Lifchitz, *Fluid Mechanics* (Pergamon Press, Oxford, 1958).
[238] G. E. Romero, S. Perez-Bergliaffa, L. A. Anchordoqui and J. A. Combi, Grav. Cosmol. **S5** (1999) 188.
[239] G. E. Romero, J. A. Combi, L. A. Anchordoqui and S. E. Perez Bergliaffa, Astropart. Phys. **5**, 279 (1996) [arXiv:gr-qc/9511031].
[240] N. Junkes, R. F. Haynes, J. I. Harnett, and D. L. Jauncey, Astron. Astrophys. **269**, 29

(1993) [Erratum, *ibid* **274**, 1009 (1993)].
[241] J. A. Combi and G. E. Romero, Astron. Astrophys. Suppl. **121**, 11 (1997).
[242] R. Schopper, G. T. Birk and H. Lesch, Astropart. Phys. **17**, 347 (2002) [arXiv:astro-ph/0106530].
[243] P. Sreekumar, D. L. Bertsch, R. C. Hartman, P. L. Nolan and D. J. Thompson, Astropart. Phys. **11**, 221 (1999) [arXiv:astro-ph/9901277].
[244] J. E. Grindlay et. al., Astrophys. J. **197**, L9 (1975).
[245] H. Steinle, AIP Conf. Proc. **587**, 353 (2001) [arXiv:astro-ph/0105482].
[246] R. W. Clay, B. R. Dawson and R. Meyhandan, Astropart. Phys. **2**, 347 (1994).
[247] V. L. Ginzburg, S. I. Syrovatsky, Ann. Rev. Astron. Astrophys. **3**, 297 (1965).
[248] E. Waxman, Phys. Rev. Lett. **75**, 386 (1995) [arXiv:astro-ph/9505082].
[249] S. Rawlings and R. Saunders, Nature **349**, 138 (1991).
[250] G. R. Farrar and T. Piran, arXiv:astro-ph/0010370.
[251] L. A. Anchordoqui, H. Goldberg and T. J. Weiler, Phys. Rev. Lett. **87**, 081101 (2001) [arXiv:astro-ph/0103043].
[252] R. L. Kinzer et. al., Astrophys. J. **449**, 105 (1995).
[253] H. Steinle et. al., Astron. Astrophys. **330**, 97 (1998).
[254] C. Isola, M. Lemoine and G. Sigl, Phys. Rev. D **65**, 023004 (2002) [arXiv:astro-ph/0104289].
[255] C. Isola and G. Sigl, Phys. Rev. D **66**, 083002 (2002) [arXiv:astro-ph/0203273].
[256] F. Aharonian, et al. [HEGRA Collaboration], Astron. Astrophys. **403**, L1 (2003) [arXiv:astro-ph/0302155].
[257] P. Sreekumar et al., Astrophys. J. **426**, 105 (1994)
[258] R. J. Protheroe, A. C. Donea and A. Reimer, Astropart. Phys. **19**, 559 (2003) [arXiv:astro-ph/0210249].
[259] C. Dermer and Y. Rephaeli, Astrophys. J. **329**, 687 (1988).
[260] V. L. Ginzburg, S. I. Syrovatsky, *The origin of cosmic rays*, (Pergamon Press, Oxford 1964).
[261] J. Wdowczyk and A. W. Wolfendale, Nature **281**, 356 (1979).
[262] J. C. Cohen , Astron. J. **119**, 162 (2000).
[263] R. Blandford, Lect. Notes Phys. **530**, 1 (1999).
[264] S. Heinz and M. C. Begelman, Lect. Notes Phys. **530**, 229 (1999).
[265] G. V. Bicknell and M. C. Begelman, Lect. Notes Phys. **530**, 235 (1999).
[266] E. J. Ahn, G. Medina-Tanco, P. L. Biermann and T. Stanev, arXiv:astro-ph/9911123.
[267] P. L. Biermann, E. J. Ahn, G. Medina Tanco and T. Stanev, Nucl. Phys. Proc. Suppl. **87** (2000) 417 [arXiv:astro-ph/0008063].
[268] J. A. Burke, Mon. Not. Roy. Astron. Soc. **140**, 241 (1968).
[269] H. E. Johnson and W. I. Axford, Astrophys. J. **165**, 381 (1971).
[270] W. G. Mathews and J. C. Baker, Astrophys. J. **170**, 241 (1971).
[271] E. N. Parker, Astrophys. J. **128**, 664 (1958).
[272] T. Stanev, D. Seckel and R. Engel, arXiv:astro-ph/0108338.
[273] L. A. Anchordoqui, M. T. Dova, T. P. McCauley, S. Reucroft and J. D. Swain, Phys.

Lett. B **482**, 343 (2000) [arXiv:astro-ph/9912081].
[274] D. Harari, S. Mollerach and E. Roulet, JHEP **0010**, 047 (2000) [arXiv:astro-ph/0005483].
[275] P. Billoir and A. Letessier-Selvon, arXiv:astro-ph/0001427.
[276] P. L. Biermann, E. -J. Ahn, P. P. Kronberg, G. Medina Tanco, and T. Stanev, in *Physics and Astrophysics of Ultra-High-Energy Cosmic Rays*, (Edts. M. Lemoine and G. Sigl, Springer-Verlag, Berlin, 2001).
[277] L. A. Anchordoqui, G. E. Romero, J. A. Combi and S. E. Perez Bergliaffa, Mod. Phys. Lett. A **13**, 3039 (1998) [arXiv:astro-ph/9811378].
[278] J. P. Rachen, T. Stanev and P. L. Biermann, Astron. Astrophys. **273**, 377 (1993) [arXiv:astro-ph/9302005].
[279] R. Mukherjee, J. Halpern, N. Mirabal and E. V. Gotthelf, Astrophys. J. 574, 693 (2002) [arXiv:astro-ph/0204489].
[280] H. Sudou and Y. Taniguchi, arXiv:astro-ph/0004194.
[281] J. A. Combi, G. E. Romero, J. M. Paredes, D. F. Torres and M. Ribo, Astrophys. J. **588**, 731 (2003) [arXiv:astro-ph/0301487].
[282] C. M. Hoffman, Phys. Rev. Lett. **83**, 2471 (1999) [arXiv:astro-ph/9901026].
[283] G. Sigl, D. F. Torres, L. A. Anchordoqui and G. E. Romero, Phys. Rev. D **63**, 081302 (2001) [arXiv:astro-ph/0008363].
[284] A. Virmani, S. Bhattacharya, P. Jain, S. Razzaque, J. P. Ralston and D. W. McKay, Astropart. Phys. **17**, 489 (2002) [arXiv:astro-ph/0010235].
[285] P. G. Tinyakov and I. Tkachev I., JETP Lett. **74**, 445 (2001) [Pisma Zh. Eksp. Teor. Fiz. **74**, 499 (2001)] [arXiv:astro-ph/0102476].
[286] P. G. Tinyakov and I. Tkachev I., Astropart. Phys. **18**, 165 (2002) [arXiv:astro-ph/0111305].
[287] P. G. Tinyakov and I. Tkachev I., arXiv:astro-ph/0301336.
[288] M. P. Veron-Cetty and P. Veron, *A catalogue of Quasars and Active Galactic Nuclei, 9th Edition,* ESO Scientific Report (2000).
[289] B. N. Afanasiev, et al., 1996 *in Proc. Int. Symp. on Extremely High Energy Cosmic Rays : Astrophysics and Future Observatories* (ed. M.Nagano, Institute for Cosmic Ray Research, Univ. of Tokyo) p.32.
[290] N. W. Evans, F. Ferrer and S. Sarkar, Phys. Rev. D **67**, 103005 (2003) [arXiv:astro-ph/0212533].
[291] D. F. Torres, S. Reucroft, O. Reimer and L. A. Anchordoqui, Astrophys. J. **595**, L13 (2003) [arXiv:astro-ph/0307079].
[292] T. Stanev, P. Biermann, J. Lloyd-Evans, J. P. Rachen and A. A. Watson, Phys. Rev. Lett. **75**, 3056 (1995) [arXiv:astro-ph/9505093].
[293] J. Linsley, *Catalog of Highest Energy Cosmic Ray,* (World Data Center of Cosmic Rays, Institute of Physical and Chemical Research, Itabashi, Tokyo) p.3, (1980).
[294] G. J. Feldman and R. D. Cousins, Phys. Rev. D **57**, 3873 (1998) [arXiv:physics/9711021].
[295] D. S. Gorbunov, P. G. Tinyakov, I. Tkachev and S. V. Troitsky, Astrophys. J. **577**,

L93 (2002) [arXiv:astro-ph/0204360].
[296] B. Punsly, Astron. J. **114**, 544 (1997).
[297] E. Boldt and P. Ghosh, Mon. Not. Roy. Astron. Soc. **307**, 491 (1999) [arXiv:astro-ph/9902342].
[298] E. Boldt and M. Loewenstein, Mon. Not. Roy. Astron. Soc. **316**, L29 (2000) [arXiv:astro-ph/0006221].
[299] M. Schmidt, Physica Scripta **17**, 135 (1978).
[300] D. Richstone et al., Nature Supp., **395**, A14 (1998).
[301] T. A. Small and R. D. Blandford, Mon. Not. Roy. Astron. Soc. **259**, 725 (1992).
[302] A. Chokshi and E. L. Turner, Mon. Not. Roy. Astron. Soc. **259**, 421, 1992.
[303] R. D. Blandford and R. L. Znajek, Mon. Not. Roy. Astron. Soc. **179**, 433 (1977).
[304] R. L. Znajek, Mon. Not. Roy. Astron. Soc. **185** 833 (1978).
[305] J. Krolik Astrophys. J. **515**, L73 (1999).
[306] T. Di Matteo et al. Mon. Not. Roy. Astron. Soc. **305** 492 (1999).
[307] A. Levinson and E. Boldt, Astropart. Phys. **16**, 265 (2002).
[308] F. Stecker, Phys. Rev. Lett. **21** 1016 (1968).
[309] D. F. Torres, E. Boldt, T. Hamilton and M. Loewenstein, Phys. Rev. D **66**, 023001 (2002) [arXiv:astro-ph/0204419].
[310] G. Giuricin, C. Marinori, L. Ceriani, and A. Pisani, Astrophys. J. **543**, 178 (2000).
[311] K. Dolag, D. Grasso, V. Springel and I. Tkachev, arXiv:astro-ph/0310902.
[312] J. Alvarez-Muniz, R. Engel and T. Stanev, Astrophys. J. **572**, 185 (2001) [arXiv:astro-ph/0112227].
[313] C. Isola, G. Sigl and G. Bertone, arXiv:astro-ph/0312374.
[314] A. Levinson, Phys. Rev. Lett. **85**, 912 (2000).
[315] A. Neronov, P. Tinyakov and I. Tkachev, arXiv:astro-ph/0402132.
[316] J. F. Hawley and J. H. Krolik, arXiv:astro-ph/0006456.
[317] L. A. Anchordoqui, G. E. Romero and J. A. Combi, Phys. Rev. D **60**, 103001 (1999) [arXiv:astro-ph/9903145].
[318] T. M. Heckman, L. Armus, and G. K. Miley, Astrophys. J. Suppl. **74**, 833 (1990).
[319] R. W. O'connell and J. J. Mangano, Astrophys. J. **221**, 62 (1978).
[320] G. H. Rieke, et al., Astrophys. J. **238**, 24 (1980).
[321] S. Satyapal, et al. Astrophys. J. **483**, 148 (1997).
[322] R. Beck, C. L. Carilli, M. A. Holdaway, and U. Klein, Astron. Astrophys. **292**, 409 (1994).
[323] T. A. D. Paglione, A. P. Marscher, J. M. Jackson, and D. L. Bertsch, Astrophys. J. **460**, 295 (1996).
[324] A. Ptak, et al., Astron. J. **113**, 1286 (1997).
[325] C. Itoh et al. [CANGAROO-II Collaboration], Astron. Astrophys. **402**, 443 (2003) [arXiv:astro-ph/0304295].
[326] J. S. Ulvestad and R. R. J. Antonucci, Astrophys. J. **488**, 621 (1997).
[327] D. A. Forbes, et al. Astrophys. J. **406**, L11 (1993).
[328] A. M. Watson, et al. Astron. J. **112**, 534 (1996).

[329] E. Keto, et al., Astrophys. J. **518**, 133 (1999).
[330] G. E. Romero and D. F. Torres, Astrophys. J. **586**, L33 (2003) [arXiv:astro-ph/0302149].
[331] P. J. McCarthy, T. Heckman, and W. van Breugel, Astron. J. **92**, 264 (1987).
[332] R. de Grijs, R. W. O'Connell and J. S. . Gallagher, Astrophys. Space Sci. **276**, 397 (2001) [arXiv:astro-ph/9903188].
[333] P. O. Lagage and C. J. Cesarsky, Astron. Astrophys. **118**, 223 (1983).
[334] A. J. Owens, and R. J. Jokipii, Astrophys. J. **215**, 677 (1977).
[335] J. R. Jokipii and G. R. Morfill, Astrophys. J. **290**, L1 (1985).
[336] J. R. Jokipii, Astrophys. J. **313**, 842 (1987).
[337] L. O'C. Drury, Rep. Prog. Phys. **46**, 973 (1983).
[338] P. L. Biermann, Astron. Astrophy. **271**, 649 (1993).
[339] C. W. Engelbracht, M. J. Rieke, G. H. Rieke, D. M. Kelly, and J. M. Achtermann, Astrophys. J. **505**, 639 (1998).
[340] L. Anchordoqui, H. Goldberg, S. Reucroft and J. Swain, Phys. Rev. D **64**, 123004 (2001) [arXiv:hep-ph/0107287].
[341] G. Bertone, C. Isola, M. Lemoine and G. Sigl, arXiv:astro-ph/0209192.
[342] L. A. Anchordoqui, H. Goldberg and D. F. Torres, Phys. Rev. D **67**, 123006 (2003) [arXiv:astro-ph/0209546].
[343] R. W. Clay [Pierre Auger Collaboration], arXiv:astro-ph/0308494.
[344] D. B. Sanders and I. F. Mirabel, Ann. Rev. Astron. Astrophys. **34**, 749 (1996).
[345] D. Downes and P. M. Solomon, Astrophys. J. **507**, 615 (1998).
[346] D. Downes, P. M. Solomon, and S. J. E. Radford, Astrophys. J. **414**, L13 (1993).
[347] D. Downes, P. M. Solomon, and S. J. E. Radford, Astrophys. J. **387**, L55 (1992).
[348] P. M. Solomon, S. J. E. Radford, and D. Downes, Astrophys. J. **348**, L53 (1990).
[349] P. M. Solomon, D. Downes, S. J. E. Radford, and J. W. Barrett, Astrophys. J. **478**, 144 (1997).
[350] L. Gao and P. M. Solomon, astro-ph/0310339.
[351] L. Gao and P. M. Solomon, astro-ph/0310341.
[352] D. F. Torres, O. Reimer, E. Domingo-Santamaria and S. W. Digel, Astrophys. J. **607**, L99 (2004) [arXiv:astro-ph/0405302].
[353] W. Saunders, et al., Mon. Not. Roy. Astron. Soc. **317**, 55 (2000).
[354] A. Smialkowski, M. Giller and W. Michalak, J. Phys. G **28** (2002) 1359 [arXiv:astro-ph/0203337].
[355] R. Della Cecca, et al., Astrophys. J. **581**, L9 (2002).
[356] F. Mannucci et. al., Astron. and Astrophys. **401**, 519 (2003).
[357] B. T. Soifer, et. al., Astrophys. J. **303**, L41 (1986).
[358] R. Coziol, et al. Astrophys. J. Suppl. **119**, 239 (1998).
[359] A. Cillis, D. F. Torres, and O. Reimer, in preparation.
[360] G. J. Fishman and C. A. Meegan, An. Rev. Astron. Astrophys. **33**, 415 (1995).
[361] B. Link and R. I. Epstein, Astrophys. J. **466**, 764 (1996) [arXiv:astro-ph/9601033].
[362] G. E. Romero, D. F. Torres, I. Andruchow, L. A. Anchordoqui and B. Link, Mon. Not.

Roy. Astron. Soc. **308**, 799 (1999) [arXiv:astro-ph/9904107].
[363] D. Band et. al., Astrophys. J. **413** 281 (1993).
[364] M. Sommer et al., Astrophys. J. **422** L63 (1994).
[365] C. A. Meegan et. al., Nature **355**, 143 (1992).
[366] M. R. Metzger et. al., Nature **387**, 878 (1997).
[367] S. R. Kulkarni et. al., arXiv:astro-ph/0002168.
[368] G. Cavallo and M. J. Rees, Mon. Not. Roy. Astron. Soc. **183**, 359 (1978).
[369] B. Paczynski, Astrophys. J. **308**, L43 (1986).
[370] J. Goodman, Astrophys. J. **308**, L47 (1986).
[371] P. Meszaros and M. J. Rees, Astrophys. J. **405**, 278 (1993).
[372] P. Meszaros, P. Laguna, and M. J. Rees, Astrophys. J. **415**, 181 (1993).
[373] T. Piran, Phys. Rept. **314** (1999) 575 [arXiv:astro-ph/9810256].
[374] T. Piran, Phys. Rept. **333** (2000) 529 [arXiv:astro-ph/9907392].
[375] E. Waxman, arXiv:astro-ph/0303517.
[376] E. Waxman, arXiv:astro-ph/0103186.
[377] W. Coburn and S. E. Boggs, Nature **423**, 415 (2003).
[378] E. Nakar, T. Piran and E. Waxman, JCAP **0310**, 005 (2003) [arXiv:astro-ph/0307290].
[379] J. Bednarz and M. Ostrowski, Phys. Rev. Lett. **80** (1998) 3911 [arXiv:astro-ph/9806181].
[380] G. Preparata, R. Ruffini and S. S. Xue, Astron. Astrophys. **338**, L87 (1998) [arXiv:astro-ph/9810182].
[381] T. Damour and R. Ruffini, Phys. Rev. Lett. **35**, 463 (1975).
[382] R. Ruffini, C. L. Bianco, P. Chardonnet, F. Fraschetti and S. S. Xue, Astrophys. J. **581**, L19 (2002) [arXiv:astro-ph/0210648].
[383] C. L. Bianco, R. Ruffini and S. S. Xue, Astron. Astrophys. **368**, 377 (2001) [arXiv:astro-ph/0102060].
[384] R. Ruffini, J. D. Salmonson, J. R. Wilson and S. S. Xue, Astron. Astrophys. **350**, 334 (1999) [arXiv:astro-ph/9907030].
[385] A. Mattei, R. Ruffini, P. Chardonnet, C. L. Bianco, F. Fraschetti, L. Vitagliano, and S. -S. Xue, *Proceedings of the Tenth Marcel Grossmann Meeting on General Relativity*, (Edited by M. Novello, S. Perez-Bergliaffa and R. Ruffini, World Scientific, Singapore, 2005).
[386] L. A. Anchordoqui, C. D. Dermer and A. Ringwald, *Proceedings of the Tenth Marcel Grossmann Meeting on General Relativity*, (Edited by M. Novello, S. Perez-Bergliaffa and R. Ruffini, World Scientific, Singapore, 2005) [arXiv:hep-ph/0403001].
[387] M. Vietri, Astrophys. J. **453**, 883 (1995).
[388] M. Schmidt, Astrophys. J. **552**, 36 (2001).
[389] D. L. Freedman and E. Waxman, Astrophys. J. **547**, 922 (2001).
[390] F. W. Stecker, Astropart. Phys. **14**, 207 (2000) [arXiv:astro-ph/9911269].
[391] S. T. Scully and F. W. Stecker, Astropart. Phys. **16**, 271 (2002) [arXiv:astro-ph/0006112].
[392] A. Loeb and E. Waxman, arXiv:astro-ph/0205272.

[393] M. Vietri, D. De Marco and D. Guetta, Astrophys. J. **592**, 378 (2003) [arXiv:astro-ph/0302144].
[394] E. Waxman, arXiv:astro-ph/0210638.
[395] M. Milgrom and V. Usov, Astrophys. J. **449**, L37 (1995) [arXiv:astro-ph/9505009].
[396] T. Stanev, R. Schaefer and A. Watson, Astropart. Phys. **5**, 75 (1996) [arXiv:astro-ph/9601140].
[397] S. D. Wick, C. D. Dermer and A. Atoyan, Astropart. Phys. (to be published) [arXiv:astro-ph/0310667].
[398] T. Piran, arXiv:astro-ph/0104134.
[399] D. A. Frail *et al.*, Astrophys. J. **562**, L55 (2001) [arXiv:astro-ph/0102282].
[400] C. D. Dermer and A. Atoyan, Phys. Rev. Lett. **91**, 071102 (2003) [arXiv:astro-ph/0301030].
[401] P. L. Biermann, G. A. Medina-Tanco, R. Engel and G. Pugliese, arXiv:astro-ph/0401150.
[402] J. P. Rachen and P. Meszaros, Phys. Rev. D **58**, 123005 (1998) [arXiv:astro-ph/9802280].
[403] G. Pugliese, H. Falcke, Y. Wang and P. L. Biermann, arXiv:astro-ph/0003025.
[404] V. A. Kuzmin and I. I. Tkachev, Phys. Rept. **320**, 199 (1999) [arXiv:hep-ph/9903542].
[405] P. Bhattacharjee and G. Sigl, *Prepared for Physics and Astrophysics of Ultrahigh-energy Cosmic Rays, Meudon, France, 26-29 Jun 2000*
[406] S. Sarkar, arXiv:hep-ph/0312223.
[407] T. Weiler, Phys. Rev. Lett. **49**, 234 (1982).
[408] T. J. Weiler, Astropart. Phys. **11**, 303 (1999) [arXiv:hep-ph/9710431].
[409] D. Fargion, B. Mele and A. Salis, Astrophys. J. **517**, 725 (1999) [arXiv:astro-ph/9710029];
[410] H. Davoudiasl, J. L. Hewett and T. G. Rizzo, Phys. Lett. B **549**, 267 (2002) [arXiv:hep-ph/0010066].
[411] O. E. Kalashev, V. A. Kuzmin, D. V. Semikoz and G. Sigl, Phys. Rev. D **65**, 103003 (2002) [arXiv:hep-ph/0112351].
[412] Z. Fodor, S. D. Katz and A. Ringwald, Phys. Rev. Lett. **88**, 171101 (2002).
[413] Z. Fodor, S. D. Katz and A. Ringwald, arXiv:hep-ph/0203198.
[414] P. W. Gorham, C. L. Hebert, K. M. Liewer, C. J. Naudet, D. Saltzberg and D. Williams, arXiv:astro-ph/0310232.
[415] A. G. Lemaître, Suppl. Nature **128**, 704 (1931).
[416] C. T. Hill, Nucl. Phys. B **224**, 469 (1983).
[417] C. T. Hill, D. N. Schramm and T. P. Walker, Phys. Rev. D **36**, 1007 (1987).
[418] P. Bhattacharjee, C. T. Hill and D. N. Schramm, Phys. Rev. Lett. **69**, 567 (1992).
[419] V. Berezinsky, X. Martin and A. Vilenkin, Phys. Rev. D **56**, 2024 (1997) [arXiv:astro-ph/9703077].
[420] L. Masperi and G. A. Silva, Astropart. Phys. **8**, 173 (1998) [arXiv:astro-ph/9706299].
[421] L. Masperi and M. Orsaria, Astropart. Phys. **16**, 411 (2002) [arXiv:astro-ph/0005593].
[422] V. Berezinsky and A. Vilenkin, Phys. Rev. Lett. **79**, 5202 (1997)

[arXiv:astro-ph/9704257].
[423] V. Berezinsky, M. Kachelriess and A. Vilenkin, Phys. Rev. Lett. **79**, 4302 (1997) [arXiv:astro-ph/9708217].
[424] V. A. Kuzmin and V. A. Rubakov, Phys. Atom. Nucl. **61**, 1028 (1998) [Yad. Fiz. **61**, 1122 (1998)] [arXiv:astro-ph/9709187].
[425] P. Jaikumar and A. Mazumdar, Phys. Rev. Lett. **90**, 191301 (2003) [arXiv:hep-ph/0301086].
[426] M. Birkel and S. Sarkar, Astropart. Phys. **9**, 297 (1998) [arXiv:hep-ph/9804285].
[427] Z. Fodor and S. D. Katz, Phys. Rev. Lett. **86**, 3224 (2001) [arXiv:hep-ph/0008204].
[428] C. Coriano, A. E. Faraggi and M. Plumacher, Nucl. Phys. B **614**, 233 (2001) [arXiv:hep-ph/0107053].
[429] S. Sarkar and R. Toldra, Nucl. Phys. B **621**, 495 (2002) [arXiv:hep-ph/0108098].
[430] C. Barbot and M. Drees, Phys. Lett. B **533**, 107 (2002) [arXiv:hep-ph/0202072].
[431] K. Hamaguchi, Y. Nomura and T. Yanagida, Phys. Rev. D **58**, 103503 (1998) [arXiv:hep-ph/9805346].
[432] K. Hamaguchi, Y. Nomura and T. Yanagida, Phys. Rev. D **59**, 063507 (1999) [arXiv:hep-ph/9809426].
[433] K. Hamaguchi, K. I. Izawa, Y. Nomura and T. Yanagida, Phys. Rev. D **60**, 125009 (1999) [arXiv:hep-ph/9903207].
[434] J. R. Ellis, J. L. Lopez and D. V. Nanopoulos, Phys. Lett. B **247**, 257 (1990).
[435] K. Benakli, J. R. Ellis and D. V. Nanopoulos, Phys. Rev. D **59**, 047301 (1999) [arXiv:hep-ph/9803333].
[436] P. Blasi, R. Dick and E. W. Kolb, Astropart. Phys. **18** (2002) 57 [arXiv:astro-ph/0105232].
[437] C. Coriano and A. E. Faraggi, Phys. Rev. D **65**, 075001 (2002) [arXiv:hep-ph/0106326].
[438] C. Barbot and M. Drees, Astropart. Phys. **20**, 5 (2003) [arXiv:hep-ph/0211406].
[439] C. Barbot, Comput. Phys. Commun. **157**, 63 (2004) [arXiv:hep-ph/0306303].
[440] C. Barbot, M. Drees, F. Halzen and D. Hooper, Phys. Lett. B **563**, 132 (2003) [arXiv:hep-ph/0207133].
[441] L. Anchordoqui, H. Goldberg and P. Nath, arXiv:hep-ph/0403115.
[442] F. A. Aharonian, P. Bhattacharjee and D. N. Schramm, Phys. Rev. D **46**, 4188 (1992).
[443] J. R. Chisholm and E. W. Kolb, arXiv:hep-ph/0306288.
[444] C. Barbot, M. Drees, F. Halzen and D. Hooper, arXiv:hep-ph/0205230.
[445] G. Sigl, S. Lee, P. Bhattacharjee and S. Yoshida, Phys. Rev. D **59**, 043504 (1999) [arXiv:hep-ph/9809242].
[446] G. Sigl, K. Jedamzik, D. N. Schramm and V. S. Berezinsky, Phys. Rev. D **52**, 6682 (1995) [arXiv:astro-ph/9503094].
[447] G. Sigl, S. Lee, D. N. Schramm and P. Coppi, Phys. Lett. B **392**, 129 (1997) [arXiv:astro-ph/9610221].
[448] P. Sreekumar *et al.*, Astrophys. J. **494** (1998) 523 [arXiv:astro-ph/9709257].
[449] G. Sigl, S. Lee and P. Coppi, arXiv:astro-ph/9604093.
[450] R. J. Protheroe and T. Stanev, Phys. Rev. Lett. **77**, 3708 (1996) [Erratum-ibid. **78**,

3420 (1997)] [arXiv:astro-ph/9605036].
[451] R. J. Protheroe and P. A. Johnson, Nucl. Phys. Proc. Suppl. **48**, 485 (1996) [arXiv:astro-ph/9605006].
[452] A. W. Strong, I. V. Moskalenko and O. Reimer, arXiv:astro-ph/0306345.
[453] U. Keshet, E. Waxman and A. Loeb, arXiv:astro-ph/0306442.
[454] D. V. Semikoz and G. Sigl, arXiv:hep-ph/0309328.
[455] S. L. Dubovsky and P. G. Tinyakov, JETP Lett. **68**, 107 (1998) [arXiv:hep-ph/9802382].
[456] V. Berezinsky, P. Blasi and A. Vilenkin, Phys. Rev. D **58**, 103515 (1998).
[457] N. E. Mavromatos and J. Papavassiliou, arXiv:hep-th/0307028.
[458] M. Kachelriess and D. V. Semikoz, Phys. Lett. B **577**, 1 (2003) [arXiv:astro-ph/0306282].
[459] H. B. Kim and P. Tinyakov, arXiv:astro-ph/0306413.
[460] T. W. Kephart and T. J. Weiler, Astropart. Phys. **4**, 271 (1996) [arXiv:astro-ph/9505134].
[461] S. D. Wick, T. W. Kephart, T. J. Weiler and P. L. Biermann, arXiv:astro-ph/0001233.
[462] L. A. Anchordoqui, T. P. McCauley, S. Reucroft and J. Swain, Phys. Rev. D **63**, 027303 (2001) [arXiv:hep-ph/0009319].
[463] N. N. Efimov, N. N. Efremov, A. V. Glushkov, I. T. Makarov, and M. I. Pravdin, in *Astrophysical Aspects of the Most Energetic Cosmic Rays,* (Eds. M. Nagano, F. Takahara, World Scientific 1991), p.434.
[464] E. E. Antonov *et al.*, JETP Lett. **69**, 650 (1999) [Pisma Zh. Eksp. Teor. Fiz. **69**, 614 (1999)].
[465] G. R. Farrar, Phys. Rev. Lett. **76**, 4111 (1996) [arXiv:hep-ph/9603271];
[466] D. J. Chung, G. R. Farrar and E. W. Kolb, Phys. Rev. D **57**, 4606 (1998) [arXiv:astro-ph/9707036];
[467] I. F. Albuquerque, G. R. Farrar and E. W. Kolb, Phys. Rev. D **59**, 015021 (1999).
[468] J. Adams *et al.* [KTeV Collaboration], Phys. Rev. Lett. **79**, 4083 (1997) [arXiv:hep-ex/9709028].
[469] V. Fanti *et al.* [NA48 Collaboration], Phys. Lett. B **446**, 117 (1999).
[470] A. Alavi-Harati *et al.* [KTeV Collaboration], Phys. Rev. Lett. **83**, 2128 (1999) [arXiv:hep-ex/9903048].
[471] I. F. Albuquerque *et al.* [E761 Collaboration], Phys. Rev. Lett. **78**, 3252 (1997) [arXiv:hep-ex/9604002].
[472] V. Berezinsky, M. Kachelriess and S. Ostapchenko, Phys. Rev. D **65**, 083004 (2002) [arXiv:astro-ph/0109026].
[473] M. Kachelriess, D. V. Semikoz and M. A. Tortola, Phys. Rev. D **68**, 043005 (2003) [arXiv:hep-ph/0302161].
[474] J. Madsen and J. M. Larsen, Phys. Rev. Lett. **90**, 121102 (2003) [arXiv:astro-ph/0211597].
[475] C. Csaki, N. Kaloper, M. Peloso and J. Terning, JCAP **0305**, 005 (2003) [arXiv:hep-ph/0302030].
[476] D. S. Gorbunov, G. G. Raffelt and D. V. Semikoz, Phys. Rev. D **64**, 096005 (2001)

[arXiv:hep-ph/0103175].
[477] S. R. Coleman and S. L. Glashow, arXiv:hep-ph/9808446.
[478] F. W. Stecker and S. L. Glashow, Astropart. Phys. **16**, 97 (2001) [arXiv:astro-ph/0102226].
[479] G. Amelino-Camelia, J. R. Ellis, N. E. Mavromatos and D. V. Nanopoulos, Int. J. Mod. Phys. A **12**, 607 (1997) [arXiv:hep-th/9605211].
[480] G. Amelino-Camelia, J. R. Ellis, N. E. Mavromatos, D. V. Nanopoulos and S. Sarkar, Nature **393**, 763 (1998) [arXiv:astro-ph/9712103].
[481] O. Bertolami and C. S. Carvalho, Phys. Rev. D **61**, 103002 (2000) [arXiv:gr-qc/9912117].
[482] R. Aloisio, P. Blasi, P. L. Ghia and A. F. Grillo, Phys. Rev. D **62**, 053010 (2000) [arXiv:astro-ph/0001258].
[483] O. Bertolami, Gen. Rel. Grav. **34**, 707 (2002) [arXiv:astro-ph/0012462].
[484] R. Aloisio, P. Blasi, A. Galante, P. L. Ghia and A. F. Grillo, arXiv:astro-ph/0205271.
[485] G. L. Alberghi, K. Goldstein and D. A. Lowe, Phys. Lett. B **578**, 247 (2004) [arXiv:astro-ph/0307413].
[486] J. Gamboa, M. Loewe and F. Mendez, arXiv:hep-th/0311014.
[487] F. Dowker, J. Henson and R. D. Sorkin, arXiv:gr-qc/0311055.
[488] A. Das, J. Gamboa, F. Mendez and J. Lopez-Sarrion, arXiv:hep-th/0402001.
[489] L. A. Anchordoqui, arXiv:hep-ph/0306078.
[490] A. Cafarella, C. Coriano and A. E. Faraggi, arXiv:hep-ph/0308169.
[491] A. Cafarella and C. Coriano, arXiv:hep-ph/0309159.
[492] E. Roulet, Phys. Rev. D **47**, 5247 (1993).
[493] T. K. Gaisser, F. Halzen and T. Stanev, Phys. Rept. **258**, 173 (1995) [Erratum-ibid. **271**, 355 (1996)] [arXiv:hep-ph/9410384].
[494] F. Halzen, Phys. Rept. **333**, 349 (2000).
[495] F. Halzen and D. Hooper, Rept. Prog. Phys. **65**, 1025 (2002) [arXiv:astro-ph/0204527].
[496] A. D. Dolgov, Phys. Rept. **370**, 333 (2002) [arXiv:hep-ph/0202122].
[497] A. Roberts, Rev. Mod. Phys. **64**, 259 (1992).
[498] I. A. Belolaptikov *et al.* [BAIKAL Collaboration], Astropart. Phys. **7**, 263 (1997).
[499] E. Andres *et al.* [The AMANDA Collaboration], Astropart. Phys. **13**, 1 (2000) [arXiv:astro-ph/9906203].
[500] E. Aslanides *et al.* [ANTARES Collaboration], arXiv:astro-ph/9907432.
[501] P. K. Grieder [NESTOR Collaboration], Nuovo Cim. **24C**, 771 (2001).
[502] J. Alvarez-Muniz and F. Halzen, AIP Conf. Proc. **579**, 305 (2001) [arXiv:astro-ph/0102106].
[503] P. Lipari, Astropart. Phys. **1**, 195 (1993).
[504] L. V. Volkova, Sov. J. Nucl. Phys. **31**, 784 (1980) [Yad. Fiz. **31**, 1510 (1980)].
[505] F. Halzen, Int. J. Mod. Phys. A **17**, 3432 (2002) [arXiv:astro-ph/0111059].
[506] K. Hirata *et al.* [KAMIOKANDE-II Collaboration], Phys. Rev. Lett. **58**, 1490 (1987).
[507] R. M. Bionta *et al.*, Phys. Rev. Lett. **58**, 1494 (1987).
[508] W. Rhode *et al.* [Frejus Collaboration], Astropart. Phys. **4** (1996) 217.

[509] V. Balkanov *et al.* [BAIKAL Collaboration], Nucl. Phys. Proc. Suppl. **110**, 504 (2002) [arXiv:astro-ph/0112446].
[510] M. Ambrosio *et al.* [MACRO Collaboration], Astropart. Phys. **19**, 1 (2003) [arXiv:astro-ph/0203181].
[511] J. Ahrens *et al.*, Phys. Rev. Lett. **90**, 251101 (2003) [arXiv:astro-ph/0303218].
[512] C. Berger *et al.* [FREJUS Collaboration], Nucl. Instrum. Meth. A **262**, 463 (1987).
[513] M. Aglietta *et al.*, Nucl. Instrum. Meth. A **277**, 23 (1989).
[514] M. Ambrosio *et al.* [MACRO Collaboration], Nucl. Instrum. Meth. A **486**, 663 (2002).
[515] M. Aglietta *et al.* [EAS-TOP Collaboration], Phys. Lett. B **333**, 555 (1994).
[516] J. W. Bolesta *et al.*, arXiv:astro-ph/9705198.
[517] I. Kravchenko *et al.*, Astropart. Phys. **20**, 195 (2003) [arXiv:astro-ph/0206371].
[518] I. Kravchenko *et al.*, arXiv:astro-ph/0306408.
[519] L. A. Anchordoqui, J. L. Feng, H. Goldberg and A. D. Shapere, Phys. Rev. D **66**, 103002 (2002) [arXiv:hep-ph/0207139].
[520] P. W. Gorham, K. M. Liewer, C. J. Naudet, D. P. Saltzberg and D. R. Williams, arXiv:astro-ph/0102435.
[521] N. G. Lehtinen, P. W. Gorham, A. R. Jacobson and R. A. Roussel-Dupre, Phys. Rev. D **69**, 013008 (2004) [arXiv:astro-ph/0309656].
[522] J. Ahrens [IceCube Collaboration], arXiv:astro-ph/0305196.
[523] X. Bertou, P. Billoir, O. Deligny, C. Lachaud and A. Letessier-Selvon, Astropart. Phys. **17**, 183 (2002) [arXiv:astro-ph/0104452].
[524] B. Eberle, A. Ringwald, L. Song and T. J. Weiler, arXiv:hep-ph/0401203.
[525] R. M. Baltrusaitis *et al.*, Phys. Rev. D **31**, 2192 (1985).
[526] S. Yoshida *et al.*[AGASA Collaboration], in *Proc. 27th International Cosmic Ray Conference*, Hamburg, Germany, 2001, Vol. 3, p. 1142.
[527] R. Gandhi, C. Quigg, M. H. Reno and I. Sarcevic, Phys. Rev. D **58**, 093009 (1998) [arXiv:hep-ph/9807264].
[528] K. S. Capelle, J. W. Cronin, G. Parente and E. Zas, Astropart. Phys. **8**, 321 (1998) [arXiv:astro-ph/9801313].
[529] I. Kravchenko *et al.* [RICE Collaboration], arXiv:astro-ph/0112372.
[530] F. Halzen and D. Hooper, JCAP **0401**, 002 (2004) [arXiv:astro-ph/0310152].
[531] E. Waxman and A. Loeb, Phys. Rev. Lett. **87**, 071101 (2001) [arXiv:astro-ph/0102317].
[532] R. Tomas, D. Semikoz, G. G. Raffelt, M. Kachelriess and A. S. Dighe, Phys. Rev. D **68**, 093013 (2003) [arXiv:hep-ph/0307050].
[533] S. Razzaque, P. Meszaros and E. Waxman, Phys. Rev. Lett. **90**, 241103 (2003) [arXiv:astro-ph/0212536].
[534] E. Waxman and J. N. Bahcall, Phys. Rev. Lett. **78**, 2292 (1997) [arXiv:astro-ph/9701231].
[535] J. Alvarez-Muniz, F. Halzen and D. Hooper, arXiv:astro-ph/0310417.
[536] A. Levinson and E. Waxman, Phys. Rev. Lett. **87**, 171101 (2001) [arXiv:hep-ph/0106102].
[537] A. Y. Neronov and D. V. Semikoz, Phys. Rev. D **66**, 123003 (2002)

[arXiv:hep-ph/0208248].
[538] L. A. Anchordoqui, H. Goldberg, F. Halzen and T. J. Weiler, arXiv:astro-ph/0404387.
[539] Y. Fukuda *et al.* [Super-Kamiokande Collaboration], Phys. Rev. Lett. **81**, 1562 (1998) [arXiv:hep-ex/9807003].
[540] A. Borione *et al.* [CASA-MIA Collaboration], Phys. Rev. D **55**, 1714 (1997) [arXiv:astro-ph/9611117].
[541] G. Rowell *et al.* [HEGRA Collaboration], Proc. 28th International Cosmic Ray Conference (Tsukuba), 2345 (2003).
[542] M. M. Hanson, Astrophys. J. **597**, 957 (2003) [arXiv:astro-ph/0307540].
[543] J. Knapp, D. Heck and G. Schatz, FZKA-5828.
[544] J. Knapp, D. Heck and G. Schatz, Nucl. Phys. Proc. Suppl. **52B** (1997) 136.
[545] J. Knodlseder, M. Cervino, D. Schaerer, P. von Ballmoos and G. Meynet, arXiv:astro-ph/0104074.
[546] S. N. Ahmed *et al.* [SNO Collaboration], arXiv:nucl-ex/0309004.
[547] V. Berezinsky and G. T. Zatsepin, Phys. Lett. B **28**, 423 (1969).
[548] R. Engel, D. Seckel and T. Stanev, Phys. Rev. D **64**, 093010 (2001) [astro-ph/0101216].
[549] O. E. Kalashev, V. A. Kuzmin, D. V. Semikoz and G. Sigl, Phys. Rev. D **66**, 063004 (2002) [arXiv:hep-ph/0205050].
[550] Z. Fodor, S. D. Katz, A. Ringwald and H. Tu, JCAP **0311**, 015 (2003) [hep-ph/0309171].
[551] Z. Fodor, S. D. Katz, A. Ringwald and H. Tu, Phys. Lett. B **561**, 191 (2003) [arXiv:hep-ph/0303080].
[552] N. Arkani-Hamed, S. Dimopoulos and G. R. Dvali, Phys. Lett. B **429**, 263 (1998) [arXiv:hep-ph/9803315].
[553] I. Antoniadis, N. Arkani-Hamed, S. Dimopoulos and G. R. Dvali, Phys. Lett. B **436**, 257 (1998) [arXiv:hep-ph/9804398].
[554] S. Nussinov and R. Shrock, Phys. Rev. D **59**, 105002 (1999) [arXiv:hep-ph/9811323].
[555] G. Domokos and S. Kovesi-Domokos, Phys. Rev. Lett. **82**, 1366 (1999) [arXiv:hep-ph/9812260].
[556] P. Jain, D. W. McKay, S. Panda and J. P. Ralston, Phys. Lett. B **484**, 267 (2000) [arXiv:hep-ph/0001031].
[557] M. Kachelriess and M. Plumacher, Phys. Rev. D **62**, 103006 (2000) [arXiv:astro-ph/0005309].
[558] L. Anchordoqui, H. Goldberg, T. McCauley, T. Paul, S. Reucroft and J. Swain, Phys. Rev. D **63**, 124009 (2001) [arXiv:hep-ph/0011097].
[559] T. Banks and W. Fischler, arXiv:hep-th/9906038.
[560] S. B. Giddings and S. Thomas, Phys. Rev. D **65**, 056010 (2002) [arXiv:hep-ph/0106219].
[561] S. Dimopoulos and G. Landsberg, Phys. Rev. Lett. **87**, 161602 (2001) [hep-ph/0106295].
[562] J. L. Feng and A. D. Shapere, Phys. Rev. Lett. **88**, 021303 (2001) [hep-ph/0109106].
[563] L. Anchordoqui and H. Goldberg, Phys. Rev. D **65**, 047502 (2002) [hep-ph/0109242].
[564] R. Emparan, M. Masip and R. Rattazzi, Phys. Rev. D **65**, 064023 (2002) [arXiv:hep-ph/0109287].

[565] A. Ringwald and H. Tu, Phys. Lett. B **525**, 135 (2002) [hep-ph/0111042].
[566] S. I. Dutta, M. H. Reno and I. Sarcevic, Phys. Rev. D **66**, 033002 (2002) [arXiv:hep-ph/0204218].
[567] M. Kowalski, A. Ringwald and H. Tu, Phys. Lett. B **529**, 1 (2002) [arXiv:hep-ph/0201139].
[568] J. Alvarez-Muniz, J. L. Feng, F. Halzen, T. Han and D. Hooper, Phys. Rev. D **65**, 124015 (2002) [arXiv:hep-ph/0202081].
[569] L. A. Anchordoqui, J. L. Feng, H. Goldberg and A. D. Shapere, Phys. Rev. D **68**, 104025 (2003) [arXiv:hep-ph/0307228].
[570] L. A. Anchordoqui, J. L. Feng, H. Goldberg and A. D. Shapere, arXiv:hep-ph/0309082.
[571] L. A. Anchordoqui, J. L. Feng, H. Goldberg and A. D. Shapere, arXiv:hep-ph/0311365.
[572] V. S. Berezinsky and A. Y. Smirnov, Phys. Lett. B **48**, 269 (1974).
[573] D. A. Morris and A. Ringwald, Astropart. Phys. **2**, 43 (1994) [arXiv:hep-ph/9308269].
[574] C. Tyler, A. V. Olinto and G. Sigl, Phys. Rev. D **63**, 055001 (2001) [arXiv:hep-ph/0002257].
[575] J. L. Feng, P. Fisher, F. Wilczek and T. M. Yu, Phys. Rev. Lett. **88**, 161102 (2002) [arXiv:hep-ph/0105067].
[576] D. Fargion, Astrophys. J. **570**, 909 (2002) [arXiv:astro-ph/0002453].
[577] L. A. Anchordoqui, J. L. Feng, H. Goldberg and A. D. Shapere, Phys. Rev. D **65**, 124027 (2002) [arXiv:hep-ph/0112247].